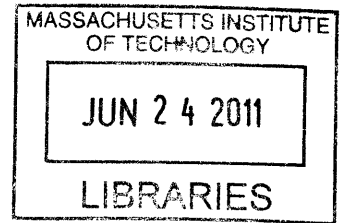# The Role of the Aerodynamic Modifications
of the Shapes of Tall Buildings

by

Jooeun Lee

B.Eng. School of Architecture and Architectural Engineering
Inha University, South Korea
1999

Submitted to the Department of Civil and Environmental Engineering
in Partial Fulfillment of the Requirements for the degree of

Master of Science in Civil and Environmental Engineering

at the

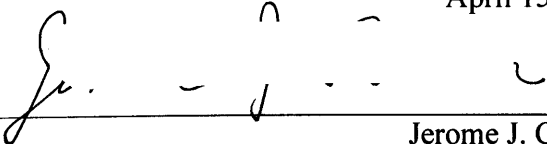Massachusetts Institute of Technology

June 2011

Signature of Author: _____

Department of Civil and Environmental Engineering
April 15, 2011

Certified by: _____

Jerome J. Connor
Professor of Civil and Environmental Engineering
Thesis Supervisor

Accepted by: _____

Heidi M. Nepf
Chair, Departmental Committee for Graduate Students

The Role of the Aerodynamic Modifications of the Shapes of Tall Buildings

by

Jooeun Lee

Submitted to the Department of Civil and Environmental Engineering
on April 15, 2011 in Partial Fulfillment of the Requirements for the degree of
Master of Science in Civil and Environmental Engineering

Abstract

With the advances in technology, recent tall building design has undergone a shift to the free-style geometric forms in the exuberant and liberal atmosphere. As a height of the building increases, it is more susceptible to vibration caused by wind because of its asymmetric distribution of mass and stiffness, increased flexibility and insufficient inherent damping. This wind-induced motion, in particular crosswind response, endangers the dynamic response of tall structures, the performance of cladding and window, and the habitability of occupants. Therefore, much research on mitigating wind induced excitations of tall buildings has been carried out.

This thesis focuses on the effect of shape modification on the wind flow pattern around tall buildings. An appropriate choice of this architectural modification can significantly reduce aeroelastic instabilities. Four aerodynamic modifications to reduce wind-induced responses of a tall building, such as a basic square model, a corner recession model, a 3-step setback model, and a 180 degree helical model, are evaluated through commercial CFD (Computational Fluid Dynamics) software, STAR-CD and compared with results from wind tunnel tests. Based on this comparison, the optimal model to effectively mitigate adverse wind excitations is recommended.

Thesis Advisor: Jerome J. Connor
Title: Professor of Civil and Environmental Engineering

Acknowledgements

존경하는 아버지, 어머니 그리고 장인어른과 장모님
사랑하는 아내 배광희와 아들 이진섭 그리고 앞으로 태어날 아기에게.

Table of Contents

Appendices

Table of Figures

List of Tables

Chapter 1 Overview

1.1 Introduction

Chief amongst reasons of constructing tall buildings have been symbolic image, power, prestige, aesthetics and visibility. Since the late 19th century, there has been a growth in the construction of tall buildings. A rapid expansion of the economy and a boom in the stock market, between the late 1890s and the early 1910s, made possible a substantial increase in capital. This increased capital significantly flows into the construction market of tall buildings to show off the richness accumulated. As the example of tall building, whose structural system is steel skeletal frames encased in massive masonry walls, built in this period, the 30 story Park Row Building in 1899 had already attained the height of about 120 meters. Also, the 47 story Singer Building, though demolished, became the tallest in the world when completed in 1908. Just one year later, the 50 story Metropolitan Life Insurance in 1909 became the world tallest building. However, this first skyscraper boom did not sustain because of the panic of 1907, one of the sharpest downturns in US economic history (Thornton 2005). After the economy stabilized, the second skyscraper boom occurred in the 1920s, benefitting from an unprecedented boom in the stock market, leading to a significant growth in the construction market of residential and commercial tall buildings including the 77 story Chrysler Building in 1930 and the 102 story Empire State Building in 1931. During these two skyscraper booms, tall buildings were influenced by the design principles such as the functionalism by Louis Sullivan and the Art Deco articulately involving with the cubism, futurism and expressionism. Therefore, such buildings showed exaggerated decorations and imagination powers with a vestige of Gothic and Renaissance motifs (Aysin 2009). In addition, the structural system prevalent in this era (1880-1940) was structural steel frame, before which load bearing masonry structure had been predominantly utilized. However, these styles and structural systems experienced considerable changes. The aftermath of the Great Depression from 1929 to the 1930s and the World War II from 1939 to 1945 retarded the advancement of tall buildings. This regression still remained strong until the 1950s. However, due to the boom

in economy in the 1960s, there was another skyscraper boom; the 52 story JP Morgan Chase World HQ in 1960, the 65 story Marina City in 1964, the 70 story Lake Point Tower in 1968, the 100 story John Hancock Center in 1970, and importantly the 108 story Willis Tower in 1974 were constructed in this skyscraper boom in which most of the tall buildings were influenced by International style, or Modernism. The feature of this style was the rectangular prism-like building. Unlike between 1880 and 1940, the decorations as vestige of Gothic and Renaissance style in tall buildings were almost absent (Aysin 2009). Also, with the significant advancement in technology and construction, buildings, whose style was a steel frame clad with glass wall, were built more efficiently. For instance in structural systems, the rigid frames, as interior structures, the 860-880 Lake Shore Drive Apartments in 1949 adopted provided flexibility in the floor planning along with fast construction (Mir M. Ali 2007). In addition, the John Hancock Center utilized the steel braced tube system as an exterior structure, which efficiently resists lateral shears by axial forces in diagonal members as shown in Figure 2.19. In fact, various modified tube systems were introduced: framed tube (Aon Center in 1973) and bundled tube (Willis Tower in 1974). Most of the tall buildings followed the modernism. However, starting from the Marina City Tower in 1964 and the Lake Point Tower in 1968, buildings such as the 333 South Wacker Drive in 1983 are of circular shape, conspicuously distinct from the boxlike buildings. This separation meant the enlightenment from the ignorance of the significance of free-style designs. However, the modernism overwhelmingly prevalent during the period from 1940 to 1980 declined with the stagflation and deep recessions from the 1970s to the early 1980s. Following modernism, post modernism elicited free forms of tall buildings with their own regional and cultural features. In addition, tall buildings with novel geometry such as the Al Faisaliah Center in 2000, the 30 St Mary Axe in 2004 and the Turning Torso in 2006 emerged. Since the 1980s, the fourth skyscraper boom has become unequivocally visible in the countries including Malaysia, Japan, China, and UAE. Although severe economic crisis in Asia, starting from the sudden collapse in stock market and deep depreciation of currency in Malaysia, was rampant, the race for tallest buildings has been consistent. Moreover, this growth gains momentum from the innovative technology and designs. For example, the diagrid system employed in

the 46 story Hearst Tower employed efficiently resists the lateral forces like wind and earthquake and the gravity forces by diagonal members without vertical columns (Moon 2005). Other examples are the space truss - exterior systems (the 72 story Bank of China Tower in 1990) and the outrigger – interior system (the 101 story 101 Taipei in 2004). These advances made unconventional designs more feasible.

However, tall buildings have more problems than low rise buildings. Although the tall buildings produce powerful iconic images and visibility, the construction cost is considerably larger and the design of them is much more difficult. Moreover, recent skyscrapers pursuit free-style forms distinct from traditional rectangular prisms as well as the height unimaginable in the past. This is due to the desire for revolutionary and innovative shapes of tall buildings from humans. This insatiable human desire, however, causes many severe problems in habitability, pedestrian comfort, wind induced noise and interference effect of neighboring buildings. Figure 3.1 shows the rapid growth of tall buildings in residential and lodging usages. This means the importance of habitability issue cannot be ignored. With the advanced structural systems and damping mechanism, tall buildings are very far from the danger of collapse and structural failure. However, the vibration and jerkiness caused by the wind to tall buildings remain an issue to be addressed for the serviceability and habitability of buildings. Especially these problems in super tall buildings are more profound.

To mitigate these adverse effects induced by the wind, there have been various strategies such as addition of viscoelastic material, the tuned mass damper, and proper aerodynamic modifications in Table 1.1. However, though equipped with the recent advancement in analysis software and wind tunnel test, the design of tall buildings based on this technology relies to a large extent on the several assumptions such as fundamental mechanics and accumulated experiences. Therefore, because the precise values of parameters in structures like damping cannot be predicted before the construction, the performance of tall buildings is highly likely to affect the serviceability and occupant comfort as previously mentioned. Therefore, the accuracy and validity of analytical results

should be assessed with respect to actual performance of tall buildings (Kijewski-Correa 2006). Nevertheless, the experiment on full-scaled model still remains so limited, even though Dryden (1930) conducted the wind pressure study on circular cylinders and chimneys. Therefore, the full-scale monitoring of the performance of actual tall buildings already built is considered a practical means for verifying and improving analytical practices.

Table 1.1 Means to suppress wind-induced responses of buildings (Ahsan Kareem 1999)

Means	Type	Methods & Aim	Remarks
Aerodynamic Design	Passive	Improving aerodynamic properties to reduce wind force coefficient	Chamfered Corners, Opening
Structural Design	Passive	Increasing building mass to reduce air/building mass ratio	Increased Material Costs
		Increasing stiffness or natural frequency to reduce non-dimensional wind-speed	Bracing Walls, Thick Members
Auxiliary Damping Device	Passive	Addition of materials with energy dissipative properties, increasing building damping ratio	SD, SJD, LD, FD, VED, VD, OD
		Adding auxiliary mass system to increase level of damping	TMD, TLD
	Active	Generating control force using inertia effects to minimize response	AMD, HMD, AGS
		Generating aerodynamic control force to reduce wind force coefficient or minimize response	Rotor, Jet, Aerodynamic Appendages
		Changing stiffness to avoid resonance	AVS

SD: *Steel Damper*; SJD: *Steel Joint Damper*; LD: *Lead Damper*; FD: *Friction Damper*; VED: *Visco-Elastic Damper*; V.D: *Viscous Damper*; OD: *Oil Damper*; TMD: *Tuned Mass Damper*; TLD: *Tuned Liquid Damper*; AMD: *Active Mass Damper*; HMD: *Hybrid Mass Damper*; AGS: *Active Gyro Stabilizer*; AVS: *Active Variable Stiffness*

Some of the most relevant characteristics of structures which affect wind-induced structural vibrations are shape, stiffness or flexibility and damping. Damping is highly uncertain, leading to unpredictability of the actual performance of tall buildings. Therefore, this paper presents an overview and a summary of past and recent work on various aerodynamic modifications to the shape of the buildings. These modifications can be grouped into minor and major modifications. Minor modifications are aerodynamic ones which, to a miner extent, affect the structural and architectural design. As various

modifications to corner geometry, chamfered corners or corner cut, corner recessions, slotted corners, corner roundness, through opening, fitting of fins and vented fins are affiliated to such modifications. On the other hands, major modifications are aerodynamic ones which considerably affect the structural and architectural concepts. Examples of these major modifications are belonged to by the modifications of a tall building shape, addition of opening and vertical or horizontal slots to building, and twisting or rotating of a building. The purpose of all the modifications is to alter the flow pattern around a tall building and reduce the wind excited vibration of tall buildings.

This paper investigates, through computational evaluations, the effects of aerodynamic modifications to a tall building on the wind force and wind pressure on the tall building. During the numerical simulation, DES (Detached Eddy Simulation) based on Standard $k - \varepsilon$ turbulence model and commercial CFD software STAR-CD is adopted. The data obtained from wind tunnel test already conducted by Tamura (2010) are utilized to validate the evaluation of various modifications. As mentioned in Tamura 2010, the square model shows much more vortex sheddings inducing acrosswind vibrations of tall buildings, while the 180 degree helical model, corner recession model and setback model present the smaller recirculation regions, leading to the suppression of vortex shedding.

1.2 Outline

Chapter 1 briefly overviews this paper by summarizing the history of tall buildings, the wind related issues with construction of tall buildings, the significance of full scale monitoring of performance of tall buildings, the effect of various aerodynamic modifications on the wind responses of tall buildings, and the computational evaluations on the wind force and moment of various shape modified models: square, corner recession, setback, and 180 degree helical model.

Chapter 2 mentions the history of tall buildings which is group into three periods. In each

period, the design trends, structural systems and economic situations are explored.

Chapter 3 reviews on the basic knowledge of the wind and elaborate on the issues related to the tall buildings concisely mentioned in chapter 1. These four issues, such as built environment for pedestrian, wind induced noise, serviceability and habitability are discussed.

Chapter 4 mentions the significance of the full scales monitoring of performance of actual tall buildings. Also, the works conducted by several researchers like Eiffel are reviewed.

Chapter 5 reviews minor modifications such as corner-cut, corner recession, corner roundness and fitting small fins and major modifications such as tapering, setback, helical shape, and openings through building. Obtained from tunnel test results, the most efficient and effective aerodynamic shapes are introduced.

Chapter 6, through computational evaluation, studies on the effect of shape modifications of tall buildings on wind induced vibration. The modifications involved in this chapter include Square Model, Model with four Corner recession, Model with Setback, 180-degree helical or twisting square model.

Chapter 7 presents the summary on each chapter, and concludes this thesis.

1.3 References

Kijewski-Correa T. et al. 2006, Validating Wind-Induced Response of Tall Buildings: Synopsis of the Chicago Full-Scale Monitoring Program, Journal of Structural Engineering, ASCE, 2006, pp.1509-1523.

Ali M.M. and Moon K.S., Structural Developments in Tall Buildings: Current Trends and Future Prospects, Architectural Science Review, Volume 50.3, PP.205-232.

Moon K.S., 2005, Dynamic Interrealationship Between Technology and Architecture in Tall Buildings, Ph.D. Dissertation, MIT

Aysin SEV. 2009, Typology for the Aesthetics and Top Design of Tall Buildings, G.U. Journal of Science, 22(4): 371-381.

Mark Thornton. 2005, Skyscrapers and Business Cycles, the journal of Austrian Economics, Vol. 8, No. 1, Spring 2005.

Kareem A., Kijewski-Correa T., and Tamura Y. 1999, Mitigation of Motions of Tall Buildings with Special Examples of Recent Applications, Journal on Wind and Structures, Vol. 2, No. 3. (1999), pp.201-251

Chapter 2 History of Tall Buildings

2.1 Introduction

Figure 2.1 shows skyscrapers are generally grouped into three periods (the first, the second and the third Skyscraper Golden age) according to the economic situations and tall building booms.
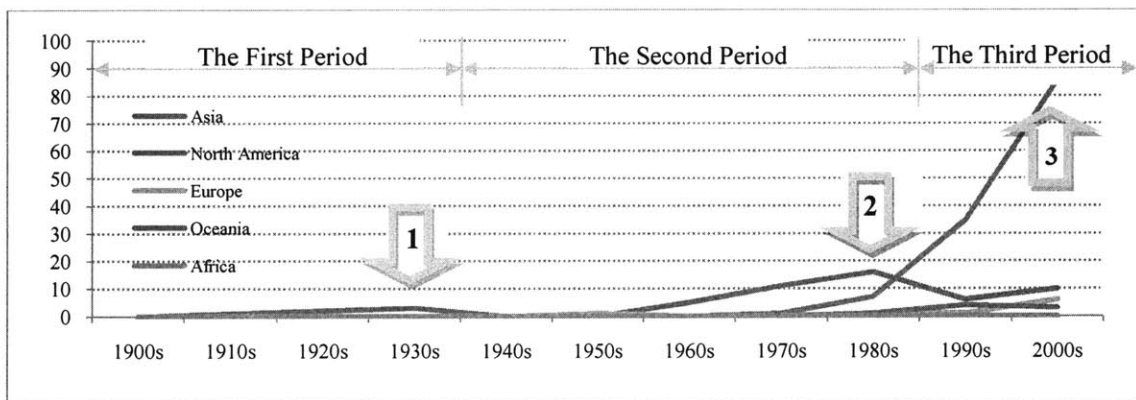
Figure 2.1 World's 200 Tallest Buildings by Continent (Emporis, 2011)
* Arrow means the skyscraper boom in each period.

The first period (1880-1940) is the time when steel and iron skeletal frame encased in massive masonry walls was introduced, and then it faced the first boom of tall buildings. Since the introduction of this steel skeletal frame in Home Insurance Building designed by William Le Baron Jenney in 1885, other advanced structural systems like portal bracing, riveted steel connection and braced frames had been utilized along with the development of elevator. However, this period was not always beneficial for tall buildings. In fact, there were two main financial risks adversely affecting the construction of tall buildings in the first boom. The first financial panic (the panic of 1907) occurred when banks regulated under the National Banking System refused to clear funds for the Knickerbocker, unregulated trust (Thronton 2005) followed by Federal Reserve Act in 1913, and the second financial downturn, Great Depression happened in 1929. In fact, resulting from the stock market boom, numerous tall buildings were constructed including the Chrysler

Building in 1930 and the Empire State Building in 1931, even though this capital-oriented boom consequently caused the Great Depression. The design characteristics of tall buildings in this period were initially followed by the principle of Louis Sullivan, Functionalism, *forms ever follows function*, later by Eclecticism in which Gothic style was adopted to the vertical design of tall buildings, and lastly by Art Deco design which was merged with cubism, futurism, expressionism and exotic motif (Aysin 2009). This period experienced vicissitude of cultures and economy, and such changes are shown in the tall buildings built in 1880-1940.

Major Economic Downturns

Panic of 1907
Significant contraction begins
Federal Reserve Act-1913
WWI (1914-1918)
Great Depression begins-1929
Economic downturn-1970
US abandons gold standard-1971
Stagflation of the 1970s
Asia Crisis and Contagion begins -1997

Singer 1908
Metropolitan Life 1909
Woolworth 1913
Manhattan Company 1930
Chrysler 1930
Empire State 1931
World Trade Center 1972–73
Sears Tower 1974
Petronas Towers 1998

Figure 2.2 Skyscrapers and Economic Crisis (Thornton 2005)

In fact, the 1940s is the time which witnessed the major social catastrophic events such as the aftermath of the Great Depression starting from 1929 and the World War II (1939-1945). These chaotic incidents led to the decline in tall building construction, a distinct

transition which significantly separated the second one from the first period of tall building boom. However, considerable amount of money from a strong economy growth during the 1960s drew the construction boom of tallest buildings such as The World Trade Center in New York and the Sears Tower in Chicago. In addition, it can be illustrated that the second period (1940-1980) is the time when the mass production become prevalent. For example, the tall buildings built just after 1950 conformed to the International style in which the significance of free-style forms was ignored, but auspicious facts from new technology were excessively valued. Most of tall buildings were preferably designed by the transparency trend with the hybrid of steel frames and glass curtain walls. The structural systems involved in this period are modified framed tube systems such as bundled tube, braced tube, composite tube and tube in tube (Aysin 2009). More interestingly, the characteristic of these buildings are the box-shaped, stereometric form designed with glass cladding system and the vertical consistency, monolithic design with little or no ornamentation and variation. However, the economic downturns, such as stagflation and deep recessions (1970-1982) and abandonment of gold standard in 1971, discouraged the competitive race for tallest buildings in United State, but this race revitalized in Asian countries from the 1980s.

The last period (1980-current) initiated when the Xerox Center in 1980 and the 333 South Wacker Drive in 1983 were constructed. The feature of these buildings is the building itself whose shape is curvilinear with a curved glass façade. This form is significantly distinct from that of the internationalism widely preferred in the second period. In addition, along with the advancements in design and construction, variations happened in shapes of tall buildings, including cylindrical, tapered, setback, helical shaped buildings. Also, influenced by post-modernism, skyscrapers with clear tripartite design of base, shaft and top reemerged after the first period because of desire of exodus from the boredom of uniform and standard form with glass and steel system. Moreover, regional architectural and cultural traditions are good design motif in design of tall buildings in this period. According to Aysin (2009), this period is called ultimate technology period in which more advanced systems like Diagrid introduce and more free style forms of tall buildings made

possible by this 'high-tech', become preferred. Although the East Asian economic crisis as well as economic recession and stagnation in Japan in the 1990s caused havoc in the tall building construction market, tall buildings are constructing in these areas with the recent boom in East Asia and China.

2.2 The First Golden Age in Tall Buildings (1880-1940).

This period, when tall buildings experienced a transition from masonry structures to steel skeletal structures encased in masonry walls, began with the Home Insurance Building (1885) by William Le Baron Jenny in Chicago. Prior to it, the structural system employed in buildings was load bearing masonry wall, which significantly limited the height of buildings. However, this limitation was solved; for example, the Home Insurance Building is one of the first tall buildings to utilize steel and iron framework, though curtain wall systems still used masonry. With the invention of steel skeletal structural system and later elevator, many tall buildings were so intensely constructed in this period in Chicago, even though the height of tall buildings was forced to be limited to 130 feet because of the Chicago zoning law (Carol Willis, 1995). In fact, it is undeniable that the introduction of the structural system led to the era of tall buildings.

In New York as well as in Chicago, prodigious amount of money was spent constructing numerous tall buildings in the late 1920s when the stock market boom and capital-oriented boom accelerated the speed of tallest building race. Therefore, this period is considered the first golden age of a tall building. Much research on structural systems was carried out. As the height of a tall building increase, needed are more efficient and innovative structural systems against lateral wind and seismic loads. Thus, following steel skeletal frame structure, portal bracing, riveted steel connection and braced frames appeared (Moon K., 2004). Among them, braced frame system was more prevalent; in fact, the Chrysler Building (1930) and Empire State Building (1931) also adopted this system. In fact, first tall buildings which utilized these systems are Tacoma Building (1889),

Monadnock Building (1891) and Manhattan Building (1891) (Moon K.S. 2005).

The race for tall buildings, starting from the economic view to attract more rent in office buildings, gradually grew enough for the public to recognize the symbolic connotation and meanings; at that time, this symbol expressed the prosperity and success. Therefore, more buildings having higher stories began to loom in the late 19th century. The bout of this race was exist from 30-story Park Row Buildings (119m, 1899) to the 77-story Chrysler Building (319m, 1930) and later 102-story Empire State Building (381m, 1931). The Empire State Building remained as the tallest skyscraper in the world, for 42 years, until the completion of 110-story World Trade Center (417m, 1973).

Unlike the rigid frame system the buildings with lower than 30 story used, the braced frame systems were utilized to resist horizontal loading for these two tallest buildings. At that time when conservative design was strong, the steel skeleton frame was not exposed because steel was vulnerable to weather condition, and masonry had been still used as cladding materials without significant advancement in technology since the 1890s. For example, as shown in Figure 1.4, most buildings, based on traditional architectural practices, have the same façade system, based on traditional architectural practices. In addition, design principles in this period were influenced by Functionalism and Eclecticism and Art Deco (Aysin 2009). In fact, these designs represented stronger symbolic power and more attractive decorations by adopting renaissance, gothic style and more recent architectural styles such as cubism, futurism, and exotic motif including Japan and China. First, functionalism mainly practiced in the late 19th century was characterized by function-based design in buildings which was manifested by Louis Sullivan. As mentioned before, the typical tall buildings were large and gigantic in scale but limited in height. The general tripartite subdivision of the tall building was organized into three parts: base, shaft and top. The classic form of tall buildings in that time is flat or triangular with the renaissance styled tops and ornamental last story from the middle height of tall building. Examples of this functionalism are the 10 story Home Life Insurance Company in 1885, the 10 story Wainwright Building in 1891, the 17 story Monadnock Building in

1891, the 13 story Guaranty Building in 1894, the 15 story Reliance Building in 1894, 30 story Park Row Building in 1899, and the 12 story Carson Pirie Scott Department Store in 1904. To evoke the religious and overpowering image, tall buildings designed in Eclecticism utilized the motif from European classical design principles, Gothic and Renaissance styles. Designed in this style, the Representative buildings are the 47 story Singer Building, though demolished, in 1908, the 50 story Metropolitan Life Insurance in 1909 and the 57 story Woolworth Building in 1913. Starting from the 1920s, rather than gothic and renaissance styles, numerous various styles from art movements famous in that time such as cubism and futurism were prevailing used in tall buildings. The main examples of this style, art deco, are the 77 story Chrysler Building in 1930, the 102 story Empire State Building in 1931, the 27 story 32 avenue of the America (formerly AT&T Long Distance) building in 1932 and the 70 story RCA Building in 1933.

This period experienced several financial crises including the Panic of 1907 and the Great Depression from 1929 until the1930s. Prior to and just after 1907, time when there was no influence of the panic of 1907, the tallest buildings in that time such as the 47 story Singer Building in 1908 and the 50 story Metropolitan Life Insurance in 1909 were constructed. However, except for the 57 story Woolworth Building, there were no other tallest buildings built after the time influenced by the panic of 1907 (Thornton 2005). Recovered from this panic during the 1910s and the 1920s, US economy showed unprecedented economic growth from which many tallest buildings could be constructed. Capital accumulated by this boom made possible the constructions of the 77 story Chrysler Building in 1930 and the 102 story Empire State Building in 1931. However, the Great Depression originated in 1929 discouraged the construction of tallest buildings and there had been no tallest building built until the 1970s since the appearance of the Empire State Building in 1931.

Table 2.1 List of Tall Buildings in 1880-1940

Completion	Building	City	Stories/ Meter
1885	Home Life Insurance Company	Chicago	10 (later 12)/42
1891	Wainwright Building	St. Louis	10/

1894	Guaranty Building	Buffalo	13/
1891	Monadnock Building	Chicago	17/66
1894	Reliance Building	Chicago	15/61
1899	Park Row Building	New York	30/119
1904	Carson Pirie Scott Department Store	Chicago	12/63
1908	Singer Building (demolished)	Philadelphia	47/187
1909	Metropolitan Life Insurance	New York	50/213
1912	Municipal Building	New York	40/177
1913	Woolworth Building	New York	57/241
1915	Equitable Building	New York	38/164
1921	Wrigley Building	Chicago	30/130
1924	Chicago Temple Building	Chicago	23/173
1925	Chicago Tribune Building	Chicago	36/141
1927	NY Telephone Building	New York	32/
1929	Palmolive Building	Chicago	37/
1930	40 Wall Street Building	New York	70/283
1930	Chrysler Building	New York	77/319
1931	Empire State Building	New York	102/381
1930	Daily News Building	New York	36/145
1931	McGraw Hill Building	New York	33/148
1932	PSFS Building	Philadelphia	36/150
1932	32 avenue of the America (AT&T Long Distance)	New York	27/167
1933	GE (formerly RCA) Building	New York	70/259

Figure 2.3
Home Life Insurance Building in 1985

Figure 2.4
Guaranty Building in 1895

Figure 2.5
Park Row Building in 1899
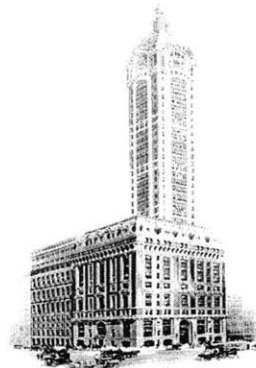
Figure 2.6
Singer Building in 1908

Figure 2.7
Metropolitan Life Insurance in 1909
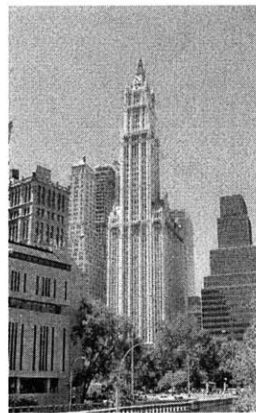
Figure 2.8
Woolworth Building in 1913

Figure 2.9
Wrigley Building in 1921

Figure 2.10
Palmolive Building in 1929

Figure 2.11
40 Wall Street Building in 1930

Figure 2.12
Empire State Building in 1931

Figure 2.13
32 Avenue of the America in 1932

Figure 2.14
GE Building in 1933

2.3 The Second Golden Age in Tall Buildings (1940-1980).

The 1940s is the time which witnessed the major social catastrophic events such as the aftermath of the Great Depression starting from 1929 and the World War II (1939-1945). In fact, these chaotic incidents suppressed tall building construction; as a result, the 1940s was a distinct transition which significantly separated the second one from the first period of tall building boom. Since the 1950s, the construction market had become recuperated, with the development of structural systems and construction technology. Before this

period, building materials such as steel and masonry acted as constraint on the design of tall buildings. However, since the steel skeleton and glass skin system introduced, tall buildings, considering aesthetics and function rather than materials and distinct from the traditional form, had emerged. The appearance of tall buildings seemed like pure rectangular box forms, and the structural systems faced a significant advancement: Framed-tube systems, Braced-Tube systems, Bundled-tube systems, and Outrigger systems. These systems enabled tall buildings to be much higher and lighter, which, ironically, arouse unwanted vibration (addressed in next chapters) from the wind. Outrigger systems are eclectic ones modified from braced frame and shear-wall frame system. This system utilized column-restrained outriggers to prevent the core including braced frames or shear walls from rotating because of the lateral loading like the wind. In particular, multi-story outriggers, with better lateral resistance and extra stiffness, enhance the efficiency in the structural response, which can be used in more than 100 story buildings (Gunel M.H., 2006). Buildings with this system are 42-story First Wisconsin Center, 88-story Jin Mao Building, and 101-story Taipei 101. Another system is the frame-tube system with the closely spaced perimeter of exterior columns and the deep spandrel beams rigidly interconnected. This system has drawbacks such as the interrupt of the view from interior and the narrow access to the public lobby, but it is considerably efficient in structural mechanism against lateral wind and gravitational load. The most notable examples of this framed tube system are the destroyed 110-story World Trade Center Twin Towers, 43-story DeWitt-Chestnut Apartment Building, and 83-story Aron Center. To improve the rigidity and efficiency of the framed tube systems, multistory diagonal bracings added onto the face of the tube are utilized. This system, Braced, or Trussed, Tube System, could make the column-spacing wider and the floor height higher, thereby providing solutions to the existing issues the framed tube systems have. Replacing numerous closely spaced columns with diagonals in both directions, the braced tube system, however, has some aesthetic problem in exterior of the buildings. The excellent examples are the 50 story 780 Third Avenue Building, 58-story Onterie Center in 1986, the 100 story John Hancock Center in 1969, and the 59 story Citigroup Center. Another system is Bundled tube system, which has several individual tubes. It is effective in tall

buildings wider and higher because of the limit in which a single framed can provide sufficient resistance. In addition, this system provides the unsymmetrical shapes to tall buildings, which opens the free-style design of a tall building. The example of this system is the 108-story Willis Tower (formerly Sears Tower) in 1974 and the 57-story One Magnificent Mile Building in 1983.

The general shape of tall buildings in this period was like a rectangular prism, which was influenced by International style or Modernism. Therefore, the tall buildings designed in this style were the steel skeletal structures with glass walls, conforming to regularity without decorations. The classical tripartite subdivision of base, shaft and top in prevalent in the previous period was little or not employed. As a result, the vertical shapes of tall buildings are continuous without any variation or ornament. However, since the 1980s, reaction against this style had appeared. The Xerox Center in 1980 and the 333 South Wacker Drive are considered the vanguards of tall buildings which showed this reaction (Aysin 2009).

Strong and sustained economic growth during the 1960s ushered in the era of the super tall building. With the advancement of technology and the introduction of computer, main tall buildings are the 100 story John Hancock Center in 1969, the 80 story Amoco Building in 1972, the 110 story World Trade Center (now collapsed) in 1973, and the 108 story Sears Tower (currently named Willis Tower) in 1974. However, major economic downturns, such as stagflation, deep recessions and high unemployment rate, sustaining from 1970 to 1982 discouraged the construction of tallest buildings. The tallest building, the Petronas Tower, had appeared in 1997 since the Willis Tower in 1974.

Table 2.2 List of Tall Buildings in 1940-1980

Completion	Building	City	Stories/ Meter
1949	860-880 Lake Shore Drive Apartments	Chicago	26/82
1952	Lever House	New York	24/92
1957	Seagram Building	Chicago	38/157
1960	JP Morgan Chase World HQ	New York	52/216

1964	Marina City	Chicago	65/179
1966	Plaza on DeWitt	Chicago	43/120
1968	Lake Point Tower	Chicago	70/197
1970	John Hancock Center	Chicago	100/344(roof)
1972	Transamerica Pyramid	San Francisco	48/260
1973	330 North Wabash (formerly IBM Plaza)	Chicago	52/212
1973	Aon (formerly Amoco) Center	Chicago	83/346
1974	Willis (formerly Sears) Tower	New York	108/442
1977	Citigroup (formerly Citicorp) Center	New York	59/279
1980	55 West Monroe (formerly Xerox Center)	Chicago	41/150
1983	333 South Wacker Drive	Chicago	36/149
1986	Onterie Center	Chicago	60/174

Figure 2.15
860-880 Lake Shore Drive Apt in 1949

Figure 2.16
Lever House in 1952

Figure 2.17
Marina City in 1964
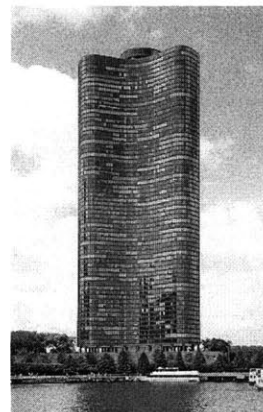
Figure 2.18
Lake Point Tower in 1968
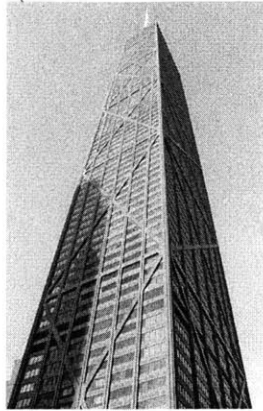
Figure 2.19
John Hancock Center in 1970

Figure 2.20
330 North Wabash in 1973
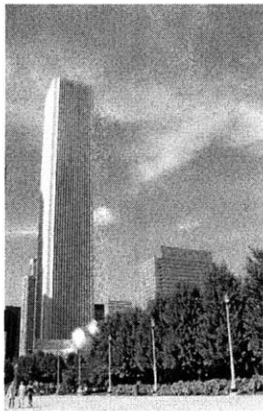
Figure 2.21
Aon Center in 1973

Figure 2.22
Citigroup Center in 1977

Figure 2.23
333 South Wacker Drive in 1983
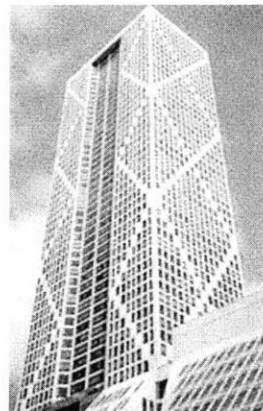
Figure 2.24
Onterie Center in 1986

2.4 The Third Golden Age in Tall Buildings (1980-Now).

Since the steel-skeletal system was first introduced in the Home Insurance Building in the 1880s, it has made a significant advancement in tall buildings. In addition, this advancement has currently been made possible along with the advanced structural systems and higher grade of materials, increased use of computerization in the design process, active and passive control systems, enhanced wind tunnel tests, and improved construction technology. For example, the diagonalized system, or braced tube system, first introduced in the John Hancock Center began to give considerable potential for super tall buildings to utilize various forms (Iyengar S.H., 1997). Following this diagonalized system, various systems such as Space Truss Structure, Megaframes, and Exo-Skeleton systems, are introduced. These systems show considerable efficiency in resisting lateral shear, producing flexibility and aesthetics in shapes of tall buildings. With the advancements in materials and structural systems, a movement known as post-modernism became prevalent in this period. The shapes of the buildings designed in post-modernism are setbacks, tapering, curvilinear, corner-modified, and helical (Aysin 2009). Therefore, the tall buildings at that time have free forms which were significantly distinct from the regularity convention long observed since 1880s. In fact, chief amongst reasons is the technological stride by which tall buildings can access to the free-style forms in the exuberant and liberal atmosphere. One of the most conspicuous shapes is 30st. Mary Axe which utilized diagrid system. It is worthwhile to note that diagrid, relatively recently recognized, creates new architectural aesthetic expressions with strengthening both bending and shear rigidity. Examples of this system are 42-story Hearst Building, 41-story Swiss Re Building, and 22-story O-14 Building.

This recent developments in the shape of tall buildings are due to the profound consideration on the inter-relationship between structural evolutions and architectural aesthetic forms. With analytical ability in computer and wind tunnel test, expression on exterior shape is given more flexibility. This flexibility provides more discretionary power to designers and makes the form possible. Moreover, tall buildings in this period adopted

various design motifs from historical, regional, cultural and imaginary contexts as well as aerodynamic forms. As example of tall buildings expressing their cultural tradition, Petronas Towers, Landmark Tower, Taipei 101 can be mentioned. Also, main examples of tall buildings having aerodynamic forms are the Shanghai World Financial Center, Guangzhou Pearl River Tower (expected in 2011), and the Kingdom Center. Another form in this period is a twisted, helical form such as Turning Torso and proposed Chicago Spire Project. More aggressive than aerodynamic and twisted or helical forms, numerous free-style forms of tall buildings have recently been designed and even actually constructed. Among several structural systems which made this freestyle forms possible, Diagrid is currently utilized to make this irregular form feasible. Fiera Milano, Oil Company Headquarter, Dancing Tower, The Sail at Marina Bay, and Phare Tower are, though proposed and not actually constructed, exemplified by free-form tall buildings (Ali M.M., 2007).
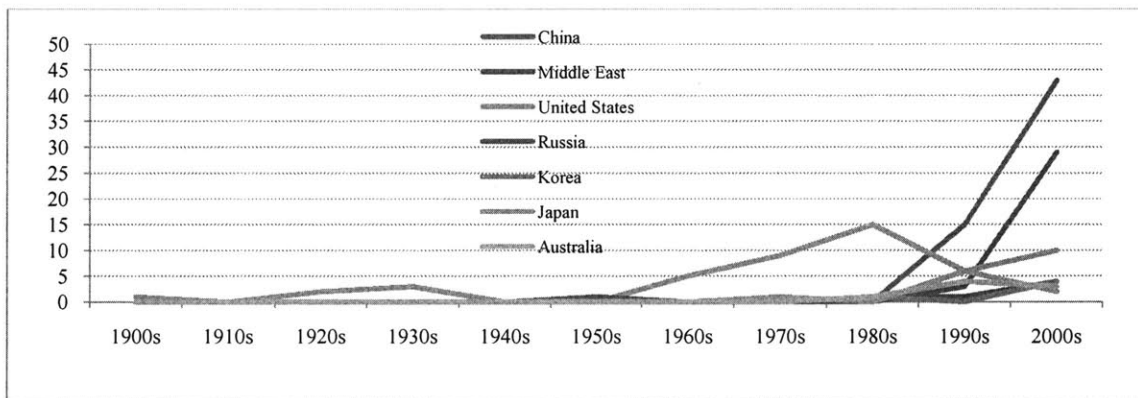
Figure 2.25 World's 200 Tallest Buildings by Region (Emporis 2011)

In fact, Starting from the 1990s, the fourth boom (the first boom between the 1880s and the 1900s, the second one between the 1910s and the 1930s, and the third one between the 1950s and the 1970s) in tall buildings has revived in Figure 2.25. Although the East Asian countries, such as Hong Kong, Malaysia, South Korea, Singapore and Vietnam, severely suffered from the economic disaster in the late 1990s, the race for height seems to be unstoppable and increasingly intense. Even at the time when Japan was in recession and stagnation during the 1990s, it has expended into Asia and Middle East. Now that symbolic power can be compatible with free-style forms of tall buildings, these forms

have been predominant. To continue this trend flourish, more research on wind engineering as well as damping mechanism should be explored.

Table 2.3 List of Tall Buildings in 1980-

Completion	Building	City	Stories/ Meter
1980	Tower 42 (The National Westminster Bank)	London	47/183
1983	Bank of America (formerly RepublicBank) Center	Houston	56/240
1983	One Magnificent Mile Building	Chicago	57/205
1984	Sony (formerly AT&T) Tower	New York	37/197
1985	HSBC Main Building	Hong Kong	44/179
1987	190 South La Salle Street Building	Chicago	40/175
1987	CitySpire Center	New York	72/248
1988	1201 Third Avenue (Washington Mutual Tower)	Seattle	55/235
1988	Maybank Tower	Malaysia	50/244
1989	900 North Michigan	Chicago	66/265
1989	Bank of China Tower	China	70/369
1989	60 Wall Street – JP Morgan Bank HQ	New York	50/227
1990	Two Prudential Plaza	Chicago	64/303
1990	311 South Wacker Drive	Chicago	65/293
1990	BNY Mellon Bank Center	Philadelphia	54/241
1990	Bank of China Tower	Hong Kong	72/315(roof)
1991	One Canada Square	London	50/230
1992	Central Plaza	Hong Kong	78/309(roof)
1992	Bank of America Corporate Center	Charlotte	60/265
1993	Yokohama Landmark Tower	Japan	70/296(roof)
1995	China Merchants Tower	China	38/150(roof)
1995	Osaka Prefectural Government Sakishima	Japan	55/256
1996	King Tower	China	38/212
1997	Baiyoke Tower II	Thailand	85/304
1998	Petronas Towers	Malaysia	88/379(roof)
1999	Yuda World Trade Center	China	45/200
1999	Jin Mao Tower	China	88/370(roof)
1999	China Insurance Building	China	38/175(roof)
2000	Capital Tower	Singapore	52/254
2000	Emirates Office Tower	UAE	54/311(roof)

2003	1 Peking Road	China	30/160(spire)
2004	Taipei 101	Taiwan	101/449(roof)
2004	30 St Mary Axe	London	40/180
2006	Hearst Tower	New York	46/182
2006	Turning Torso	Sweden	54/190
2007	The New York Times Building	New York	52/228(roof)
2008	Shanghai World Financial Center	China	101/484(roof)
2010	Burj Dubai	UAE	163/828(roof)
2010	Blue Cross Shield Tower	Chicago	57/243(roof)
on hold	Plaza Rakyat	Malaysia	79/382
under const.	Pearl River Tower	China	71/310(roof)

Figure 2.26
Tower 42 in 1980
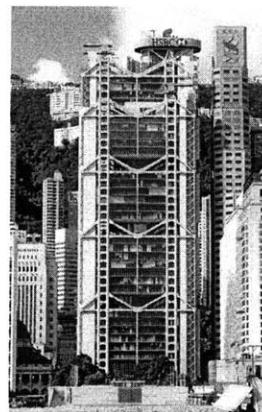
Figure 2.27
HSBC Main Building in 1985
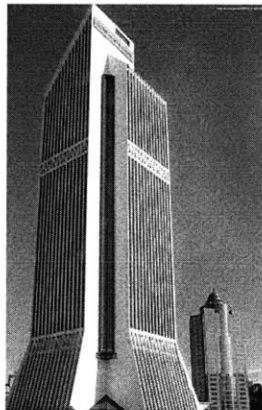
Figure 2.28
Maybank Tower in 1988

Figure 2.29
900 North Michigan in 1989

Figure 2.30
Two Prudential Plaza in 1990

Figure 2.31
Yokohama Landmark Tower in 1993

Figure 2.32
Petronas Towers in 1998

Figure 2.33
Jin Mao Tower in 1999

Figure 2.34
Al Faisaliah Center in 2000

Figure 2.35
30 St Mary Axe in 2004
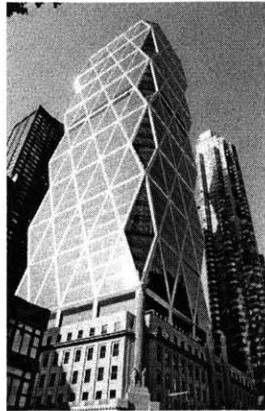
Figure 2.36
Hearst Tower in 2006
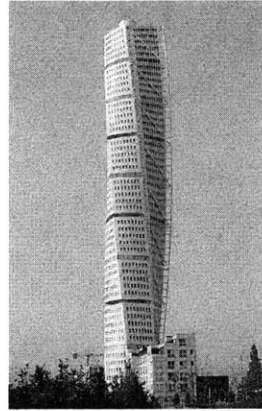
Figure 2.37
Turning Torso in 2006

Figure 2.38
Shanghai World Trade Center in 2008
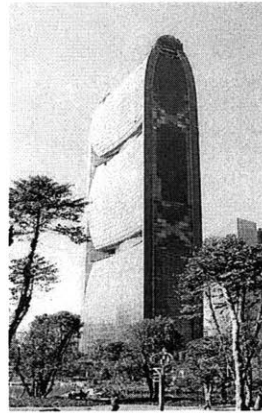
Figure 2.39
Pearl River Tower under Cons.

2.5 References

Ali M.M. and Moon K.S., Structural Developments in Tall Buildings: Current Trends and Future Prospects, Architectural Science Review, Volume 50.3, PP.205-232.

Iyengar S.H., 1997, Tall building Systems for the Next Century, Structures in the new millennium, Lee (ed.) 1997, pp.19-30.

Moon K.S., 2005, Dynamic Interrealationship Between Technology and Architecture in Tall Buildings, Ph.D. Dissertation, MIT

Willis, C., 1995., Form Follows Finance: Skyscrapers and Skylines in New York and Chicago, Princeton Architectural Press, New York

Gunel M.H. and Ilgin H.E., 2007, A Proposal for the classification of structural systems of tall buildings, Building and Environmental 42 (2007) 2667-2675.

Aysin SEV. 2009, Typology for the Aesthetics and Top Design of Tall Buildings, G.U. Journal of Science, 22(4): 371-381.

Mark Thornton. 2005, Skyscrapers and Business Cycles, the journal of Austrian Economics, Vol. 8, No. 1, Spring 2005.

Chapter 3 Wind-Related Issues with Construction of Tall Building

3.1 Introduction

Tall buildings have more disadvantages than lower ones. The construction cost of taller ones is considerably larger and the design of them is also much more difficult. Moreover, several constraints on tall buildings such as zoning laws can be a burden. However, these drawbacks can easily be overwhelmed by the symbolic power tall buildings provide. The shapes adopted in design of tall buildings have traditionally been symmetric rectangular, circular or triangular prisms because this design little causes torsional vibrations induced from eccentricity. However, recent high-rise buildings pursuit free-style forms completely distinct from symmetry shapes. This is due to the fact that architects, clients and engineers all demand for revolutionary and innovative forms of tall buildings along with the advancement in technology. In addition, since the threshold of the free-style period, irregular and unsymmetrical buildings have been fervently proposed and currently constructed. Although the current technology appears to sufficiently predict and prevent the adverse responses of tall buildings induced by the wind, some problems such as habitability have been unavoidable. Moreover, the residential type of tall buildings built since the 1990s has increased substantially, as shown in Figure 3.1. This means the importance of habitability issue cannot be ignored.
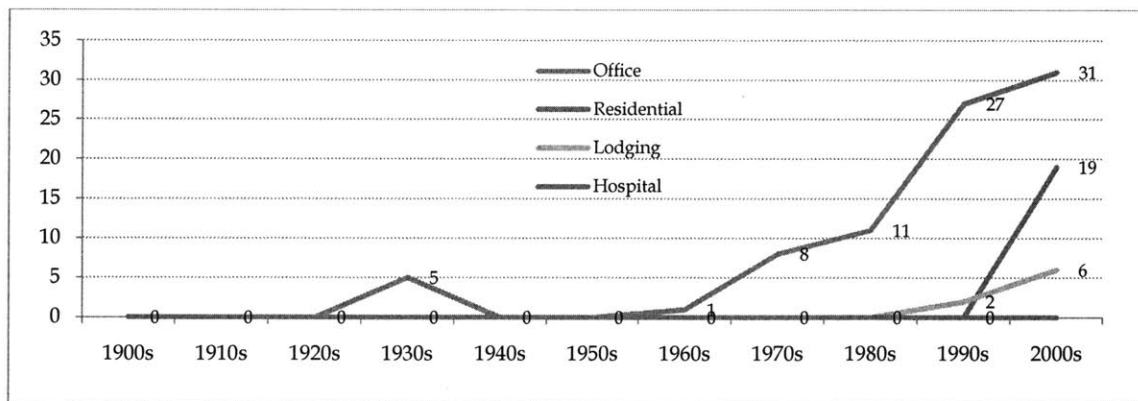
Figure 3.1   Buildings equal to and higher than 250m by Usage (Emporis 2010)

Therefore mitigation of wind responses of tall buildings has also been of keen interest, for chief amongst the wind related problems is the habitability in residential buildings. With highly advanced damping and structural systems, structural safety against lateral loads has been guaranteed. However, issues, such as serviceability, interference effect between buildings, built environment for pedestrians, and wind-induced noise, still remain to be solved. Wind-induced responses cause various problems to structural frames, cladding systems, equipment and importantly occupants as shown in table 1. To mitigate these issues, quantitative criteria and other systems must be considered and adopted.

Table 3.1 Problems to be suppressed relevant to wind-induced responses (Tamura 1998)

Physical item	Purpose	Building or equipment
Displacement, rotation	Safety	High-rise buildings, long-span buildings, expansion joints
Inter-story deformation	Serviceability	Elevators, antennae, furniture, cranes
	Safety	High-rise buildings
	Serviceability	Cladding, interior walls, equipment piping, expansion joints
Acceleration	Safety	Furniture, occupant
	Serviceability	Equipment, elevators
	Habitability	Hotels, residential buildings, high-rise office buildings

3.2 Habitability

The purpose of structural design is to effectively and efficiently resist lateral and gravitational loads in structures. Moreover, tall buildings are expected to meet wind-induced drift- serviceability and acceleration-occupant comfort criteria (Bashor, 2007). However, a tall building is much more susceptible to wind responses because of its lower damping and higher flexibility than general buildings. Although multiple damping systems are applied to tall buildings for satisfactorily mitigating motions caused by the wind, the complex modes of vibrations, which are induced by along-wind, across-wind and torsion, adversely affect the serviceability for occupants. Because this oscillation can be generated due to the irregularities in mass and stiffness, the subject of considerable attention is the issue of the habitability and the quantification of acceptable level for occupant comfort in

the era of freely shaped tall buildings. In fact, Drift criteria is not solely an adequate index to govern the habitability limit states in tall buildings in which occupants can feel the limit of tolerance, or discomfort, under fluctuating accelerations in the strong wind (Kijewski – Correa 2009). Therefore, wind-sensitive buildings can be vulnerable to excessive vibrations that cause discomfort and interruption of activities of occupants. To deal with this subject, several guidelines have been introduced: ISO6897 (1984), BS6841 (1987), ECCS (1987), NBCC (1990), ISO2631-1 (1997), AIJ-Guidelines (2004), and ISO10137 (2007). Among them, AIJ-Guidelines and ISO10137 use 1-year recurrence peak acceleration, while ISO6897 employs root mean square (RMS) value to evaluate habitability under lateral vibrations of tall buildings (Tamura, 2009). In detail, motion perception criteria based on frequency of 5-year recurrence standard deviation acceleration, or root mean square, have been adopted in ISO6897 (1994) for low frequency motion ranging from 0.063 to 1 Hz. On the other hand, Peak acceleration criteria related with strong winds, such as extreme windstorm or cyclones, have also established numerous contemporary design codes. To illustrate, the peak acceleration criteria of 15 milli-g for residential buildings and 25 milli-g for commercial buildings under 10-year return period of wind conditions are recommended in the Canada code (NBCC 1995), the Chinese code (JGJ 3-2002), and the Hong Kong code (HKCOP 2005). Based on experimental motion simulator research, the Japanese code, AIJ-GEH 2004 provides frequency dependent peak acceleration criteria (Chan 2010). The standard deviation acceleration and peak acceleration are two significant factors in assessing motion perception of vibrations in tall buildings. Generally, the motion perception can be more influenced by long duration events of a stationary vibration leading to the fact that the standard deviation acceleration can be a more reasonable index. Nevertheless, under the thunderstorms and hurricanes, this root mean square value over 10 minutes of this non-stationary motion is inappropriate. Therefore, one of these two criteria can be considered, with understanding on the nature of prevailing winds influenced by the topology and geography on which a tall building is located (Chan 2010). However, unfortunately, habitability issue is closely related to psychological situations for occupants in tall buildings. Moreover the criteria for occupant comport have not been free from

debate so far. This is due to the uncertainty and complex in human perception of motion, accurately acceleration. Furthermore, discrepancy among individual human perceptions on motion can be wide, according to visual, acoustic, posture effects and mental and physical effects and other social and economic conditions (Tamura, 2009). Therefore, finding more clear criteria for qualifying accelerations which negatively impact occupants still remains a daunting work. Since Reed first experimented on human responses under full-scale conditions in 1971, numerous studies have been performed. These previous works generally are divided into three types of studies which are the first, field experiments and surveys of building occupants conducted in tall buildings induced by wind excitation; the second, motion simulator and shake table experiments to evaluate test subjects; and the last, field experiments performed in artificially excited buildings (3) (Kwok, 2009). In the first, field experiments and surveys of building occupants conducted in tall buildings induced by wind excitation, Denoon (2000) conducted field experiments at three towers to assess occupant reaction to wind-induced vibration of buildings. The survey investigated that motion perceptions are dependent on peak accelerations and also evaluate the thresholds of motion perception, annoyance levels and onset of fear and nausea. This work suggests that exposure duration and vibration waveform play an important role in human perception of motion and tolerance threshold. Moreover, it indicates that the acceptance criteria should be based not on occupant perception of vibration but on occupant comfort and general well-being with the assessment of occupant comfort in tall buildings excited by the wind (Kwok, 2009). In the second, motion simulator and shake table experiments, Michaels (2009) reported on empirical results form a series of experiments by motion simulators. This work suggested that the comfort level, under bi-directional narrow-band random motion, was dependent on the increasing frequency of motion, acceleration and duration. As the frequency increases, the number of test subjects who became nauseated, fatigued and distracted also increases. More interestingly, the number of test subjects who felt these symptoms at 0.50 Hz is more than twice than at 0.16Hz. In the last, field experiments performed in artificially excited buildings. Kijewski-Correa (2009) evaluated occupant comfort by comparing the full-scale accelerations form an instrumented tall building with the results from motion simulators which involved the effect of frequency,

amplitude, duration and waveform on human group. The study catalogued the number of full-scale occurrences of short duration events that can be task disruptive and long ones that can be nauseating in motion simulator studies. In addition, it presented the number of occurrences annually and the percentage of occupants likely affected. Bashor (2007) presented a probabilistic framework to evaluate occupant-comfort performance of a building at different recurrence interval winds including parametric uncertainties such as damping and wind speed. To better evaluate the effect of such uncertainties on occupant comfort, the paper used FORM based analysis and Monte Carlo simulation. It also proposed the checking procedures based on occupant comfort for evaluating habitability of tall buildings. Since the work by Reed (1971), much research on human perception has been performed. However, because of the fact that human perception and tolerance of the response of tall buildings induced by wind excitation are subjective, there have been no clearly accepted criteria for occupant comfort (Kwok, 2009). However, the research on human perception of wind induced vibration in tall buildings is still an active topic, and therefore it is expected to develop more practical and reasonable code for occupant comfort in the near future.

3.3 Pedestrian level winds

Many factors affect the wind conditions around a tall building, some of which are the local topology, local climate, building height and mass, local vegetation, the proximity of other tall buildings. In addition, the construction of a building unavoidably leads to changes of the climate at the environs of the building: in specific, wind speed, wind direction, air pollution, radiation and daylight, and driving snow and rain. These factors are dependent on the shape, size, and orientation of the building and the interaction of the building with neighboring buildings and obstacles such as trees (Blocken 2004). Cochran (1979) reported a wind environment around the base of a building will depreciate the attraction of the building and estrange the perspective residents and clients of the buildings, for example, leading to unsuccessful outdoor restaurants and cafes nearby the base of tall

buildings. To (1995) investigated wind environment around the base of a row of identical tall buildings through wind-tunnel experiments. This paper presented the results of pedestrian-level winds of three test cases: case 1, isolated building; case 2, four buildings arranged in a row, and wind flow direction perpendicular to the row; and case 3, wind flow along the row of four buildings. The results attained in this test show the distribution of mean wind speed for three cases, with use of the reference wind speed of the approaching flow at the building-roof height. In case 1, it is observed that a region of high pedestrian-level wind ,the speed of which is 1.2 times more than the reference speed (RWS), extends from the upwind corners. In case 2, the windiest conditions occur in the upwind corners with the speed 1.3 times more than the RWS, which is like in case of the isolated building. In case 3, wind pattern, around the most upstream building, the first building, is somewhat similar from those of the isolated building in case 1. Around the second and other downwind buildings, the regions of high pedestrian-level wind speeds are not detected at their upwind corners. This is due to the strong shielding provided by the first building. Large velocity gradients are detected for all buildings at the downwind corners, but low pedestrian-wind speed is observed in the regions behind the buildings. Penwarden (1975) suggests The Beaufort Scale shown in Table 4, which classifies the speed effect on pedestrian; the wind speed is averaged in 10-minute interval at 10 m height above the ground. Davenport adopts the criteria in Table 2 for the situation considered, which indicates several activities such as sitting, standing and walking in different areas. To illustrate, the main activities in an outdoor restaurants or café only need to sit or stand for a long time; therefore, the tolerable wind speed can be up to 3.4-5.4 m/s (or Beaufort number 3), and the frequency can be less than once a week. If the wind speed is between 8.0-10.7 m/s, the frequency should be less than once a month. These criteria by Davenport suggest that the evaluation of the pedestrian wind should not be based on the extreme weather conditions (Wang 2004). Ahuja (2006) assesses through wind tunnel test the wind comfort and safety of pedestrian area around a building. The paper mentions that there are two principal types of flow that affect the pedestrian comfort: downwash flow brings higher energy wind to lower elevations and horizontally accelerated flow. Therefore, it suggests the remedial methods to reduce this effect by providing a large canopy at the

main entrance and a podium on which a building is constructed for comfortable pedestrian-wind condition.

Table 3.2 Summary of wind effects on people based on the Beaufort Scale

Beaufort number	Description	Wind Speed (m/s)	Effect
0,1	Calm, light air	0-1.5	Calm, no noticeable wind
2	Light breeze	1.6-3.3	Wind felt on face
3	Gentle breeze	3.4-5.4	Wind extends light flag
			Hair is disturbed, Clothing flaps
4	Moderate breeze	5.5-7.9	Raises dusts, dry soil and loose paper, Hair disarranged
5	Fresh breeze	8.0-10.7	Force of wind felt on body
			Drifting snow becomes airborne
			Limit of agreeable wind on land
6	Strong breeze	10.8-13.8	Umbrellas used with difficulty
			Hair blown straight, Difficult to walk steadily
			Wind noise on ears unpleasant, Windborne snow above head height (blizzard)
7	Near gale	13.9-17.1	Inconvenient felt when walking
8	Gale	17.2-20.7	Generally impedes progress, Great difficulty with balance in gusts
9	Strong Gale	20.8-24.4	People blown over by gusts

Table 3.3 Tentative comfort criteria (unit: Beaufort number)

Activity	Area applicable	Relative comfort		
		Tolerable	Unpleasant	Dangerous
Walking fast	Sidewalks	6	7	8
Strolling, skating	Parks, entrances, skating rinks	5	6	8
Standing, sitting-short exposure	Park, plaza area	4	5	8
Standing, sitting-long exposure	Outdoor restaurants, bandstands, theatres	3	4	8
Representative criteria for acceptability		<1 occasion/week	<1 occasion/month	<1 occasion/year

3.4 Wind-Induced Noise

Generated from the corners, the cladding systems, the ventilating openings of a tall building, wind-induced noises can have an adverse effect on serviceability, especially occupants in residential buildings (Tamura 2009). Moreover, the desire for increased natural ventilation, even in a tall and green building, can degrade the acoustic performance of facades, leading to producing additional noise sources located in and nearby the façade of the building (Swift 2008). In addition, As previously mentioned by Diemling in 1983, aesthetic elements like ornaments, coronets, gird, steel pipes, and structural or functional elements like solar lamella shields, external rigidity frames can cause the wind to make noise. As a recent example, the coronet of the Strijkijzer tower 130- meter high in Hague was enforced to be shrouded with plywood to reduce the sound level (Vambersky 2008). Therefore, prediction and mitigation of wind-excited noise on buildings, especially residential tall buildings, should be considered even in the process of architectural and structural design. This wind-related noise issue has been of particular interest to many researchers since Curle mentioned this issue in 1955. With reviewing the noise transmission issues across facades on green buildings, Swift (2008) mentions that it is possible that a noise problem may occur in a place where there are repetitive geometric elements, such as sunshade element, louvers, decorative meshes and gratings, exposed on a building. It proposes that the potential for generating disturbing noise can be reduced by modifying the repeating elements into a more random pattern. Kim (2009) compares, in the peak of SPL (Sound Pressure Level), experiment results and numerical simulation ones for three types of building shape: circular, rectangular and triangular. It identifies the peak SPL in circular > in rectangular > in triangular, which means that different angles can also produce distinct SPLs. Recent research on wind-excited noise has been conducted through CFD analyses.

3.5 Interference Effect

The response of an isolated tall building by wind excitation is considerably distinct from that of a tall building adjacent to other buildings or structures. Such influence by these neighboring buildings is generally known as interference effect, which depends on the shape, arrangement and orientation of the buildings with the direction of wind and its topology (Khanduri 1997). Therefore, newly constructed buildings often have more adverse effects upon the wind loading on the existing buildings, for cities become denser nowadays; moreover, new buildings higher than other existing ones more contribute to this effect (Uffelen 2009). The study on this issue is not a recent one. In fact, interference effect has been interested since the 1930s when the tallest buildings such as Empire State building and Chrysler Building were built. With wind tunnel experiments, Harris (1934) mentioned that if two building blocks were built across the two streets adjacent to the building, torque on the Empire State building in New York would be doubled. Bailey (1942) studies on general relationship between the wind speed and the distribution of wind pressure on three distinct roof shapes: sloped, flat, and stepped roofed buildings. In 1965, three out of the eight natural draft cooling towers at Ferrybridge, England were collapsed due to interference effects, which draw attention on this issue from many researchers (Armitt 1980). Kareem (1987) investigates the interference effects on the dynamics of bluff bodies of equal height and plan dimensions in two approach boundary layers. It identifies that the magnitude of the localized fluctuating pressure on buildings may be influenced differently under distinct boundary conditions.
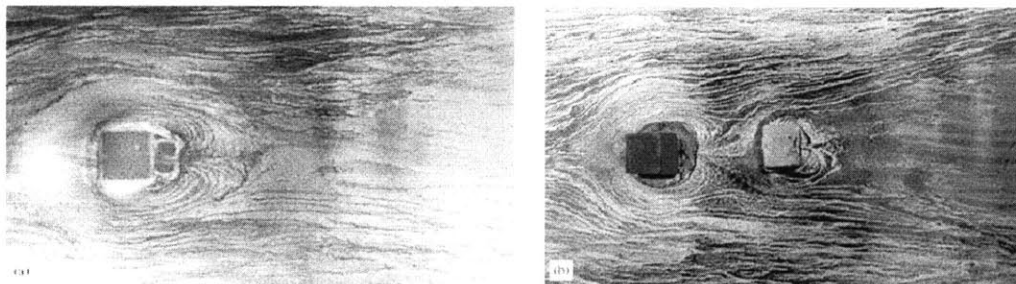
Figure 3.2 Flow around a building (a) and a pair (b), win flowing from the left side (Khanduri 1997)

The Austrian Standard 1989 presents a brief guideline on this issue that flow around any structure in a group will usually differ from flow around a similar isolated one, and interference effects are prevalent in structures located less than 10b apart, where b is the dimension of the structure normal to the wind (AS 1170.2). Khanduri (1997) presents that an upstream taller building more significantly affects downstream buildings than in the reverse case: with reduction of mean along-wind loads but increase of dynamic loads by more than 70% for taller upstream buildings. Moreover, it observes that interference effects are more pronounced in open country exposure while they are gradually decreased in suburban or urban exposure; buildings positioned along open spaces like deserts, park or coastal areas are more vulnerable to interference effects. Also, it shows the case of shield effects, in which with a large group of buildings of significant sizes, the wind loadings of a building can be decreased. As shown in Figure 1, Khanduri (1998) discussed the physical mechanism underlying wind interference. It shows turbulent eddies separate from the upwind building at the corners and edges of the building, then hitting the existing downwind building with overpressure increasing. As mentioned in the report by Taniike (1992), if the buildings are not positioned right behind each other, unlike in figure 1, the flow released from the new building can be forced through the space between the buildings and then generates increasing suction at the flank of the existing one, leading to a cross force. This uneven, partial shielding can induce torsion moments around the vertical center line of the existing downwind building. This effect are related with the height of the new building; if the height of the new one is significantly high, wind from higher layers can be forced downwards, or downwash, causing a further increase of the wind loads which acts upon the downwind, existing building (Uffelen 2009). In addition, such interference can be influenced by the distance between buildings. The wind interference can be negligible at very small mutual distance between buildings. This is a reason that the vortex shedding of the upwind building can be disturbed by the presence of the downwind building. The wind flow grows less organized; large eddies have difficulty being into smaller ones that have a higher angular velocity. Therefore, it is unlikely that higher peaks be generated (Uffelen 2009). Recently, Xie (2007) investigates, through a series of wind tunnel tests analyses by correlation and regression methods, effect of the

upstream terrain conditions, the relative heights of the interfering buildings, and the spacing between two and three buildings. This study shows that the two upstream buildings can more adversely affect the principal buildings than a single upstream one. It further finds that two interfering buildings can generate stronger along-wind dynamic interference effects than a single one, but induced by two interfering buildings, the dynamic interference effects in the across-wind direction may be weaker than by a single interfering building. As identified by many researchers, higher interfering building has stronger effects on the principal buildings while in the case that the height ratio of the interfering buildings to the principal building is less than 0.5, this effect can be negligible. It proposes the simple regression equations which reflect the relationship, inherently complex, in the mean and dynamic interference factors for different configurations of height ratios and upwind terrains. Systematic scientific research on interference still requires more generalized data. Furthermore, long lasing on-site measurements are considerably significant to enhance the reliability of wind tunnel tests and computer simulation results on wind interference.

3.6 References

Habitability

Tamura Y. 2009, Wind and Tall Buildings, EACWE 5 Florence, Italy, July 2009.

Tamura Y. 1998, Application of Damping Devices to Suppress Wind-Induced Responses of Buildings, Journal of Wind Engineering and Industrial Aerodynamics, 74-76 (1998), pp.49-72.

Amin J.A. and Ahuja A.K., 2010, Aerodynamic Modifications to the Shape of the Buildings: A Review of the State-of-the-Art, Asian Journal of Civil Engineering (Building and Housing) Vol. 11, No. 4 (2010)

McNamara R. et al., 2002, "Perception of Motion Criteria for Tall Buildings Subjected to Wind: A Panel Discussion".

J.W. Reed. (1971). "Wind induced motion and human comfort", Research Report 71-42, Massachusetts Institute of Technology.

Melbourne W.H. and Palmer T.R. 1992, Accelerations and Comfort Criteria for Buildings Undergoing Complex Motions, Journal of Wind Engineering and Industrial Aerodynamics, 41-44 (1992) 105-116.

Kijewski-Correa T. et al. 2009, Pseudo-Full-Scale Evaluation of Occupant Comfort in Tall Buildings, 11th Americas Conference on Wind Engineering, 2009.

Michaels M.N. et al. 2009, Human Body Response to Low Frequency Narrow Band Random Building Motions, The Seventh Asia-Pacific Conference on Wind Engineering, 2009.

Bashor R. and Kareem A. 2007, Probabilistic Performance Evaluation of Buildings: An Occupant Comfort Perspective, ICWE12 Cairns 2007.

Kwok K.C.S., Hitchcock P.A. et al. 2009, Perception of Vibration and Occupant Comfort in Wind-Excited Tall Buildings, Journal of Wind Engineering and Industrial Aerodynamics 97 (2009) 368-380.

Denoon R.O. et al. 2000, Field experiments to investigate occupant perception and tolerance of wind-induced building motion, Research Report No. R803, Department of Civil Engineering, University of Sydney, Australia.

Pedestrian level winds

Cochran L. 2004, Design Features to Change and/or Ameliorate Pedestrian Wind
  Conditions, Structures Building on the Past: Securing the Future Proceedings of
  Structures Congress, ASCE 2004.

Tamura Y. 2009, Wind and Tall Buildings, EACWE 5 Florence, Italy, July 2009.

To A.P. and Lam K.M. 1995, Evaluation of Pedestrian-level Wind Environment around a
  Row of Tall Buildings Using a Quartile-Level Wind Speed Descripter, Journal of Wind
  Engineering and Industrial Aerodynamics 54/55 (1995) 527-541.

Blocken B. and Carmeliet J. 2004, Pedestrian Wind Environment Around Buildings,
  Journal of Thermal Envelope and Building Science 28(2): 107-159.

Shiau B.S. and Tsai B.J. 2009, Wind Tunnel Measurement and Assessment on the
  Pedestrian Wind Environment, 10th International Conference on Fluid Control,
  Measurements, and Visualization, 2009, Moscow, Russia

Penwarden AD, Wise AFE. 1975, Wind Environment around Buildings. Building
  Research Establishment Report, HMSO.

Davenport AG, 1972, An approach to human comfort criteria for environmental Wind
  Conditions, CIB/WMO Colloquium on Building Climatology, Stockholm.

Wang B.M. 2004, Evaluation of pedestrian winds around tall buildings by numerical
  approach, Meteorology and Atmospheric Physics 87, 133-142.

Ahuja R., Dalui S.K. and Gupta V.K. 2006, Unpleasant Pedestrian Wind Conditions
  Around Buildings, Asian Journal of Civil Engineering, Building And Housing Vol.7,No.2,
  pp.147-154

Wind-Induced Noise

Fricke F.R. 1972, Noise Inside Buildings due to External Air Flows, Applied Acoustics,
  VOL 5, Issue 3, 1972, pp. 223-235.

Curle N. 1955, The Influence of Solid Boundaries Upon Aerodynamic Sound, Proceedings
  of the Royal Society of London, Series A, Vol. 231, No. 1187, pp.505-514

Swift P.B. 2008, Noise and Vibration Sources and Mitigation in Green Buildings, CTBUH

8th World Congress 2008.

Kim Y.D. et al. 2009, A Study on Numerical Simulation on Flow-Fields & Wind-Induced Noise Around Buildings, The Seventh Asia-Pacific Conference on Wind Engineering, 2009.

Vambersky J. 2008, Wind-Induced Sound Produced by High Buildings, Building Physics and Technology: Wind, 2008.

Diemling A. et a.. 1983, Wind-Induced Vibrations of a Façade Element, Journal of Wind Engineering and Industrial Aerodynamics, 11 (1983) 133-148.

Interference Effect

Khanduri A.C. et al. 1998, Wind-Induced Interference Effects on Buildings, Engineering Structures, Vol. 20, Issue 7, pp. 617-630.

Minimum Design Loads on Structures (SAA Loading Code), Part 2: Wind Loads, AS 1170.2, Standards Association of Australia, North Sydney, Australia, 1989.

Harris C.L. 1934, Influence of Neighboring Structures on the Wind Pressure on Tall Buildings, Part of Bureau of Standards Journal of Research, Vol. 12, 1934, 12, 103-118.

Bailey A. and Vincent N.D.G., Wind Pressure on Buildings including Effects of Adjacent Buildings, Journal of the Institute of Civil Engineering, 19-20, I, November 1942.

Armitt J., Wind Loading on Cooling Towers, Journal of Structural Division, Vol. 106, No.3, 1980, pp.623-641.

McLaren F.G. et al.1971, The Interference Between Bluff Sharp Edged Cylinders in Turbulent Flows Representing Models of Two Tower Buildings closed together, Technical Note, Building Science 6, 1971, 273-274.

Taniike Y. 1992, Interference Mechanism for Enhanced Wind Forces on Neighboring Tall Buildings, Journal of Wind Engineering and Industrial Aerodynamics, Vol. 42, Issues 1-3, 1992, pp. 1073-1083.

Kareem A. 1987, the Effects of Aerodynamic Interference on the Dynamic Response of Prismatic Structures, Journal of Wind Engineering and Industrial Aerodynamics, Vol.25, Issue 3, pp. 365-372.

Uffelen G.M. 2009, Wind-Induced Building Interference: Increase of Wind Loads on

Existing Buildings after Erection of New High-Rises, EACWE 5, Italy, 2009.

Xie Z.N., Gu M. 2007, Simplified Formulas for Evaluation of Wind-Induced Interference Effects among Three Tall Buildings, Journal of Wind Engineering and Industrial Aerodynamics, 95 (2007) 31-52.

Davenport A.G., 2002, Past, Present and Future of Wind Engineering, Journal of Wind Engineering and Industrial Aerodynamics, 90 (2002), 1371-1380.

Chapter 4 Monitoring

4.1 Introduction

Recently, along with the development in computer, more advanced structural analysis software and wind tunnel test have introduced. However, the design of tall buildings based on this technology depends to a large extent on the several assumptions like fundamental mechanics and accumulated experiences. Therefore, the performance of tall buildings constructed in this way can affect the serviceability and occupant comfort because the precise values of parameters in structures such as damping cannot be predicted before the construction. Therefore, the accuracy and validity of analytical results should be assessed with respect to actual performance of tall buildings (Kijewski-Correa 2006). Nevertheless, the experiment on full-scaled model is so limited, so full-scale monitoring of the performance of actual tall buildings already built becomes the pragmatic means for verifying and improving analytical practices. Moreover, with advances in technology, the instrumentation systems used for full-scale monitoring have improved. These systems involve accelerometers, strain gauges, inclinometers and global positioning systems (Isyumov, 2010).

4.2 Monitoring of the performance of actual buildings

This full-scale measurement has progressed since the 1930s. After the completion of the tower, Eiffel conducted a pioneer work on response monitoring at the top of the Eifel tower which was 300m high. The study of wind at this height was unprecedented. From the table 1, for the ratio of mean deflection to square of mean wind speed, the drag of the tower assumed in the design is of the order of 3.5 times the observed one. In addition, it shows the gust factors are of the order 1.4 to 1.7 (Davenport 1975).

Table 4.1: Deflection of Eiffel Tower in Wind (after Eiffel)

	Mean Wind speed /Direction	Mean Deflection cm	Dynamic sway		Gust Factor	Mean deflection/square of mean wind speed
			Drag (cm)	Lift (cm)		
Design	**24**	**20**				**0.035**
Observed:						
20 Dec 1893	31.8 SSW	7	±5	±3	1.71	0.007
12 Nov 1894	28.8 S	8	±3.5	±2	1.44	0.010

Arnstein in 1936 reported full scale measurements on the Akron airship dock which had the vaulted cross-section. The pressure of coefficients derived from a wind tunnel test is referenced to the same internal pressure coefficient. It observes that the peak negative sections are significantly less at full scale than at model scale while the positive pressures are similar (Davenport 1975). Dryden (1930) conducted the wind pressure study on circular cylinders and chimneys. Rathbun (1940) carried out full-scale experimentation on the Empire State Buildings. Many full scale measurements have been conducted since then. In recent, Li (2005) took the full-scale monitoring of typhoon effects on two super tall buildings: 78-story Central Plaza Tower (374m) in Hong Kong and 78-story Di Wang Tower (384m) in Shenzhen. It investigates the characteristics of typhoon-generated wind-induced vibrations of these buildings by comparing the dynamic characteristics of the buildings obtained through the field measurements with those calculated from computational models. Two accelerometers were installed orthogonally at the elevation of the 73rd floor of Central Plaza Tower and two Gill-propeller-type anemometers installed on the top of the building, approximately at 300m in height. Similarly, two accelerometers were orthogonally positioned at the height of 298m of DWT, and two same anemometers at an elevation of 247.5m. To sufficiently study wind-induced response characteristics, this installation is later added by two more anemometers on each building. the results of spectral analysis of acceleration response measured from CPT and DWT shows that the wind-induced responses of these buildings were primarily in the two fundamental sway

modes of vibrations, though higher modes are observed. In Table 2, the natural frequencies of the first three modes of CPT and Dwt buildings are listed both from the measured spectra and from the computational models of the same buildings.

Table 4.2: Natural frequencies (Hz) of the two buildings

	Frequencies (Mode 1, sway)			Frequencies (Mode 2, sway)			Frequencies (Mode 1, torsion)		
	Measu.	Calcu.	Diff.(%)	Measu.	Calcu.	Diff.(%)	Measu.	Calcu.	Diff.(%)
CPT	0.244	0.206	15.6	0.253	0.208	17.8	0.557	0.606	-8.08
DWT	0.173	0.168	2.9	0.208	0.181	13.0	0.293	0.286	2.45

Measu.=Measured, Calcu.=Calculated, Diff.=Difference=(Measured-Calculated)/Measured.

As shown in Table 2, the difference between the calculated and measured natural frequencies range from approximately 2.9 to 17.8% for the first and second modes of the buildings. Consequently, it is noted that the measured natural frequencies for the two fundamental sway modes of the buildings are larger than those calculated. As the reasons of these differences, Li (2005) pointed out the effective mass values of the buildings less than those assumed at the design stage and the effective stiffness values of the buildings higher than those determined at the design stage because of nonstructural components. As mentioned by Li (2005), Isyumov (2010) also indicates the discrepancies between calculated and monitored frequencies by listing some of the structural modeling assumptions: first, stiffness degradation of concrete structural members; second, Contribution of non-structural elements to building stiffness; third, Unpredictability of material properties under transient loading; and fourth, Soil-structure interaction. In the third case, it is noted that concrete, when loaded at an increase strain rate, exhibits a significant increase in both strength and stiffness (Isyumov 2010). Pauley (2002) finds that the increase in stiffness may be of the order of 16 % or more. Therefore, the third case can be explained from the fact that the effect of this increased stiffness has commonly been disregarded in practice of structural engineering. In the case of Soil-structure interaction, it is assumed that all buildings are supported on soil or rock strata not infinitely rigid. This

induces rigid body motions that are both linear and rotational at the foundation and the supporting soil interface. To illustrate, for a building propped up on piles, flexibility of the building is increased by the lateral stiffness of the pile assembly. Typical buildings are modeled on the assumption of a rigid foundation, leading to overestimating the frequencies (Isyumov 2010). Building monitoring programs generally initiate after construction of the main structure and the damping tanks completes. However, Isyumov (2010) utilizes this program, during the as-built periods when the building reached about 70% of its final height, in order to precisely predict the frequencies of vibration of the building. Rather than computational models based on numerous assumptions, such building monitoring program during the as-built periods can provide more accurate data, thus assuring a more effective design of tuned supplementary damping systems. Yigit (2010) investigates a 30-story tall reinforced concrete building used for a hotel in Turkey through the full scale measurement with GPS, inclination sensor and anemometer. Gikas (2009) observes dynamic measurement of displacement by utilizing RTS and TLS (robotic total station and terrestrial laser scanning) (Yigit 2010). In conclusion, full-scale measurement on an actual tall building directly shows its actual performance in terms of accelerations, which is significant for evaluating occupant comfort. In addition, this monitoring provides the opportunity to validate the modeling and design assumptions and enhance the existing accumulated databases such as damping levels (Kijewski-Correa 2006).

4.3 References

Kijewski-Correa T. et al. 2007, Dynamic behavior of tall buildings under wind: Insights from Full-Scale Monitoring, The Structural Design of Tall and Special Buildings, 471-486.

Davenport A.G. 1975, Perspectives on the Full-Scale Measurement of Wind Effects, Journal of Wind Engineering and Industrial Aerodynamics, 1, 23-54.

Campbell S. et al. 2005, Dynamic Characteristics and Wind-Induced Response of Two High-Rise Residential Buildings during Typhoons, Journal of Wind Engineering and Industrial Aerodynamics, 93, 6, 2005, 461-482.

Rathbun J.C. 1940, Wind Forces on a Tall Building, Transactions, American Society of Civil Engineers, Paper 2056, 105: 1-41.

Isyumov N. et al. 2010, Monitoring of Tall Buildings to Assist the Design of Supplementary Damping Systems, Structures Congress 2010, ASCE.

Paulay T. and Preistley M.J.N., 2002, Seismic Design of Reinforced Concrete and Masonry Buildings, John Wiley & Sons, INC., NY, 1992, 163p.

Kijewski-Correa T. et al. 2006, Validating Wind-Induced Response of Tall Buildings: Synopsis of the Chicago Full-Scale Monitoring Program, Journal of Structural Engineering, ASCE, 2006, pp.1509-1523.

Li Q.S et al. 2005, Full-Scale Monitoring of Typhoon Effects on Super Tall Buildings, Journal of Fluids and Structures 20 (2005) pp.697-717.

Yigit C.O. et al. 2010, Analysis of Wind-Induced Response of Tall Reinforced Concrete Building based on Data collected by GPS and Precise Inclination Sensor, FIG Congress 2010, Facing the Challenges – Building the Capacity, Sydney, 11-16 April 2010.

Gika V. 2009, Contribution of Combined RTS and TLS to Dynamic Monitoring of Wind Energy Turbines, International Conference on Optical 3-D measurement Techniques, Vienna, Austria, July 1-3.

Chapter 5 Effect of Shape Modifications of tall buildings on wind induced vibrations

5.1 Introduction

Some of the most relevant characteristics of structures which affect wind-induced structural vibrations are shape, stiffness or flexibility and damping. In the previous chapter, it is mentioned that damping is still a much more approximate characteristic in building while mass and stiffness as structural variables are in the high level of reliability. This chapter presents an overview and a summary of past and recent work on various aerodynamic modifications to the shape of the buildings. These modifications can be grouped into minor and major modifications. Minor modifications are aerodynamic ones which, to a minor extent, affect the structural and architectural design. As various aerodynamic modifications to corner geometry, chamfered corners or corner cut, corner recession, slotted corners, corner roundness, through opening, fitting of fins and vented fins are affiliated to such modifications. On the other hands, major modifications are aerodynamic ones which considerably affect the structural and architectural concept. Examples of these major modifications are belonged to by the modification of a tall building shape, addition of opening and vertical or horizontal slots to building, and twisting or rotating of a building. The detailed information about these two modifications is presented with the pictures of tall buildings later in this chapter. In fact, the purpose of all the modifications is to alter the flow pattern around a tall building and reduce the wind-incited vibration of tall buildings.

5.2 Minor modifications

A square or rectangular shaped building, whose height is greater than 300m and its aspect ratio is larger than 8, are generally susceptible to the aero-elastic instabilities. This is the reason that approaching wind separates from the windward corner of the building and

generates strong vortices by rolling up of the separated shear layer (Kawai 1998). In fact, the aerodynamic responses of a tall building are induced by the atmospheric turbulence and wake excitation due to vortex shedding. In detail, this atmospheric turbulence causes fluctuating alongwind structural loading while wake excitation induces fluctuating acrosswind loads (Kareem 1982). Therefore, the use of corner modifications such as slotted corners and chamfered corners is effectively beneficial in mitigating the wake-excited response by up to 30% at the low range of reduced velocities (Kim and You, 2008). Davenport (1971) finds that peak deflection of the model with circular cross section is roughly half of the model with square cross section; the cross-section of most 70-story tall buildings is generally square-shaped. Kwok (1995) investigates that corner modifications of a tall building can significantly mitigate the along-wind and across-wind responses when compared to its basic shape of corner. Approaching a roughly circular shape, significant corner roundness of a building significantly improves the response of the building (Kareem 1999). Hayashida (1990) studies the comparison between cross-wind aerodynamic characteristics for various cross section shapes of a super high-rise building through wind tunnel test. The author identifies that the aerodynamic shape effect of corner cutting is pronounced in the square cross section under wind direction normal to the face and is shown as a slightly smaller peak in the power spectrum, thus controlling vortex shedding by corner cutting. However, for corner modification to the cross-section based on triangular shapes, such effect is not significant, compared to that of the square cross section. Miyashita (1993) clarifies that a method of cutting corners or making openings is effective to reduce wind-induced motions for high-rise buildings with a square plane. The author further investigates on the effect of the wind direction not perpendicular to the face of the building. Kawai (1998) investigates effect of corner cut, recession and roundness on aero-elastic instabilities such as vortex induced excitation and galloping oscillation, through wind tunnel tests for square and rectangular prisms. The researcher finds that small corner cut and recession are significantly effective to prevent aero-elastic instability by increasing the aerodynamic damping. For a deep depth rectangular prism, however, this effectiveness by the corner modifications is insignificant. The benefits of corner modification have still remained debated, for these modifications to buildings corners, in

some cases, are ineffective and even have negative effects according to wind direction (Miyashita 1993). Irwin (2006) mentions corner modifications in Taipei 101 building provide 25% reduction in base moment when compared to the original square section. Holmes (2001) finds that chamfers of the order of 10% of the building width reduces both the along wind response by 40% and the across wind response by 30%, when compared to the rectangular cross sectional shape without any corner modification. Many researchers have identified that corner modifications such as corner roundness, corner recession, chamfered corners, fitting of small fins and vented fins to the corners and slotted corners are considerably effective to reduce the alongwind and crosswind response, compared to original building plan shape without any corner modification. In addition, these modifications effectively preclude the aero-elastic instability.
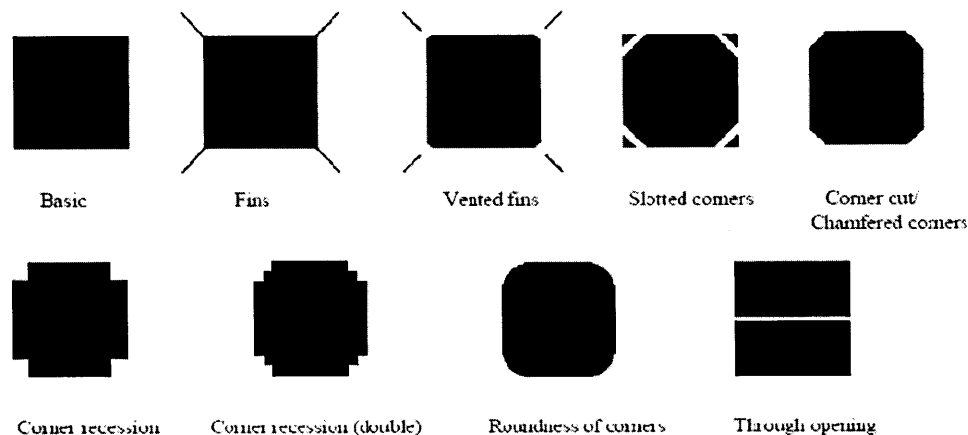
Figure 5.1 Various aerodynamic modifications to corner geometry (Amin J.A. 2010)

5.2.1 Effect of small fins and Vented fins and Slotted corners

Kwok and Bailey (1987) employ a basic square tower shape with a height h to width b ratio of 9:1 as the subject of wind tunnel tests. Model configurations used include the fitting of small vertical fins to the corners and the cutting of slots near the corners. Tested as a scale of 1/400, the models have the equivalent full scale height of 216m and a width and depth of 24m. Five model configurations are as follow: plain square tower; tower with 10mm wide vertical fins fitted to corners; tower with 5mm wide vertical fins and 5mm

gap between fins and corners; tower with 5mm wide slots cut through corners over the entire tower height; and tower with slotted corners about the top half of the model. The authors find that the fitting of fins and vented fins to the corners increases the along-wind response because of the increase in the projected area perpendicular to the wind. They also observe that for the fins, the crosswind response increases at the critical reduced wind velocities; therefore, the fins should be used at the low range of reduced velocities. It is noted that the slotted corners is very efficient in the alongwind and crosswind responses. Therefore, they conclude that the usage of the slotted corners can be useful in the design of tall buildings.

5.2.2   Effect of Slotted corners, Chamfered corners and Horizontal slots

Kwok (1988a) investigates the effect of building shape on the wind-induced responses of a tall building with rectangular cross section with minor modifications which involve the removal of the sharp corners, the cutting of slots near the corners and horizontal slots at half and three-quarter height of building. Tests are conducted in two 1/400 scale models of natural wind flow: open terrain and suburban terrain. The mean (or static) and standard deviation (or dynamic) alongwind displacement response and the standard deviation crosswind displacement response at the top of the building model are measured at reduced wind velocities which range from 4 to 20 and at a structural damping value of 1% of critical damping. For alongwind responses, slotted corners and two horizontal slots significantly reduce the mean and standard deviation, and chamfered corners cause more substantial reduction up to 40% in response when compared to the rectangular plain shape with no modification. While the response reduction is little affected by the change of terrain category, standard deviation responses are much higher in suburban terrain because of the turbulence buffeting increased by this more turbulent terrain. For crosswind responses, chamfered corners, slotted corners and the horizontal slots are effective in reducing the response within the range of reduced velocities, up to a 30% reduction in wake-excited response. At reduced velocities being approximately the critical value of 10,

observed are significant reductions in response by a factor of 2 or more. The chamfered corners lower the critical reduced velocity to a value of 8, and slotted corners to a value of 9. With the incident wind perpendicular to the narrow face of the building, the horizontal slots or slotted corners show up to 30% reduction in the cross wind response. This elongated rectangular building may prevent the vortex shedding corners, leading to reduction in the crosswind response. The author examines the wake spectra because peaks in the wake spectrum suggest the critical reduced wind velocity and the frequency. With the incident wind normal to the wide face of the building, the wake spectrum of the no-modification building peaks at a reduced velocity of 10. The slotted corners or the horizontal slots considerably reduce the wake spectrum, and the chamfered corners more significantly reduce the wake energy. The chamfered corners more reduce the wake energy than other models, at the high reduced frequency or low reduced velocity, with the incident wind perpendicular to the narrow face of the building. The researcher concludes that slotted corners, horizontal slots, and in particular chamfered corners effectively reduce both the alongwind and the crosswind response.

5.2.3   Effect of Slotted corners, Chamfered corners and Combinations of these corners

Kwok, Wilhelm and Wilkie (1988b) study on effectiveness of modification to the building corners in reducing the alongwind and crosswind responses of the building. A number of configurations are investigated in the same experiment as in the study of Kwok (1988a). For alongwind responses, chamfered corners more significantly reduce both the mean and standard deviation responses than slotted corners. When compared to the plain building shape, up to 40% reduction in the response is observed. For crosswind responses, the plain building shape shows a significant peak in the crosswind response, with the incident wind perpendicular to the wide face of the building model. However, slotted corners and chamfered corners are effective in reducing the responses; there are up to 30% reduction in wake-excited response. With the incident wind perpendicular narrow face of the building model, there is no significant response peak. Slotted corners reduce the responses

up to 30%, and chamfered corners shows larger reduction in responses. Both slotted corners and chamfered corners are effective in reducing the responses of a tall building; however, the chamfered corners are the better modification in both responses. For wake spectra, the plain building shape shows peaks at a reduced velocity of about 10 with the incident wind perpendicular to the wide face of the building. However, chamfered corners shows the wake spectrum peaks at a value of 8, leading to substantial reduction in wake energy around the vortex shedding frequency. On the other hand, the wake spectrum of the plain building has a small peak at a reduced wind velocity of 12, with the incident wind normal to the narrow face of the building. However, chamfered corners show a noticeable reduction around reduced velocity of 10. The author also considers all directions of wind. As the angle of incident wind increases, it is more likely that the separated shear layer reattaches onto the windward face of the building. This reattachment reduces excitation force, then decreasing responses. In fact, the plain building shape, over the first 20 degrees, significantly decreases the response. Chamfered corners follow the same trends. However, at angles of 60 and 70 degrees, responses in chamfered corners are higher than those in the plain building shape, even though these angles are considered insignificant in terms of design. All the tests results are obtained in open terrain similar to the fringes of a city. The author considers urban terrain where the level of wind turbulence is high. The author points out that in this terrain, the effect of the corner modifications may be diminished, in particular in the crosswind direction because the vortex shedding process is very sensitive to the level of turbulence. Therefore, this study mentions that, under the situation such as this urban terrain and interference by adjacent tall buildings, the benefit of corner modifications to the tall buildings is uncertain.

5.2.4 Effect of Chamfered corners and Corner roundness

Hayashida and Iwasa (1990) investigate the effect of chamfered corners and roundness of corners on aerodynamic forces and aerodynamic response of a super high-rise building with an assumed height of 600m and floor area of 6400m^2 in a wind tunnel. Five models,

in this test, are basic shapes and the other models are deformed shapes with corners-cut. The plain building shape with no modification shows the cross-wind response becomes larger than the alongwind response when design wind velocity exceeds about 30m/s. This means cross-wind response is more significant for the wind resistant design of tall buildings under this strong wind conditions. For the maximum crosswind displacement response, corner roundness is found to be more effective in resisting the responses than chamfered corner and plain rectangular shape; the corner roundness is followed by chamfered corner and then plain shape. For power spectra, a conspicuous peak fluctuation in the crosswind force spectrum occurs by the vortex shedding. For a chamfered corner, there is no noticeable peaks in both alongwind and crosswind response, but in corner roundness, crosswind response shows a well-defined peak which is smaller than in plain shape but which is larger than in chamfered corner. The author concludes that the corner modification to the 600-meter high-rise building, under the strong wind excited by vortex shedding, is effective in reducing the dynamic response behavior. Hayashida, Mataki and Iwasa (1992) investigate a change of the air force caused by the difference in the shape of the building and the dynamic effects induced by the vibration of the building. They use some of the same model shapes adopted in the test of Hayashida and Iwasa (1990): (1) square shape; (2) Y-shaped model; (3) equilateral triangle shape; and (4) circular shape. They conclude that except for the circular plane section, the response value obtained from the dynamic test is smaller than that from the analysis using the measured fluctuating external force. This is the reason that aerodynamic damping affects the response value. Under the resonance wind velocity, the value, obtained from the dynamic test of the circular plane section, is larger than that of the response analysis. This value is about three times larger in the alongwind direction and about 1.8 times larger than the value from the response analysis. It is observed that the vortex moved from the upper levels down to the lower levels through measurements of the fluctuating pressure of the side face. The moving speed of this vortex is about three times the wind velocity of the approaching flow.

5.2.5   Effect of Corner-Cut, Corner Recession and Through openings

Miyashita et al. (1993) investigate the responses of a square building with chamfered corners or openings from the wind tunnel tests, considering wind direction not perpendicular to a certain face of the building. The models adopted are (1) rectangular plain shaped model, (2) a model with through opening along the X axis, (3) a model with through opening along the Y axis, (4) a model with through openings along both X axis and Y axis, (5) a model with corner-cut and (6) a model with corner recession. Each through opening is located at three positions, respectively h/6, 2h/6, 3h/6 from the top of the building. To identify the effect of wind direction, the tests are conducted for the wind direction of every 5 degree from 0 degree to 45 degree. For corner cuts or openings, the fluctuating wind force coefficient along Y-axis around 0 degree is smaller than that of the basic model. Moreover, the reduction of the value of the value of model with openings in both directions of X and Y is conspicuous. For the model with corner-cuts like a square, the maximum value of the fluctuating wind force coefficient along the Y-axis occurs at the wind direction of 10 degree. The model shape little affects the fluctuating wind force coefficients for X-axis. A model (3) with openings in the across-wind direction has a sharp peak in power spectrum. A model (6) with corner recession shows the highest vortex shedding frequency. In the wind direction of 0 degree, the correlation between the wind forces is mostly low while a high correlation, in the directions from 5 degree to 20 degree, is observed near the vortex shedding except for model (2). In the direction of 45 degree, a high correlation occurs in the low frequency range.

5.2.6   Effect of Corner-cut, Corner recession and Corner roundness

Kawai (1998) studies on the effect of minor shape modifications such as corner recession on aeroelastic instabilities such as vortex induced excitation and galloping oscillation through wind tunnel tests. The test adopts 15 square prisms: five corner-cut square prisms – in b/B 0.05, 0.10, 0.15, 0.20, 0.25; five square prisms with recession corners – in b/B like corner-cuts; and five square prisms with corner roundness like in b/B above. The test

also 11 rectangular prisms with corner-cuts, corner recessions and corner roundness varying in b/B: It is, through the tunnel test, observed that there is aeroelastic instability of galloping along with vortex-excited vibration in the case of corner-out model. Moreover, the corner-cut with the smallest values of b/B = 0.05 is considerably effective in reducing the amplitude at high reduced velocity. In the damping ratio of 1.4%, the prism with corner-cut modification remains stable except around the reduced velocity of 7.5 for corner-cut models with large value of b/B = 0.2 and 0.25. For models with the large values of b/B = 0.2 and 0.25 and with the damping ratios of 0.3% and 0.4%, vortex induced vibration is observed to occurs. As the corner recession values become larger, the onset velocity tends to be smaller. It is noted to the small corner recession of b/B=0.05 effectively reduces the instability. In the case of the corner roundness, as its value increases from b/B=0.05 to 0.25, its effectiveness also enhances. Nevertheless, the circular cylinder model shows instable vortex induced vibration, at the reduced velocity of U/nB=7, with the damping ratio of 0.3% and 1.4%. For the rectangular prism with side ratio D/B=1/2, or with deep depth, the large corner cut and corner recession increase the instability at low velocity while they decrease the instability at high velocity. When in the damping ratio of 0.2% and 1.2%, the corner roundness little affects the instability; however, when in the damping ratio of 4%, large corner-cut, corner recession and corner roundness effectively suppress the instability. For the elliptical cylinder, stability is noticeable at the damping ratio of 1.2% and 4%. For the rectangular prism with side ratio D/B=2/1, or shallow depth, corner modifications such as corner recession, corner-cuts and corner roundness have little beneficial effect on the vibration, while such modifications influence the maximum amplitude. In fact, the corner recession model with the b/B ratio of 0.21 makes the maximum amplitude one fourth of that in the rectangular prism without any modification. The author also investigates the reason that small corner cut and corner recession effectively reduce the instability of a square prism in the very small damping ratio, by comparing the power spectra of the responses of the corner recession models with the b/B ratio of 0.05 and 0.2. For b/B=0.2, instability is observed at the range of the reduced velocity of U/nB from 5 to 15 while for b/B=0.05, this instability is reduced. Under the reduced velocity less than 6, two peaks, one of which is related to vortex

shedding and the other of which result from the natural vibration of the model, in the power spectra of the response appear. In addition, the peak at the lower frequency occurs smaller in 0.2 than in 0.05, and the shedding vortex is weaker in 0.2 than in 0.05. For the small corner recession of the ratio b/B of 0.05, highly sharp and large peak at the natural frequency and at the reduced speed of 2.8 appears, with the weak instability occurring. This instability is assumed to be motion induced vibration, then making the peak become blunt as the velocity increases. This may mean that this blunting is associated by the increase of the aerodynamic damping. Therefore, the author concludes that for the small corner modification, the reduction of the aerodynamic instability result not from the suppression of the vortex shedding but from the increase of the aerodynamic damping. For the rectangular prism with the D/B ratio of 1/2, or with the shallow depth, the corner cur and corner recession, both with large b/B ratio, promote the instability at low velocity, thus reducing the onset velocity of the instability. This phenomenon is similar in the case of a model without a corner modification. Two peaks occur before and after the onset of the instability. One peak associated to vortex shedding is not conspicuous in the corner recession with a large b/B before the onset of the instability. However, the peak becomes distinct and sharp after the onset. From the fact that when the vibration amplitude is about similar to the width of the model, it is suggested that the locking phenomenon is not significant, the instability is not related not to vortex shedding but to the low-speed galloping. The researcher identifies that the prevention of the vortex shedding by the corner modifications negatively affects the instability in case of low-speed galloping. He also mentions that for the rectangular prism with deep depth, the motion induced vibration occurs at the reduced velocity of 5. From this observation, it is noted that corner modifications little affect the vibration, but these modifications significantly reduce the response at the reduced velocity more than 10.

5.2.7   Effect of Incremental Corner chamfers

Mara and Case (2009) investigate, through wind tunnel test, the effect of incremental

corner chamfers, whose dimensions are 1/10 and 1/6.7 of the building face, on the mean and dynamic response of a square building. Base on the high-frequency base balance technique, the tests use five configurations: (baseline) unmodified model; (1) one-corner chamfered model; (2) two-corner chamfered model; (3) all-corner chamfered model with a chamfer dimension of 1/10 of the building face; and (4) all-corner larger chamfered model with the dimension of 1/6.7. The length scale adopted in this test is 1/400 which means in full-scale chamfer dimensions of 3.05m and 4.57m. For mean base bending and torsion moment coefficient, a single chamfered corner in the windward reduces the alongwind mean loading by 20%. Both chamfered corners on the windward face decrease the loading by about 35%. A significant reduction is observed in the range of wind directions from -30 degree to +30 degree. It is observed that the increase of the chamfered dimension little affects the mean loading for winds directly on to the face. All corner chamfered models (3) and (4) at the critical angles significantly reduce the torsion coefficients by 30%. The increase of the chamfer dimension additionally reduces this coefficient by up to 10% when compared to the smaller chamfer dimension at critical wind directions. Researchers investigate the influence of chamfered corners relative to a range of building periods. In case the vibration-periods of a building are short, corner modifications have little beneficial effect on resonant response. However, In case of larger vibration-periods of the building, corner modifications significantly affect the response. In addition, the larger chamfer model (4) is observed to be more effective in reducing the response than model with smaller modification (3). This is not related to building period. Moreover, they study the orientation of the corner chamfer relative to the statistically significant wind direction. For a wind climate with equal preference from north and south directions, the corner modifications of (1) and (2) shows little benefit regardless of period. However, for a wind climate with a predominantly northern preference, these modifications, (1) and (2), have benefit when compared to the baseline model as the corner modifications are aligned with northern directions. However, with the corner modifications aligned away from the southern wind directions, models (1) and (2) increase the resonant response when compared to the baseline model: particularly for longer periods of building. Regardless of the period of vibration, for torsion, incremental corner modifications consistently improve

the resonant behavior. Authors conclude that corner modifications to the rectangular building can be effective in suppressing the responses induced by the wind, but they emphasize the necessity of comprehensive study on building geometry such as size, shape and slenderness, the building properties such as vibration periods and the local wind climate.

5.3 Major Modification

As the height of tall building increases, the building is more susceptible to wind induced vibration. To mitigate this adverse effect of the wind, there are various methods introduced, particularly one of which is an aerodynamic modification to the building. This modification can be grouped into two types according to its effect on structural and architectural concept. Therefore, the major modification, which considerably affects the architectural and structural design of tall buildings, contains tapering, or setbacks along the height, sculptured building shape, openings, varying the shape of buildings, and twisting of building. Building codes admit a reduction of the wind pressure design loads for circular or elliptical buildings up to 40% of those of rectangular buildings (Schueller 1977). You and Kim (2008) identify that a tapered tall building effectively reduce crosswind responses by spreading the vortex-shedding over a broad range of frequencies. Dutton and Isyumov (1990) mention that openings completely through the building considerably reduce vortex shedding induced forces and the crosswind dynamic response; this effect is particularly more evident when the openings are positioned near at the top of the building.

5.3.1 Effect of Helical models and Setback model

Tamura, Tanaka et al. (2010) investigate the relationships among structural properties, aerodynamic modifications and aerodynamic force characteristics acting on 31 tall

building models. These models have various modifications including square plan, rectangular plan and elliptical plan, with chamfered corner, with corner recession, tilted, tapered, inversed tapered, with setbacks, twisting, and openings. The models have the same height (400m, or 80 stories) and floor areas (2500 square meter), giving an aspect ratio of 8. There are four basic models including square, circular, elliptical and rectangular. The side ratio of elliptical and rectangular models is 1/2. For chamfered corners and corner recessions, the modification ratio of b/B is 1/10. For the tilted model, the base floor is shifted by 2B from the top floor of the model. For the shaking model, the floors at 0.25H and 0.75H are shifted by 0.5B respectively in the left direction and then the right direction, thereby appearing like a smoothly curved shaking prism. Authors use two types of tapered models: 2-tapered models having two tapered surfaces and 4-tapered models having four tapered surfaces. For tapered models, the area ratio of top floor to base floor is 1/6. An inverse 4-tapered model means the inverse shape of the 4-tapered model. The drum model is designed to have its floor area of 0.5H which is three times the top and base floor areas. The sectional shapes of the helical models, which have the same floor areas, are square, rectangular and elliptical, with the twist angle used as a prefix of the model name. To illustrate, 270-helical rectangular means helical rectangular model with twist angle of 270 degree. They investigate the effect of twist angle on aerodynamic force characteristics by the twist angles of 90, 180, 270 and 360 degree. For cross void model, the opening of the void model is located at the top center and for oblique void model, at the top corner of the surface. To identify the effect of opening size on the aerodynamic force characteristics, various opening sizes of 2/24H, 5/24H and 11/24H are utilized. They also use the combination models such as 360-degree helical model with corner-cuts, setback model with corner-cuts, and 4-tapered and 360-degree helical model with corner-cuts. For aerodynamic force measurements, the square, corner-cut, 4-tapered, setback, 90-helical square and 180-helical square are investigated. The maximum value of mean wind force coefficient occurs in the square model with 0.6 at a wind direction of 45 degree, while the minimum value appear in setback model with 0.43, indicating 70% of the value of the square model. For fluctuating wind force coefficient, square model and corner-cut model show the across wind component which is larger than the alongwind component.

However, the inverse trend happens in the other models, showing smaller values in the acrosswind components.
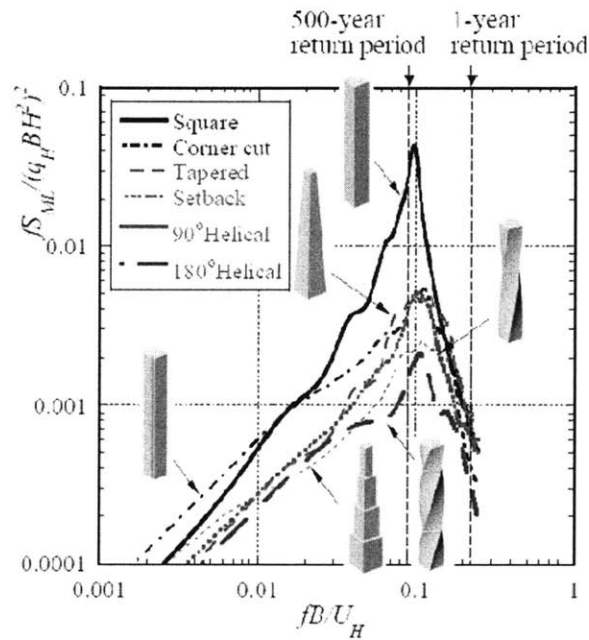
Figure 5.2 Power spectral density of across-wind force coefficients (Tamura 2010)

The maximum value in the square model is observed while the minimum value comes from the setback model, with being 60% of that of the square model. 180-degree helical model and 90-degree helical model are found to be little affected by the wind direction. Moreover, the 180-degree helical model almost remains the same value regardless of the direction. For the acrosswind power spectra in Figure 5.2 for the specified wind directions at which the peak is the largest, the square model shows the sharp peak significantly reduces when compared to those of the other models. The peak value corresponding to a 500-year return period wind speed of the 180-degree helical model is about 0.05 that of the square model, which shows the helical model is a conspicuously effective design. Obtained from the spectral modal method, the maximum displacement of the square model is 0.015H while that of the 180-degree helical model is 0.003H. Similarly, the displacement of the setback model is 0.004H. Judged from the values corresponding to a 1-year return period wind speed, the maximum acceleration of the 180-degree helical

model is almost half that of the square model while the maximum acceleration of the setback model is larger than that of the square model. Therefore, it is concluded from the authors that the 180-degree helical model is the most effective structural shape of models in terms of safety and habitability criteria.

5.3.2 Effect of Tapering

Kim and You (2002) investigate the tapering effect on the wind induced responses of tall buildings through high-frequency force-balance test. They use four models including three tapered models with the taper ratio of 5%, 10% and 15% and the basic square model: type (1), the ratio of the top floor area of a square prism to the base floor area of the square prism is 100:100; type (2) is 64:100; type (3) is 36:100; and type (4) is 16:100. Two typical boundary layers are considered: BL1 representing suburban wind climate with turbulence intensity at the top of the model about 10% and BL2 indicating urban wind climate about 15%. For mean alongwind force coefficients, normal reduction ratios of type 4 for suburban and urban terrains are about 10% of those of the basic square model, type 1. Around at 60 degree of wind direction, maximum reduction ratio of 30% is shown in BL1. For mean acrosswind force coefficients, tapering effect in open terrain BL1 is more conspicuous than in urban terrain, with increasing wind direction. However, for rms alongwind force coefficients, the values of rms-force coefficients in BL2 are larger than those in BL1. Tapering effect for reducing fluctuating acrosswind forces is pronounced, especially when wind direction is 0 degree. However, this effect becomes weaker as the wind direction increases. For fluctuating alongwind force spectrum, although the taper ratio increases, no conspicuous changes, though there is slight reduction, in spectral configuration appear. For fluctuating acrosswind force spectrum, as the taper ratio increases, it is observed that the magnitude of the spectral peak decreases and the band width becomes broad. It is interestingly noted that a tapered tall building can spread the vortex shedding over a broad range of frequencies, thereby effectively reducing acrosswind responses. Authors identify that tapering effect is more effective in reducing

the large size of vortex shedding than in the smaller one. For rms-displacement of acrosswind direction, tapering effect in BL1 is more evident than in BL2, particularly when wind direction is around 0 degree. It is also found that increased taper ratio is not effective for reducing acrosswind and alongwind accelerations. Kim and You conclude that the wind induced responses of a tapered building are not always mitigated compared to that of basic square prism building, even though a beneficial tapering effect is more evident in acrosswind direction than in alongwind direction.

5.3.3 Effect of Through-Building Openings

Miyashita et al. (1983) investigate wind forces acting on tall buildings (H: 300m, W:50m, D:50m) with openings (Type 1, square shape without opening; Type 2, along X axis; Type 3, along Y axis; and Type 4, along X and Y axis) in various wind directions (every 5 degree, from 0 degree to 45 degree) through wind tunnel tests. Each model has 3 openings evenly distributed from 0.5H to H along the height of the building. For the fluctuating wind force coefficient, the reduction of the value of Type 4 is significantly pronounced, even though Type 2 and Type 3 both show smaller reductions than Type 1. For the power spectral densities of the fluctuating wind force along the Y-axis of wind direction of 0 degree, Type 1 shows the largest value. The wind force power spectra for Type 2 and Type 4 have peaks at the reduced velocity of 0.08 and 0.18 respectively. Type 3 is also observed to have a sharp peak.

Dutton and Isyumov (1990) use three models including square model, model with alongwind opening, and model with both alongwind and acrosswind openings. Each model with opening has three openings, whose dimension is 1.25D high and which are 0.25D separated from others, along the vertical axis of the building. Utilization of the openings results in a conspicuous reduction of the vortex shedding induced forces, leading to reducing the acrosswind dynamic deflection of the building. The venting of the flow through the opening into the base region causes this base pressure recovery, suppressing

the vortex shedding process and mitigating the acrosswind excitation.

5.4 Examples of utilizing modifications

It is well known that modifications such as corner-recession, chamfered corner, helical shape, tapered shape, setback shape are significantly effective in reducing wind induced responses of tall buildings. Armed with these modifications, tall buildings can be aesthetically and innovatively designed by suppressing adverse effects by the wind. In addition, along with advance in visco-elastic materials like tuned mass damper as well as structural systems like diagrid, the shape of a tall building becomes distinct from the rectangular and symmetrical prisms which have traditionally and compulsorily been a norm of the shape of tall building. This trend in the shape of a tall building was initiated in 1974 by 108-story Willis Tower (formerly named the Sears Tower) in Chicago in Figure 5.3 which utilized the advantages of reducing the plan area along the height to minimize the wind induced vibrations. The 152-meter, 34-story Mitsubishi Jyuko Yokohama Building and the 346-meter, 83-story Aon Center (formerly Amoco) in Figure 5.4 exploits corner modifications; four corners of the building are made chamfered. This modification reduces the wind forces which is stronger in water front areas like open terrains on which the building is built. The tall building which adopted the double step corner recession modifications to the cross section is 101-story Taipei 101 building in Taiwan (2004) in Figure 5.5. It is found that this building with such modifications can reduce the base moment by 25% when compared to the building of basic square section (Irwan 2006). The Marian City in Figure 5.6, Lake Point Tower in Figure 5.7, and 333 South Wacker Drive in Figure 5.8 used the corner roundness. This circular plane section effectively reduces the crosswind forces, suppressing vortex shedding. Recent examples of this modification are the 30 St Mary Axe in Figure 5.9, the Burj Dubai in UAE, and the Millennium Tower in Tokyo. The Shanghai World Trade Center in Figure 5.10, the Pearl River Tower in Figure 5.11, and the Kingdom Center in Figure 5.17 utilize the effect of through-building opening. The Shanghai World Trade Center benefits from the conspicuous reduction of vortex

shedding while Pearl River Tower exploits through wind turbines the wind energy as well as mitigating the across-wind excitation. As representative of major modification, Al Faisaliah Center in Figure 5.12 employs the tapering effect, which reduces the upper level plan areas. As examples of setback modifications, the 40 Wall Street building in figure 5.13, the Jin Mao Building in Figure 5.14, the Chrysler building and the Petronas Towers are mentioned. Since the 2000s, there has been a sharp growth in the freestyle shapes of tall buildings. Distinct among these shapes is the helical or twist shape. These helical shapes are applied to the Shanghai Tower under construction in Figure 5.15 and Turning Torso in Figure 5.16.

Figure 5.3
Willis Tower in 1974
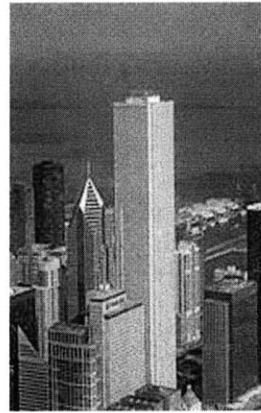
Figure 5.4
Aon Center in 1973
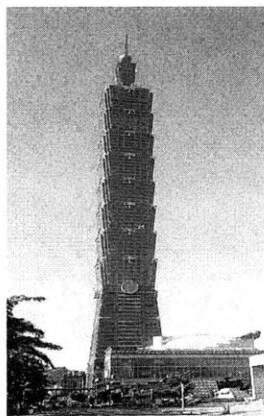
Figure 5.5
Taipei 101 in 2004

Figure 5.6
Marian City in 1964
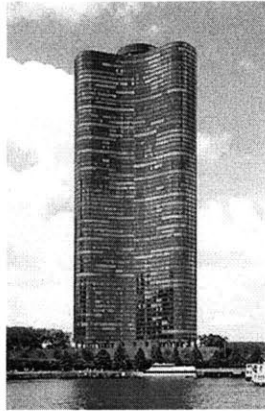
Figure 5.7
Lake Point Tower in 1968

Figure 5.8
333 South Wacker Drive in 1983

Figure 5.9
30 St Mary Axe in 2004

Figure 5.10
Shanghai Tower under cons

Figure 5.11
Pearl River Tower under cons.

Figure 5.12
Al Faisaliah Center in 2000

Figure 5.13
40 Wall Street Building in 1930
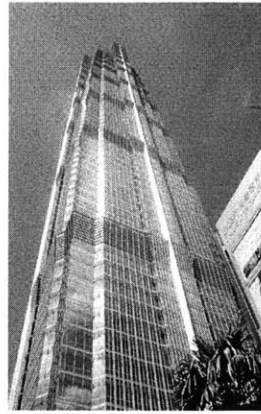
Figure 5.14
Jin Mao Building
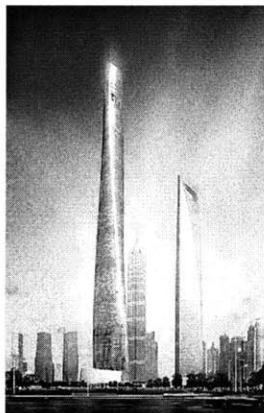
Figure 5.15
Shanghai Tower under cons.

Figure 5.16
Turning Torso in 2006

Figure 5.17
Kingdom Center in 2002

5.5 References:

Minor Modifications

Amin J.A. and Ahuja A.K. 2010, Aerodynamic Modifications to the Shape of the Buildings: A Review of the State-of-the-Art, Asian Journal of Civil Engineering (Building and Housing) VOL.11, NO. 4 (2010), pp.433-450.

Ilgin H.E. and Gunel M.H. 2007, The Role of Aerodynamic Modifications in the Form of Tall Building Against Wind Excitation, METU JFA 2007/2, 24:2, 17-25.

Kawai H., 1998, Effect of Corner Modifications on Aeroelastic Instabilities of Tall Buildings, Journal of Wind Engineering and Industrial Aerodynamics 74-76 (1998), pp.719-729.

Kwok K.C.S. 1995, Aerodynamics of Tall Buildings, A State of the Art in Wind Engineering: International Association for Wind Engineering, Ninth International Conference on Wind Engineering, New Delhi.

Kareem A. 1982, Fluctuating Wind Loads on Buildings, Journal of the Engineering Mechanics Division, Vol. 108, No. 6, 1982, pp.1086-1102.

Miyashita K. and et al. 1993, Wind-Induced Response of High-Rise buildings: Effects of corner cuts or openings in square buildings, Journal of Wind Engineering and Industrial Aerodynamics, 50, pp.319-328.

Hayashida H and Iwasa Y. 1990, Aerodynamic Shape Effects of Tall Building For Vortex Induced Vibration, Journal of Wind Engineering and Industrial Aerodynamics, 33, pp.237-242.

Hayashida H., Mataki Y and Iwasa Y. 1992, Aerodynamic Damping Effects of Tall Building for a Vortex Induced Vibration, Journal of Wind Engineering and Industrial Aerodynamics, 43(3), pp.1973-1983.

Kareem A., Kijewski-Correa T., and Tamura Y. 1999, Mitigation of Motions of Tall Buildings with Special Examples of Recent Applications, Journal on Wind and Structures, Vol. 2, No. 3. (1999), pp.201-251.

Davenport A.G. 1971, The Response of Six Building Shapes to Turbulent Wind, Philosophical Transactions of the Royal Society of London. Series A, Mathematical and

Physical Sciences, Vol. 269, Issue 1199, pp. 385-394.

Irwin P.A. 2006, Developing Wind Engineering Techniques to Optimize Design and Reduce Risk, 7th UK Conference on Wind Engineering, Wind Engineering Society, ICE.

Holmes J.D. 2001, Wind Loading of Structures, Spon Press, London.

Kwok KCS and Bailey P.A. 1987, Aerodynamic Devices for Tall Building and Structures, Journal of Engineering Mechanics, ASCE, Vol. 113, Issue 3, pp.349-365.

Kwok KCS, 1988, Effects of Building Shape on Wind-Induced Response of Tall Buildings, Journal of Wind Engineering and Industrial Aerodynamics, 28(1988) pp.381-390.

Kwok KCS and Wilhelm P.A. et al. 1988, Effect of Edge Configuration on Wind-induced Response of Tall Buildings, Engineering Structure, 10(1988) pp.135-140.

Mara T.G. and Case P.C. 2010, The Effects of Incremental Corner Modifications on a 200m Tall Building, 2010 Structures Congress, 2010 ASCE, pp.2949-2960.

Wind tunnel tests for Wind-Excited Benchmark Building

Major Modification

Cooper K.R., Nakayama M. et al. 1997, Unsteady Aerodynamic Force Measurements on a Super-Tall Building with a Tapered Cross Section, Journal of Wind Engineering And Industrial Aerodynamics, Vo.72, pp.199-212.

Kim Y.M. and You K.P. 2002, Dynamic Response of a Tapered Tall Building to Wind Loads, Journal of Wind Engineering And Industrial Aerodynamics, Vol.90, Issues 12-15, pp.1771-1782.

You K.P. and Kim Y.M. and Nag H.K. 2008, The Evaluation of Wind-Induced Vibration Responses to a Tapered Tall Building, The Structural Design of Tall and Special Buildings, Vol.17, Issue 3, pp.655-657.

Kim Y.M., You K.P. and Ko N.H. 2008, Across-wind Responses of an Aeroelastic Tapered Tall Building, Journal of Wind Engineering And Industrial Aerodynamics, Vol.96, Issues 8-9, pp.1307-1319.

Dutton R. and Isyumov N. 1990, Reduction of Tall Building Motion by Aerodynamic Treatments, Journal of Wind Engineering And Industrial Aerodynamics, Vol.36, Part 2, pp.739-747.

Schueller W. 1977, High-Rise Building Structures, John and Wiley Sons Inc., New York.

Tamura Y. 1998, Application of Damping Devices to Duppress Wind-Induced Responses of Buildings, Journal of Wind Engineering And Industrial Aerodynamics, 74-76 (1998), pp.49-72.

Irwin P.A. 2006, Developing Wind Engineering Techniques to Optimize Design and Reduce Risk, 7th UK Conference on Wind Engineering, Wind Engineering Society, ICE.

Gu M and Quan Y. 2004, Across-Wind Loads of Typical Tall Buildings, Journal of Wind Engineering and Industrial Aerodynamics, 92, 1147-1165.

Tse K.T. Hitchcock P.A. and Kwok K.C.S. et al., 2009, Economic perspectives of aerodynamic Treatments of Square Tall Buildings, Journal of Wind Engineering and Industrial Aerodynamics, No. 3, 43, 1973-1983.

Davenport A.G. 1971, The response of Six Building Shapes to Turbulent Wind, Philosophical Transactions, Royal Society, A269, 285-394.

Browne M., Garber J., 2009, Implications of Solid-Walled Balconies on Wind Loading, Technotes, Issue No. 34, RWDI.

Hayashida K., Katagiri J. et al. 1993, Wind Induced Response of High Rise Building: Effects of Corner Cuts or Openging in Square Building, Journal of Wind Engineering and Industrial Aerodynamics, 50(1993) pp. 319-328.

Melbourne N.H. and Cheung J.C.K. 1988, Designing for Serviceable Accelerations in Tall Buildings, 4th International Conference on Tall Buildings, Hong Kong and Shanghai, pp.148-155.

Melbourne N.H. 1989, Wind Loading and Environment of Tall Building, International Conference on Tall Buildings and City Development, Brisbane, pp.159-164.

Chapter 6 Numerical Analysis on Aerodynamic Modifications

This chapter investigates the effects of aerodynamic modifications to a tall building on the wind force and wind pressure on the tall building. With DES (Detached Eddy Simulation) which combines features of classical RANS formations with elements of Large Eddy Simulations (LES) methods, commercial CFD code, STAR-CD V4.14 is adopted. In order to validate CFD results, four models already conducted by Tamura (2010) are used; therefore, these results from the numerical analysis of the wind flow are compared.

6.1 Test models

To determine wind forces and wind pressures, Tamura et al. (2010) performed wind tunnel tests on 31 tall building models with various configurations, four of which are analyzed through CFD (Computational Fluid Dynamics) in this paper. These models, as shown in the figure 1, are square, corner-cur, setback and 180 degree helical shaped tall building models. Like in Tamura (2010), the model heights are 400 meter, and floor areas are 2500 square meters in common. For square model as a basic model, an aspect ratio is 1:8, while for the corner-recession model, the corner modification length is 0.1 of the building length. For the 180 degree helical model, the twist angle is 180 degree, and the sectional shape is square. The setback model has a three step setback involving 28-meter, 41-meter, 52-meter from 69-meter base floor length.

(a) Square Model   (b) Corner-recession   (c) Setback Model   (d) 180 Helical Model
                        Model
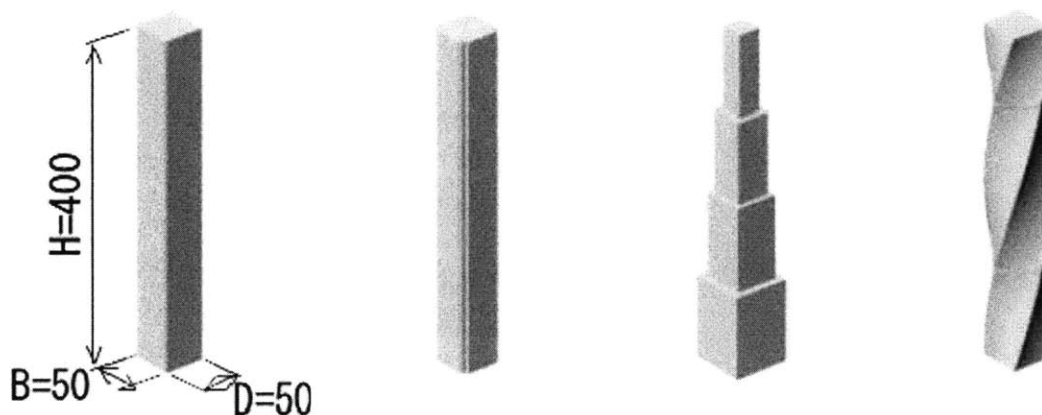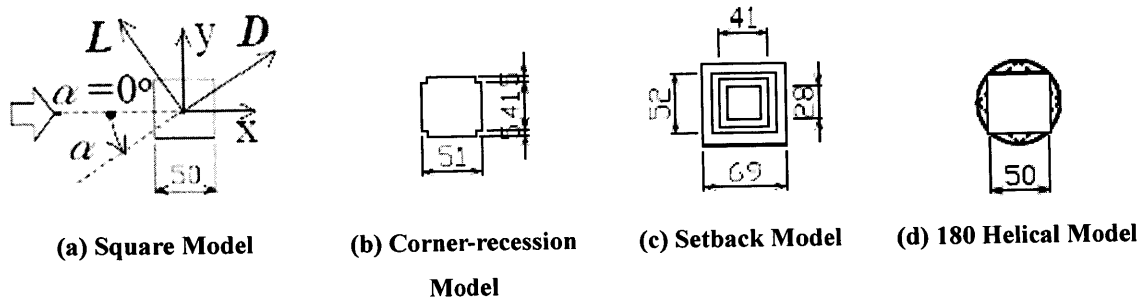
Figure 6.1 Geometry of Tall Building Models (Tamura 2010)

At the time when the wind around a tall building acts as a wind pressure on the surface of the building as in the figure 2, aerodynamic characteristics on the tall building are determined by wind velocity and turbulence. In order to numerically analyze such characteristics, this paper considers the profile of an urban area which represents power-law exponent of 0.27 and wind speed at model height of 7.0m/s. Based on the results by Tamura et al. (2010), this paper studies effects of the shape modifications of tall building on the aerodynamic forces and pressure of the tall building.
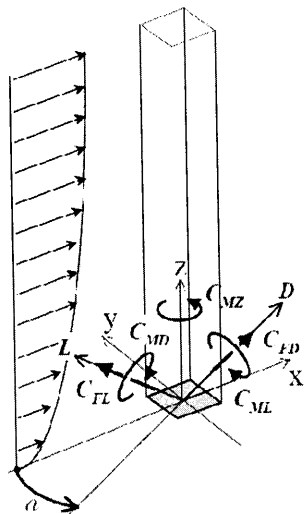
Figure 6.2 Aerodynamic characteristics

(Tamura 2010)
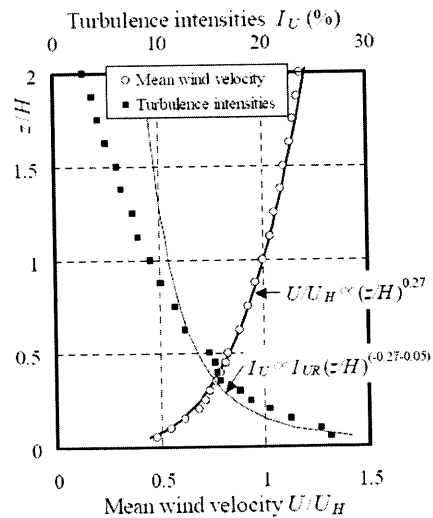
Figure 6.3 Wind tunnel flow

(Tamura 2010)

6.2 Numerical Method

Mass and momentum conservation equations, or the 'Navier-Stokes' equations, solved by STAR-CD to analyze the flow around a tall building model are,

$$\frac{\partial u_i}{\partial x_i} = 0 \tag{1}$$

$$\frac{\partial}{\partial x_j}(u_i u_j) = \frac{\partial}{\partial x_j}\left[(v + v_t)\frac{\partial u_i}{\partial x_j}\right] - \frac{1}{\rho}\frac{\partial p}{\partial x_i} \tag{2}$$

where u – velocity vector

v – dynamic viscosity

$v_t(= C_\mu k^2 / \varepsilon)$ – isotropic eddy viscosity

ρ – density

p – pressure

In the case of the building model (400m in height, 1/1000 scale, and 7m/s in wind-speed), Re (Reynolds number) is 1.86E+5. One of the most common models to calculate the turbulent flow is standard $k - \varepsilon$ turbulence model which can be, as shown in equation (3) and (4), represented as transport equations for turbulent kinetic energy and eddy dissipation rate.

$$\frac{\partial}{\partial x_j}(k u_j) = \frac{\partial}{\partial x_j}\left[\left(v + \frac{v_t}{\sigma_k}\right)\frac{\partial k}{\partial x_j}\right] + v_t S_{ij}\frac{\partial u_i}{\partial x_j} - \varepsilon \tag{3}$$

$$\frac{\partial}{\partial x_j}(\varepsilon u_j) = \frac{\partial}{\partial x_j}\left[\left(v + \frac{v_t}{\sigma_\varepsilon}\right)\frac{\partial \varepsilon}{\partial x_j}\right] + c_{\varepsilon 1}\frac{\varepsilon}{k}v_t S_{ij}\frac{\partial u_i}{\partial x_j} - c_{\varepsilon 2}\frac{\varepsilon^2}{k} \tag{4}$$

$$\text{where } S_{ij} = \frac{\partial u_i}{\partial x_j} + \frac{\partial u_j}{\partial x_i}$$

where S_{ij} – mean stress tensor

         $c_{\varepsilon 1}$ – coefficient for turbulent model (1.44)

         $c_{\varepsilon 2}$ – coefficient for turbulent model (1.92)

In this paper, to represent characteristics of anisotropic turbulence, RNG model, rather than standard $k-\varepsilon$ turbulence model, is utilized because it adopts modified turbulence dissipate rate which is shown in equation (5). η_0 (4.38), β (0.012) are empirical coefficients, and coefficients for RNG turbulence model are $c_{\varepsilon 1}$ (1.42) and $c_{\varepsilon 2}$ (1.68).

Standard $k-\varepsilon$ turbulence model and RNG turbulence model as models involved in RANS (Reynolds-Average Numerical Simulation) investigate the mean properties of turbulent flows. However, to accurately predict the turbulent flow features like pressure fluctuation acting on building models, it is necessary is to compute unsteady flow fields.

$$\frac{\partial}{\partial x_j}\left(\varepsilon u_j\right) = \frac{\partial}{\partial x_j}\left[\left(\nu + \frac{\nu_t}{\sigma_\varepsilon}\right)\frac{\partial \varepsilon}{\partial x_j}\right] + c_{\varepsilon 1}\frac{\varepsilon}{k}\nu_t S_{ij}\frac{\partial u_i}{\partial x_j} - c_{\varepsilon 2}\frac{\varepsilon^2}{k} - \frac{C_\mu \eta^3\left(1-\eta/\eta_0\right)}{1+\beta\eta^3}\frac{\varepsilon^2}{k} \tag{5}$$

$$\text{where } \eta = S\frac{k}{\varepsilon}$$

Equation (5) reveals that the distinctive feature of the RNG model is the additional, last term in the dissipation equation. This is a term from the RNG analysis, representing effect of mean flow distortion on the turbulence (Rodi 1979).

As shown in Figure 4, as a hybrid RANS (Reynolds-averaged Navier-Stokes) - LES (Large-Eddy Simulation) method, DES (Detached Eddy Simulation) is in this study used. Turbulence kinetic energy and turbulence dissipation rate are considered in Equation (6) and (7).
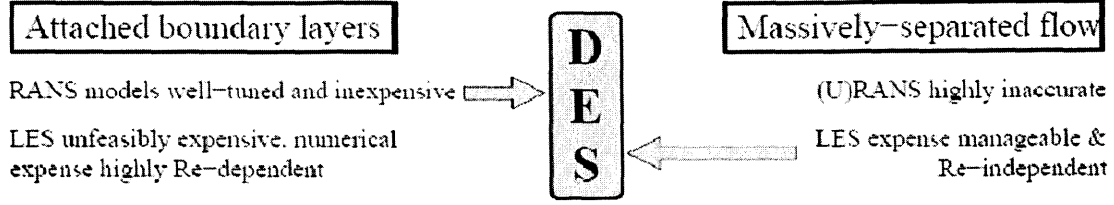
Figure 6.4 Diagrammatical summary of the motivation of DES (Mockett 2009).

$$\partial_t \rho k + \partial_x \rho U k = \partial_x \left(\nu + \frac{\nu_t}{\sigma_k^{k-\varepsilon}} \right) \partial_x k + \rho P_k - D_k^{k-\varepsilon} \tag{6}$$

$$\partial_t \rho \varepsilon + \partial_x \rho U \varepsilon = \partial_x \left(\nu + \frac{\nu_t}{\sigma_\varepsilon^{k-\varepsilon}} \right) \partial_x \varepsilon + \rho \alpha P_k \frac{\varepsilon}{k} - \rho C_{\varepsilon 2} \frac{\varepsilon^2}{k} \tag{7}$$

where $\quad D_k^{k-\varepsilon} = \rho \varepsilon$

∂_t – temporal derivative term

U – velocity

σ – empirical constant of turbulence model

α – constant of turbulence model

P – production of turbulence kinetic energy

D – dissipation of turbulence kinetic energy

The length scale of DES model is determined by equation (8).

$$\tilde{l} = \min\left(\frac{k^{3/2}}{\varepsilon}, C_{DES}, \Delta \right) \tag{8}$$

where Δ is the maximum of the grid spacing for the sides of computational cell (X,Y,Z), and C_{DES} is a constant which takes the value 0.65. Dissipation term along with length

scale is modified as in equation (9).

$$D_k^{k-\varepsilon} = \frac{\rho k^{3/2}}{\tilde{l}}$$ (9)

6.3 Solution strategy

The dimension of the model considered in the computational study is a 1:1000 scale model of the tall building. Computational domain, coordinate definition and boundary conditions for this study are shown in Figure 5 and Figure 6.
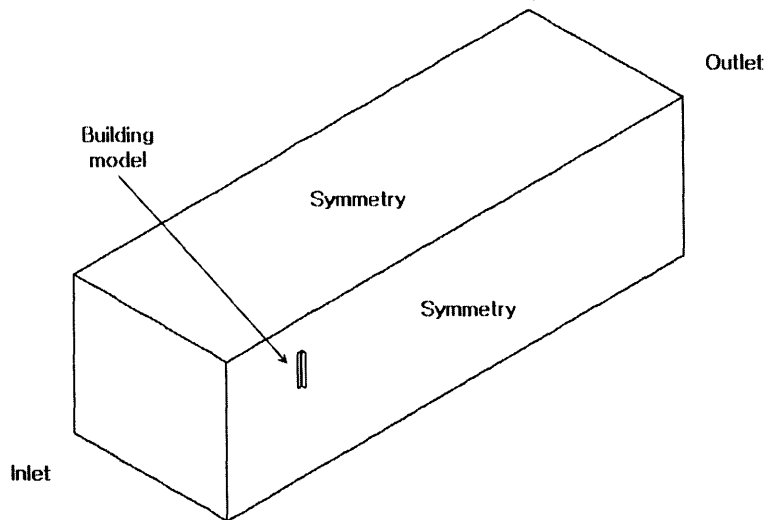
Figure 6.5 Computational domain including building model and boundary conditions

The Reynolds numbers involved in the simulations are in the range of about 1.86E+5, which is the same range as in the wind tunnel test of Tamura (2010). As in the figure 6, the computational domain covers 120B (B is the building width of the building) in stream-wise (X) direction (-40 < X/B < 80) and 40B in lateral or normal (Y) direction (-20<Y/B<20) and 29B in vertical (Z) direction. The reason for such configurations is to eliminate the flow obstacle effect on the inflow and outflow boundary conditions (Murakami 1998).
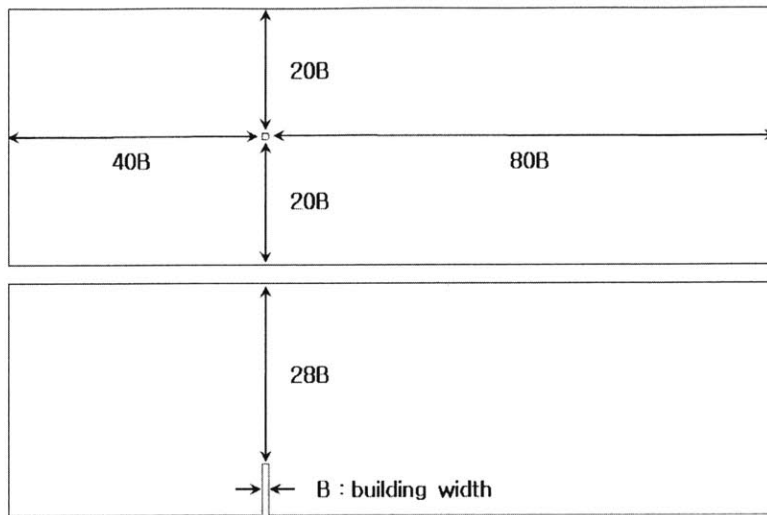
Figure 6.6 Size of computational domain based on the building width showing plan view (top) and section view (bottom)

The computational meshes are automatically created through the function of pre-process in STAR-CCM+ V5.06. As shown in figure 6, the grid topology is trimmed grid, and the total number of this mesh in all cases is 8,900,000. The mesh number must be as low as possible for efficient computation, even though the mesh near and aligned with the surfaces of the models is more refined for better analysis as in figure 7.
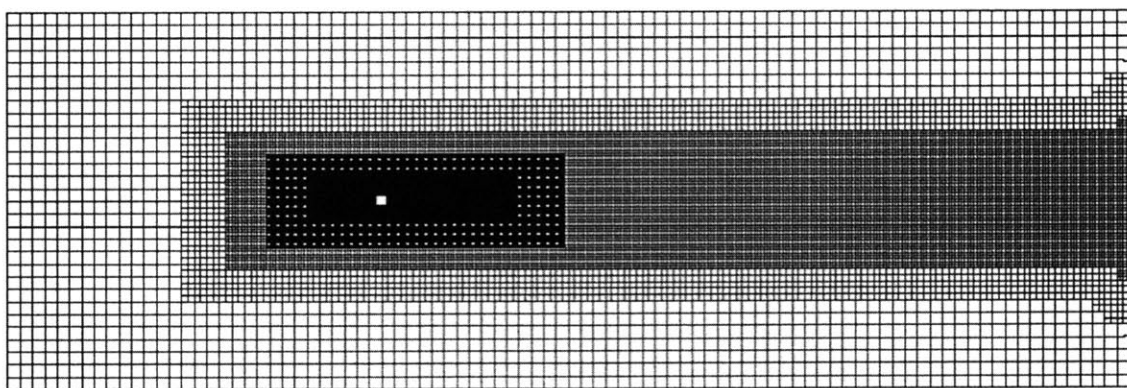
Figure 6.7 Section view of meshes at the 0.3 m height from ground showing mesh refinement technique to resolve complex flow around building model

Wind force coefficient and wind moment coefficient acting on the wall surfaces of tall

is due to the flow instability. In addition, instability at the recirculation region causes the flow separation region where the flow detaches from the surface of the model to move in the direction of the flow, which is a phenomenon called vortex shedding.
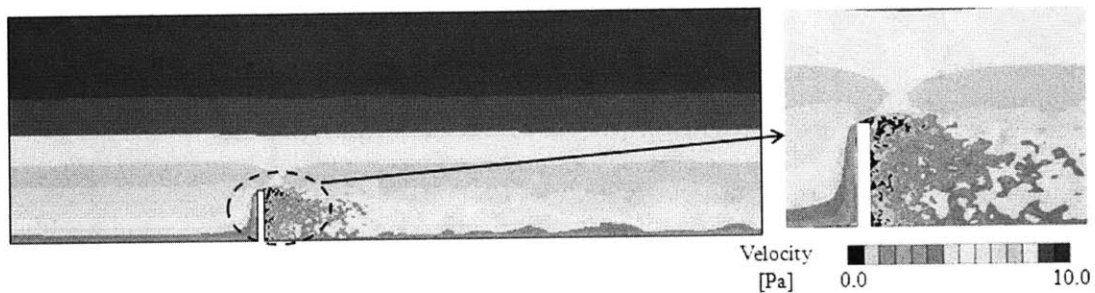
Figure 6.8 Velocity magnitude distribution around the square model (x-z section at y=0)
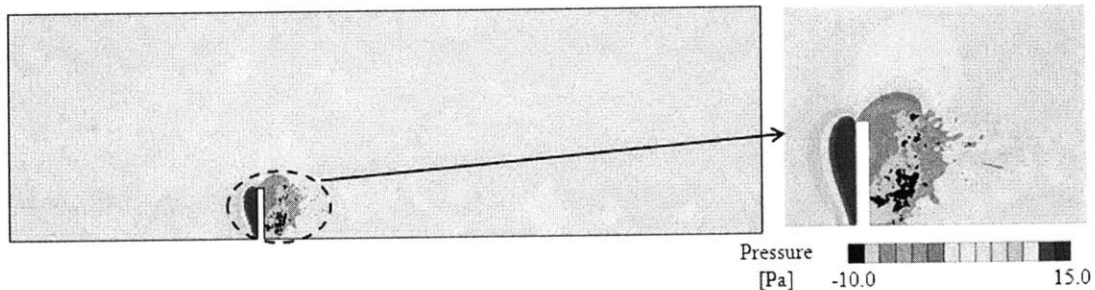
Figure 6.9 Pressure distribution around the square model (x-z section at y=0)

This vortex shedding is affected by the turbulence effect, and small scaled vortex shedding as well as big scaled vortex shedding can exist. The vortex shedding resulting from the flow separation induces the pressure difference, which, according to time, acts on the building model periodically. Finally, this fluctuating pressure creates unfavorable vibration on the building model. In case that the fundamental frequency of the building model is in accordance with the frequency of the vibration, the building can be susceptible to the damage or partial collapse. Characteristics of vortex shedding around the tall building are, as in Fig. 11, evaluated as the velocity distribution and pressure distribution in x-y section. The features of the vortex shedding in horizontal section are influenced by those of the air flow around the building; they are can be affected by the height from the ground and the flow at the top face of the building. For the flow characteristics in height, the flow velocity in the vicinity of the building at the 0.25H is low, thereby leading to showing low pressure.
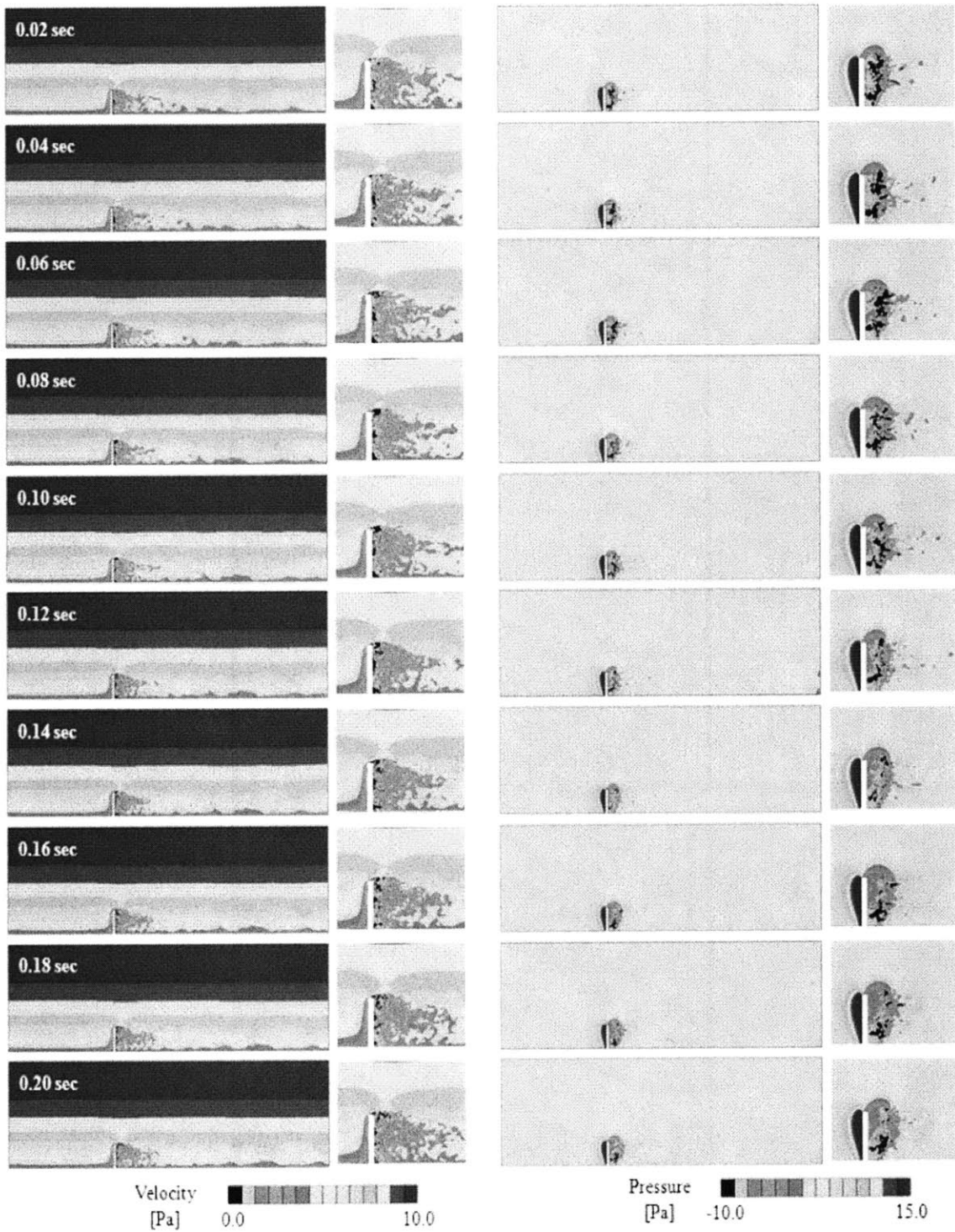
(a) Velocity distribution   (b) Pressure distribution

Figure 6.10 Transient flow characteristics around the square model (x-z section at y=0)

z = 0.25 H	
z = 0.50 H	
z = 0.75 H	
z = 1.00 H	

Velocity [Pa] 0.0 — 10.0

Pressure [Pa] -10.0 — 15.0

(a) velocity distribution   **(b) pressure distribution**
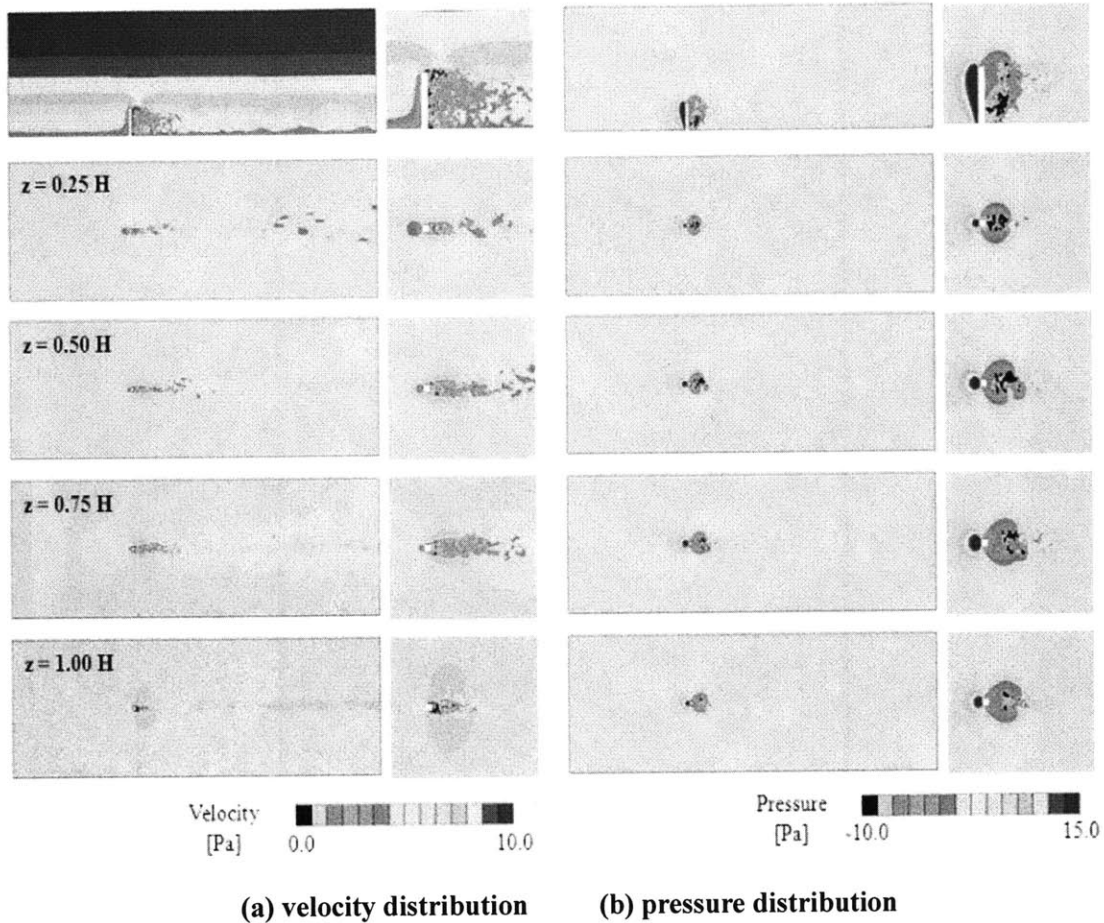
Fig. 6.11 Flow characteristics around the square model (x-y section)

Moreover, at the section of 1.00H or the top of the building, the pressure difference between at two faces is shown low because of vortex shedding. In the other hand, at 0.50H where vortex shedding occurs actively, the pressure difference at two faces is shown large. As illustrated in Fig. 12, for transient flow characteristics around the square model in x-y section at z=0.50H, because of the instability of the recirculation region occurring at the both sides (left and right sides) of the building, vortex is shown to be shedding form left to right or from right to left alternatively. Created by this alternating vortex shedding, periodical pressure differential induces vibrations of the building. Therefore, to mitigate the pressure gradient caused by this vortex shedding can be one of the methods to reduce the motion regularly acting on the building.
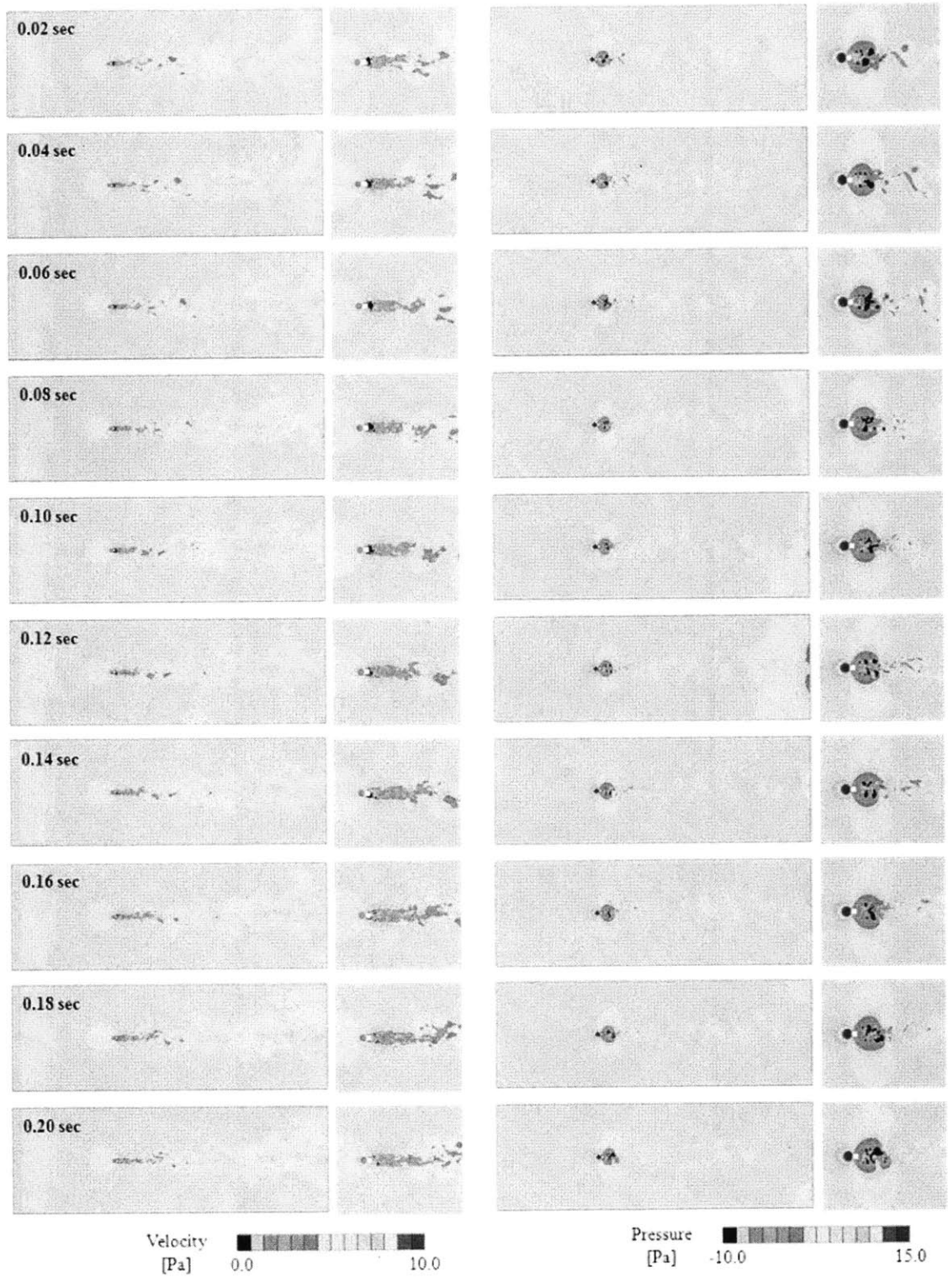
0.02 sec

0.04 sec

0.06 sec

0.08 sec

0.10 sec

0.12 sec

0.14 sec

0.16 sec

0.18 sec

0.20 sec

Velocity [Pa] 0.0 10.0

Pressure [Pa] -10.0 15.0

(a) velocity distribution

(b) pressure distribution

Fig. 6.12 Transient flow characteristics around the square model (x-y section at z=0.5H)

0.02 sec

0.04 sec

0.06 sec

0.08 sec

0.10 sec

0.12 sec

0.14 sec

0.16 sec

0.18 sec

0.20 sec

Velocity [Pa]   0.0   10.0

Pressure [Pa]   -10.0   15.0
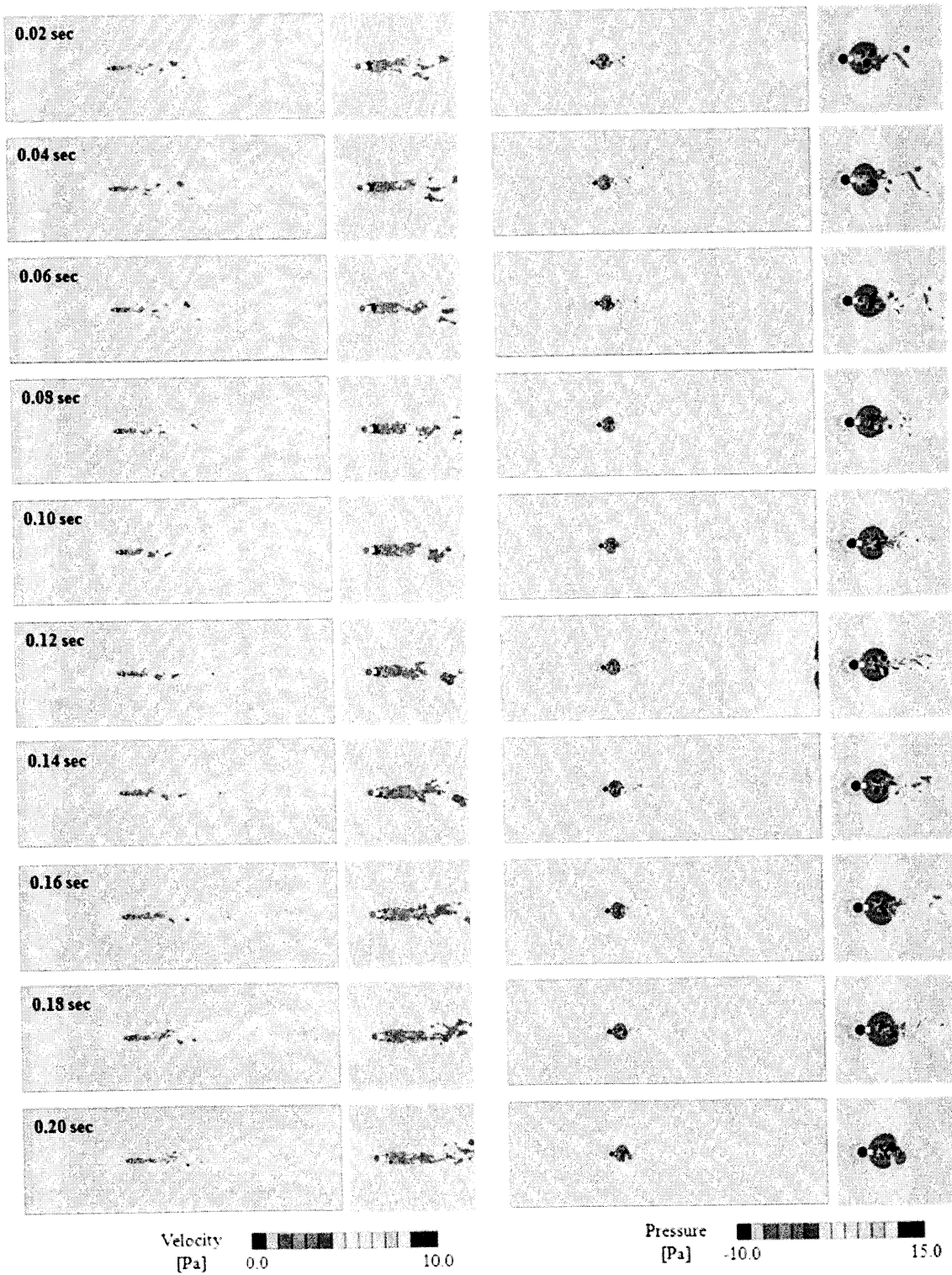
(a) velocity distribution

(b) pressure distribution

Fig. 6.12 Transient flow characteristics around the square model (x-y section at z=0.5H)

6.4.2 Flow characteristics with various building models.

In this study, to mitigate the vibration, induced by the characteristics of the vortex shedding in the flows around a building, regularly acting on the building, flow characteristics around the various shapes of building models as illustrated in Fig 1 are evaluated through numerical analysis. Obtained from the analysis on the various shapes of tall buildings, velocity and pressure of the flow around each model - (a) square model, (b) corner-recession model, (c) setback model and (d) 180 degree helical model - are seen in Fig. 13. From this figure, in the direction of height of the building (x-y section), it is noticeable that aerodynamic characteristics are determined by the position and the area of the section facing the flow. By modifying the shape of the corner at which vortex shedding occurs, the corner-recession model makes the recirculation region less than that of the square model, leading to effectiveness on reducing the pressure gradient. In the case of setback model, as the distance from the ground increases, the section area of the model decreases. Thus, the pressure difference between two faces of the model at the top of the model is shown much smaller than that of the square model. Moreover, for the 180 degree helical model, according to the height, square section forms specific angles by which the smooth flows are made; therefore, the helical model suppresses the vortex shedding. Accordingly, when compared to the square model, the models with shape modifications reduce the recirculation regions and then lessen the pressure gradient induced by vortex shedding. This eventually leads to the decrease in the vibration characteristics of the tall buildings. To evaluate general characteristics of the pressure periodically acting on the surface of a tall building, mean wind pressure acting on the surface in the time span of 1.5 seconds are shown in Fig. 14 and Fig. 15. From the figures, between the front and back face of the square model occurs the pressure difference of 20Pa. However, it is significantly noticeable that the pressure differences decrease by 2Pa or 3Pa in all the case of other models with aerodynamic shape modifications. The reason for this decrease is that the pressure gradient between two faces is reduced because such modification makes the recirculation region smaller. In addition, it is shown that the reduction of the pressure difference between two left and right sides as well as between the front and back face of a

tall building significantly suppresses vibrations by modifying the shape of the building.

(a) square model

Velocity [Pa] 0.0   10.0

Pressure [Pa] -10.0   15.0

(b) Corner-recession model

Velocity [Pa] 0.0   10.0

Pressure [Pa] -10.0   15.0

(c) Setback model

Velocity [Pa] 0.0 — 10.0   Pressure [Pa] -10.0 — 15.0
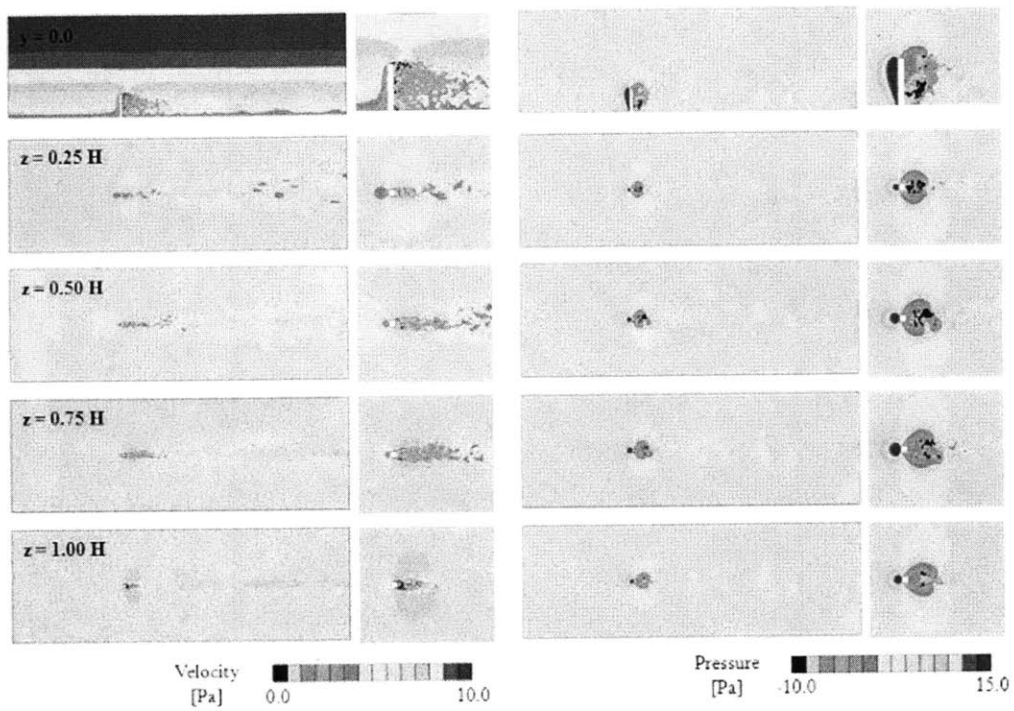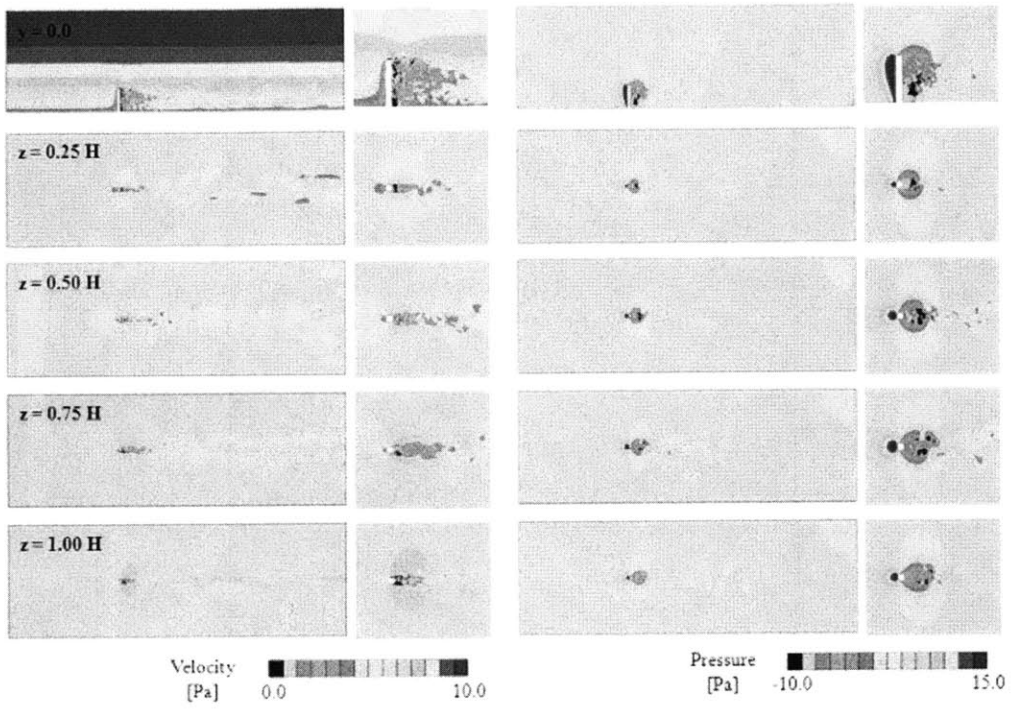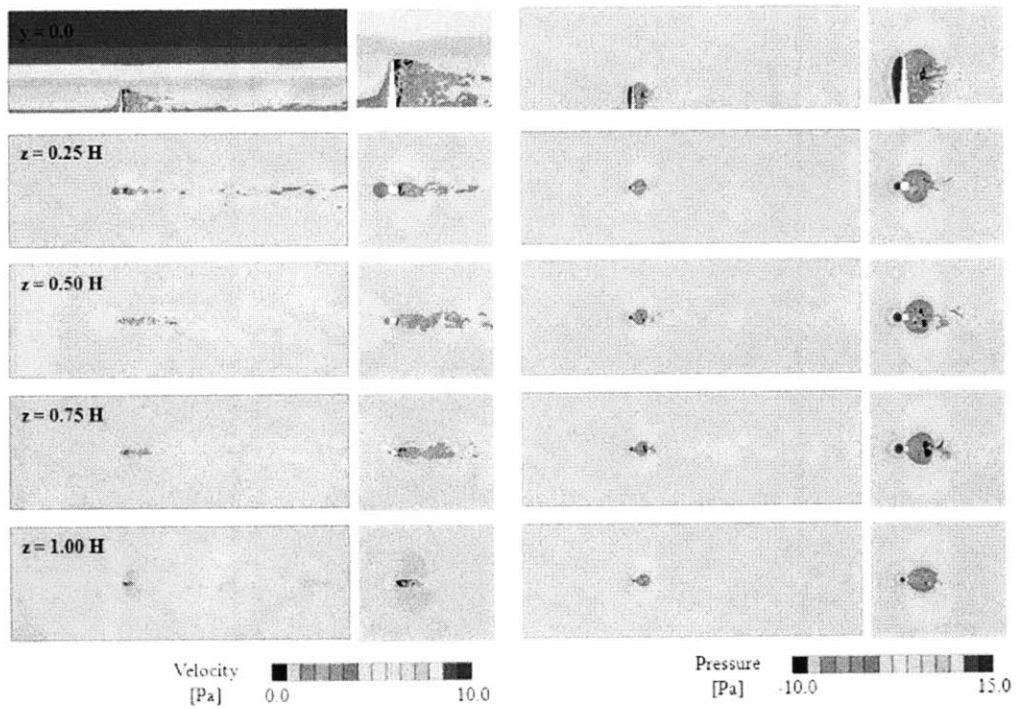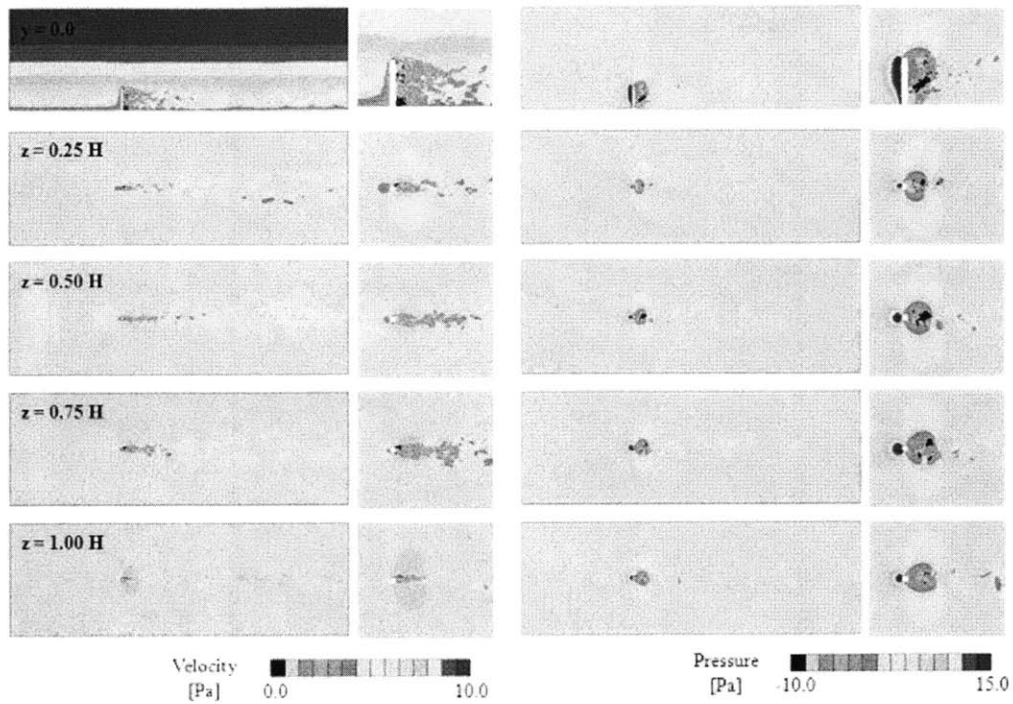
(d) 180 degree Helical model

Figure 6.13 Flow characteristics around various types of building model (x-y section)
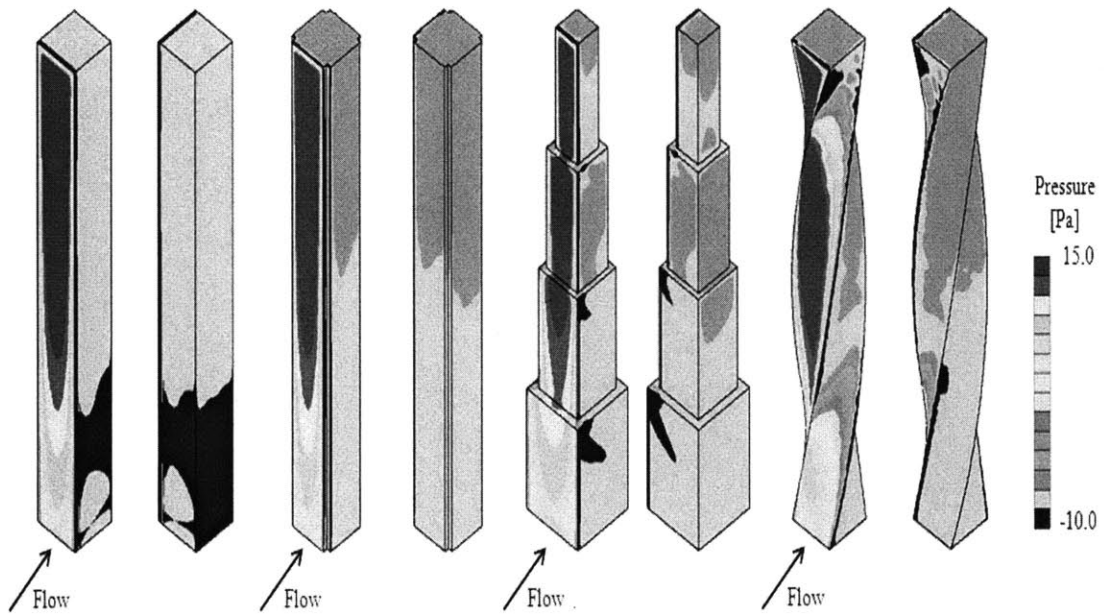
Pressure [Pa] 15.0 -10.0

(a) square model   (b) corner-recession model   (c) setback model   (b) helical model

Figure 6.14 mean wind pressure I on various building models
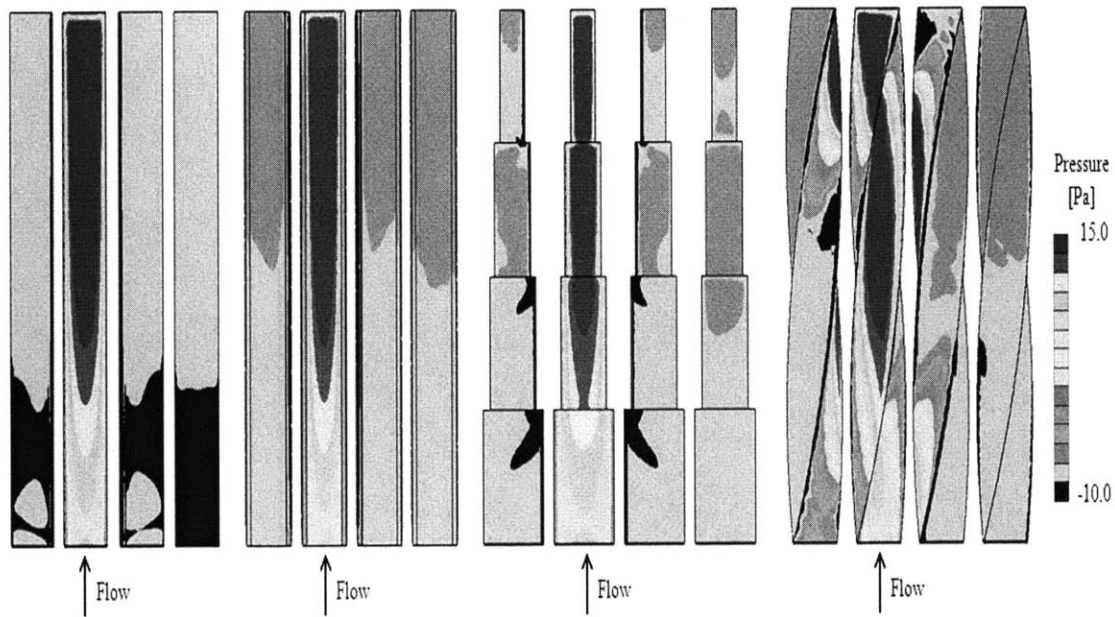
(a) square model   (b) corner-recession model   (c) setback model   (b) helical model

Figure 6.14 mean wind pressure II on various building models

6.4.3 Characteristics of wind force and moment with various building models

From the numerical analysis of flow around a tall building model, flow characteristics such as wind force and wind moment are evaluated. Fig. 16 shows wind force coefficient and wind moment coefficient acting on the wall of each of various models. The reason that wind force coefficient of each model has the mean value of about 0.15 to 0.18 is that a certain force acts on the front face of a building model. As vortices are shed alternatively first from one side and then the other side after the flow develops, the feature that coefficient values fluctuate within certain ranges is shown. Wind force coefficient acting on left and right side of a building model has a mean value of about 0.0. For the force acting on these sides, vortices are shed alternatively to the left and the right side of a model, thereby inducing pressure difference. Like wind force coefficients in the direction of the wind and two sides of a building, wind moment coefficient shows similar patterns. Table 1 shows mean and standard deviation of wind force and wind moment acting on various models. As shown in Fig. 15, wind force and wind moment in the direction of

wind flow are observed to be within certain values and to be fluctuating due to the effect of vortex shedding. However, wind force and wind moment in the direction of two sides of a model is shown to only fluctuate due to the effect of vortex shedding. Therefore, as compared to the square model, models with shape modification reduce the recirculation region, and then models have smaller wind force and wind moment than those of square model. Moreover, it is noticeable that fluctuation

Table 6.1 Mean and standard deviation of wind force and moment with various models

	C_{FD}	C_{FD}'	C_{FL}	C_{FL}'	C_{MD}	C_{MD}'	C_{ML}	C_{ML}'
Square model	0.1759	0.0020	0.0002	0.0022	0.0950	0.0012	0.0950	0.0012
Corner-recession Model	0.1529	0.0011	-0.0001	0.0017	0.0827	0.0005	0.0827	0.0005
Setback model	0.1539	0.0017	0.0006	0.0024	0.0691	0.0006	0.0691	0.0006
Helical modal	0.1541	0.0012	0.0013	0.0019	0.0826	0.0006	0.0826	0.0006

ranges decrease in standard deviation showing characteristics of fluctuation. Also, in the case of wind moment than in case of wind force, setback model, whose sectional area decreases as the height from the ground increases, shows the smaller value of wind moment. Unlike other models, helical model, whose twist is made in the horizontal direction (x-y section), has a certain value of wind force and wind moment in the lateral direction. The power spectral densities of the wind force and moment coefficients are shown in Figure 16 and Figure 17. The power spectra of the square model show a sharp peak around a reduced frequency of 1. However, those of other models with shape modification show a reduced value at the same frequency. For wind force, the power spectra of corner-recession model are shown much smaller than those of other models in x direction.
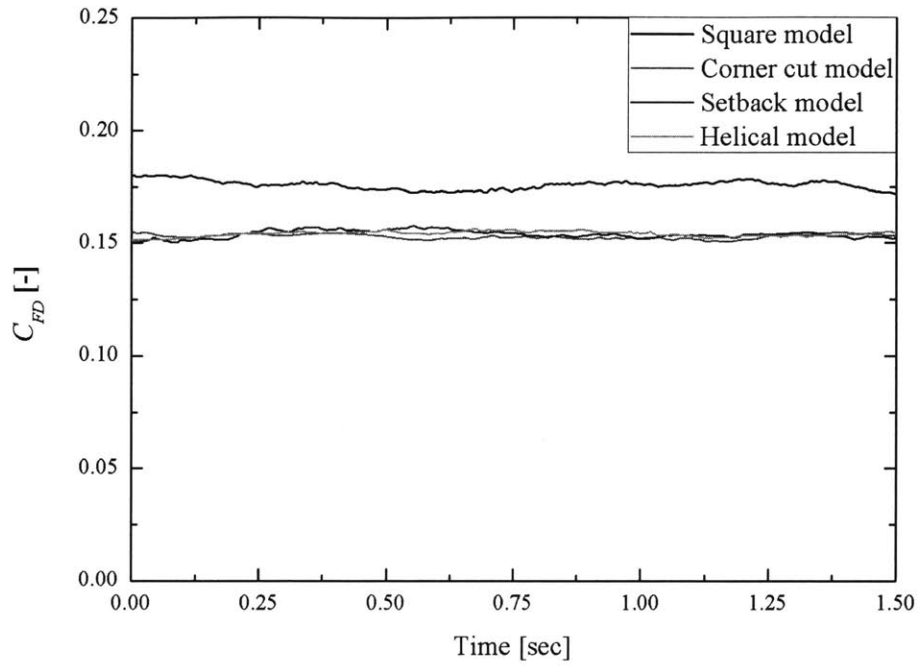
(a) C_{FD}, **wind force coefficient in the wind direction**
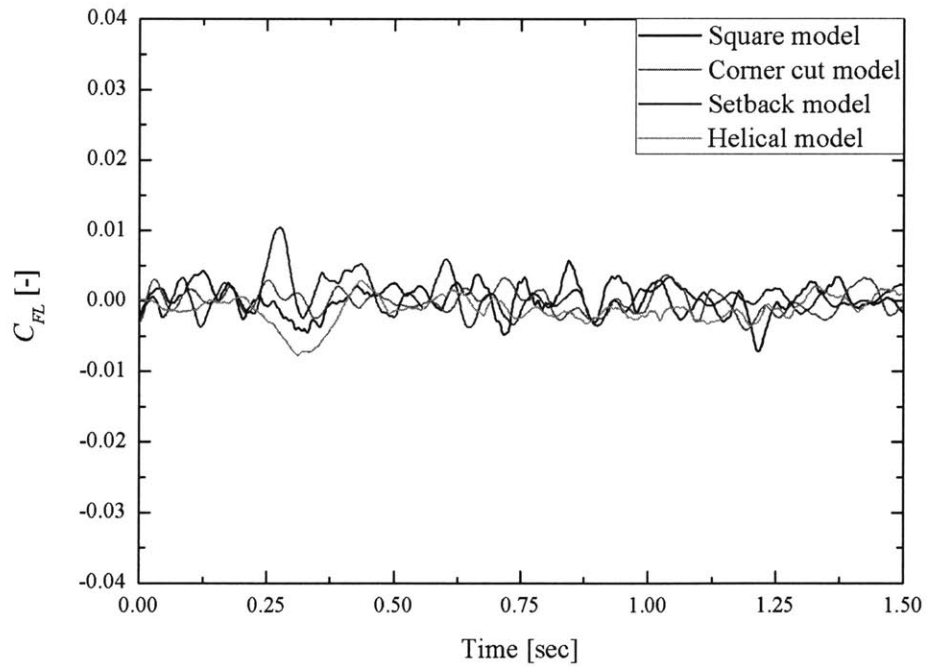
(b) C_{FL}, **wind force coefficient in the side direction**
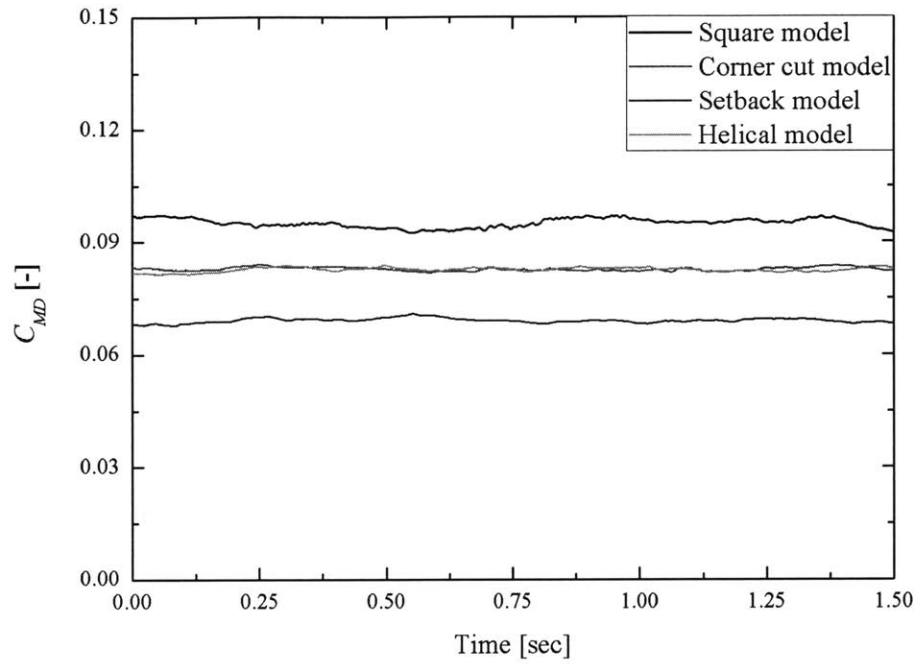
(c) C_{MD}, wind moment coefficient in the wind direction
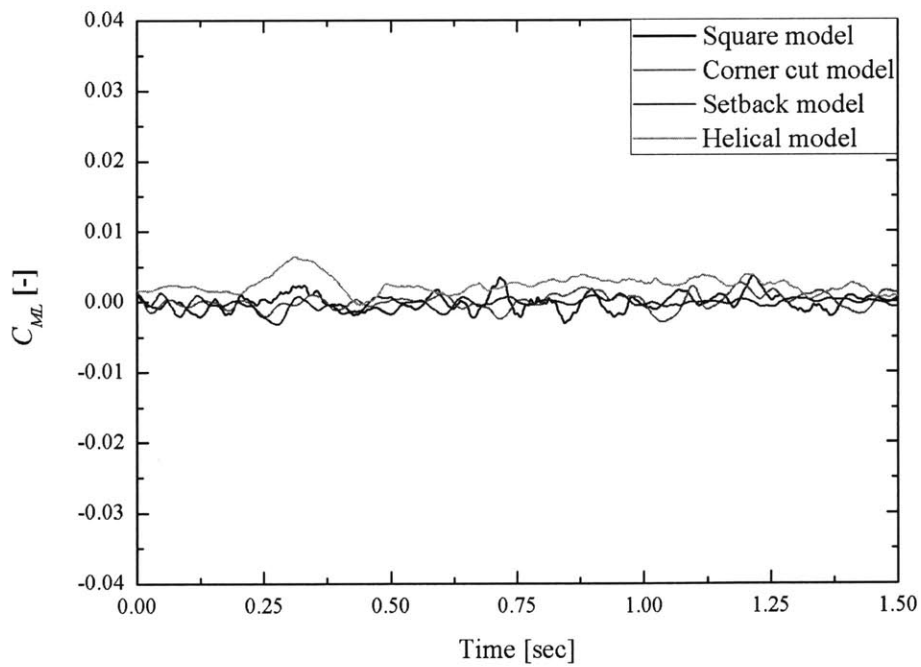
(d) C_{ML} wind moment coefficient in the side direction

Fig. 6.15 Characteristics of wind force and moment with various building models
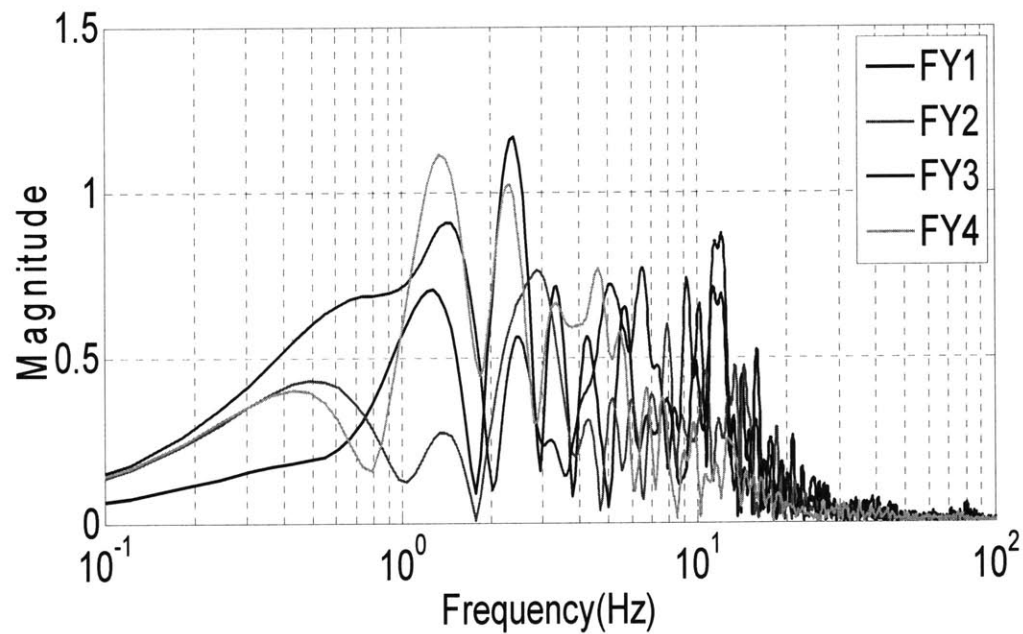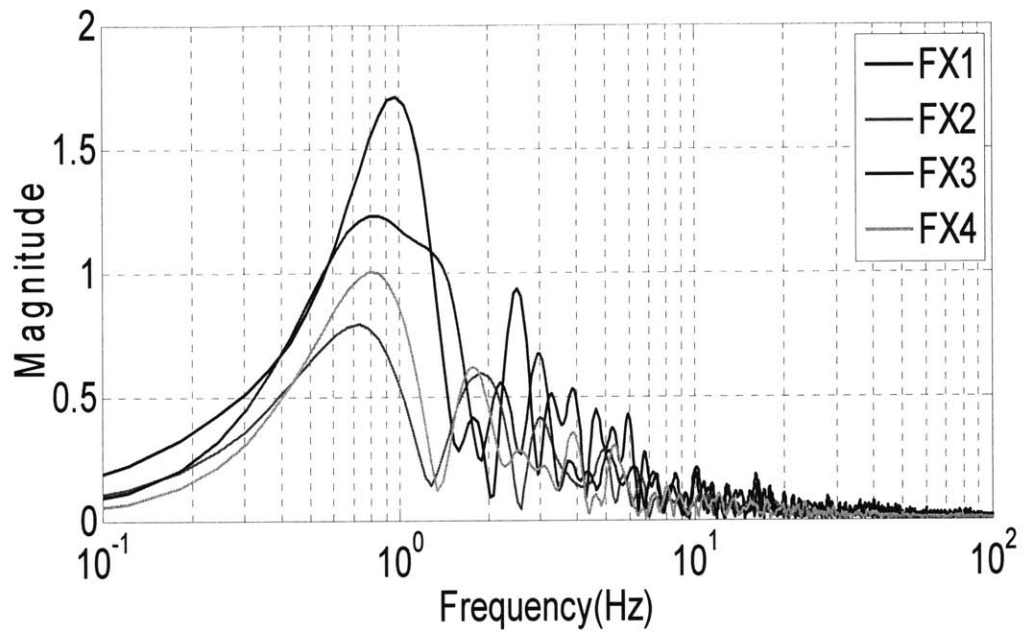
(a) wind force

1: Square, 2: Corner-recession, 3: Setback 4: 180 degree helical

Figure 6.16 power spectral density of wind force coefficients
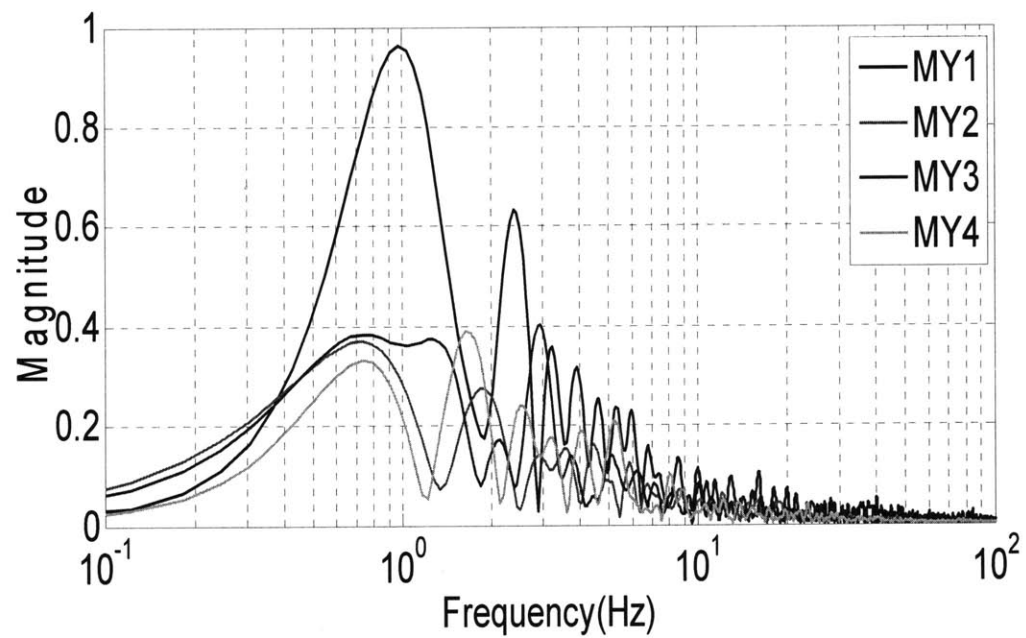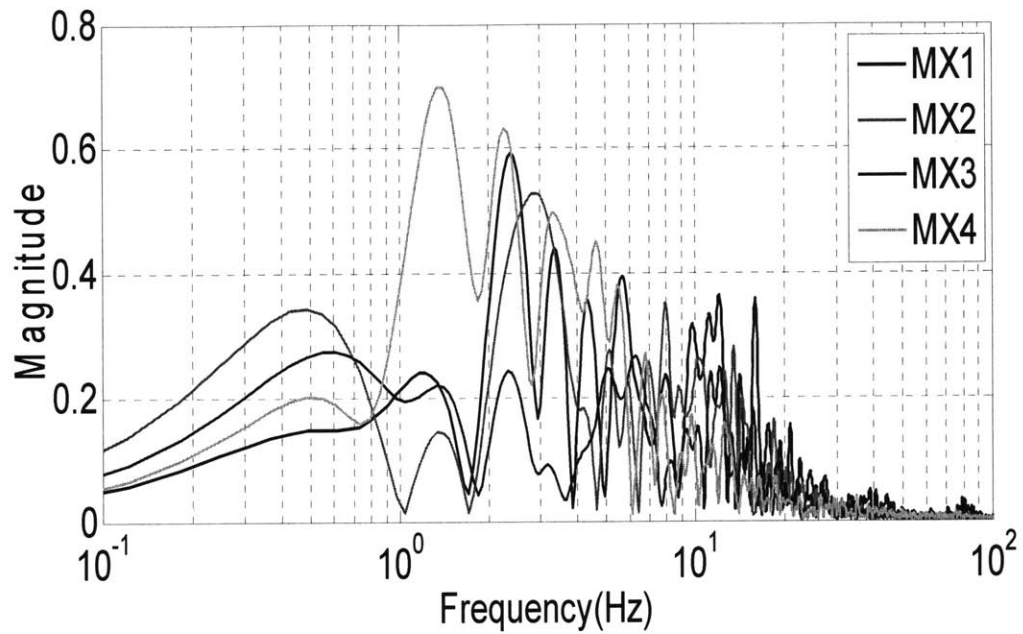
(b) wind moment

1: Square, 2: Corner-recession, 3: Setback 4: 180 degree helical

Figure 6.17 power spectral density of wind moment coefficients

6.5 References

Murakami S. Overview of Turbulence Models applied in CWE-1997. Journal of Wind Engineering and Industrial Aerodynamics 1998; 74-76: 1-24.

Rodi W. 1979, Influence of Buoyance and Rotation on Equations for the Turbulent length Scale, Proc. 2nd Symp. On Turbulent Shear Flows.

Mockett C. 2009, A Comprehensive Study of Detached-Eddy Simulation, PhD Thesis.

STAR-CD Adapco 2009, Methodology, STAR-CD Version 4.12

Tamura Y. 1998, Application of Damping Devices to Duppress Wind-Induced Responses of Buildings, Journal of Wind Engineering And Industrial Aerodynamics, 74-76 (1998), pp.49-72.

Chapter 7 Conclusions

There have been three skyscraper booms throughout history since the 1880s. The first boom had been from the 1880s, through the panic of 1907, until the Great Depression in the 1930s. This period utilized the steel skeletal frames encased in masonry walls which made construction of tall buildings higher than 300m possible. Designed in Art-Deco, many tall buildings still had tripartite subdivisions and florid decorations from Gothic and Renaissance styles.

⇒ Section 2.2

During the second one, Modernism since the 1950s had affected the shapes of tall buildings. These buildings are like rectangular prism with no or little decorations. More based on high technology and materials rather than on exterior decorations, tall buildings (1940-1980) employed modified framed tube systems like Aon Center and John Hancock Center and Willis Tower.

⇒ Section 2.3

For the third skyscraper boom since the 1980s, postmodernism with technological innovations has permeated into tall buildings. Exuberant and liberal atmosphere produces the free forms of tall buildings which also represent eclecticism; Jin Mao Building carries the regional and cultural features. Moreover, tall buildings like art sculpture are proposed and constructed like the 71 story Phare Tower.

⇒ Section 2.4

Although tall buildings express powerful iconic images, esthetics, affluence, and visibility, the construction cost is considerably larger and the design of them is much more daunting. Moreover, the recent high rise buildings pursuit free-style forms completely distinct from symmetry shapes. Although seemingly the current technology sufficiently predict and prevent the adverse responses of tall buildings excited by the wind, some problems such

as habitability, pedestrian comport and wind induced noise have long remained to be solved.

⇒ Section 3.2 to 3.5

With the development of sophisticated structural design and computer analysis, various irregular, sculpture-like shapes of tall buildings emerged since the 2000s can be feasible enough to be constructed. However, the design of tall buildings based on this technology depends to a large extent on the several assumptions like accumulated experiences. Therefore, the performance of tall buildings constructed in this way can affect the serviceability and occupant comfort because the precise values of parameters in structures such as damping cannot be predicted before the construction. Thus, the accuracy and validity of analytical results should be assessed with respect to actual performance of tall buildings. Nevertheless, the experiment on full-scaled model is so limited, so the full scale monitoring of the performance of actual tall buildings already built becomes the pragmatic means for verifying and improving analytical practices.

⇒ Section 4.1 to 4.2

Uncertainty in structural design and wind tunnel test and irregular, unsymmetrical shapes and flexibility in tall building make tall buildings highly vulnerable to excessive levels of vibrations under wind activities, thereby severely affecting serviceability and occupant comfort. Various methods to mitigate these adverse effects have been introduced. Example of these means are aerodynamic modifications like corner-cut and changing sectional areas or plan shape with height, auxiliary damping devices like Tuned Mass Damper and Active Variable Stiffness and structural design like increasing mass or stiffness.

⇒ Section 5.1

Many researchers have identified that corner modifications such as corner roundness, corner recession, chamfered corners, fitting of small fins and vented fins to the corners and slotted corners are considerably effective to reduce the alongwind and crosswind

response, compared to original building plan shape without any corner modification. In addition, these modifications effectively preclude the aero-elastic instability. In particular, chamfered model reduces the across wind responses by 30% when compared to the model without modification (Holmes 2001). However, the larger corner-cut and corner recession increase the instability at low velocity while they decrease the instability at high velocity (Kawai 1998a). Moreover, the effect of the corner modifications may be diminished in the cross-wind direction because the vortex shedding process is very sensitive to the level of turbulence; therefore, the benefit of corner modifications is uncertain in urban terrain and interference by neighboring buildings where the level of wind turbulence is high (Kowk 1998b).

⇒ Section 5.2

In addition, changing the cross sectional shape or areas along the height of a tall building significantly suppresses the crosswind responses. Although increasing taper ratio shows no conspicuous changes in along-wind direction, this increasing taper ratio in across-wind direction decreases the peak of force spectrum and broadens its band width (Kim and You 2002). As one of major modifications, opening completely through a tall building considerably reduce vortex shedding induced forces and the crosswind dynamic response; this effect is particularly more evident when the openings are positioned near at the top pd the building (Dutton and Isyumov 1990).

⇒ Section 5.3

The mean wind force coefficient value of setback model indicates 70% of that of square model. For fluctuating wind force coefficient, square model and corner recession model show the across-wind component larger than the along-wind component. However, the inverse trend is shown in setback model and helical model. Therefore, the square model shows that the sharp peak, in the acrosswind power spectra, significantly reduces when compared to other models. The peak value corresponding to a 500-year return period wind speed of the 180 degree helical model is about 0.05 that of the square model. The

maximum displacement of the square model is 0.015H, while that of the 180 degree

helical model is 0.003H; the setback model's is 0.004H. Therefore, the 180 degree helical

model is the most effective structural shape of models in terms of safety and habitability

criteria (Tamura 2010).

⟹ Section 5.3.1

Based on the results obtained from many researchers, the square model without

modification, corner-recession model, setback model, and 180 degree helical model are

evaluated. Shown is good agreement between the wind tunnel test results conducted by

Tamura and the numerical simulation results by DES version. Rather than in square model,

the other models are shown to effectively reduce the wind force and moment. This is the

reason that aerodynamic modifications suppress the vortex shedding with the smaller

recirculation regions.

⟹ Section 6.4 to 6.4.1

Like in the research (Tamura 2010), the distributions of mean wind pressure on the

windward surfaces of four models are almost identical. However, on the across-wind

surface of the square model, negative regions are distributed mainly in the area from the

bottom to 0.3H. For the corner recession model, negative wind pressure much smaller than

that of the square model is distributed more widely. The 180 degree helical model and the

setback model shows better distribution of wind pressure than those of the others.

⟹ Section 6.4.2

The wind force coefficient in the wind direction remains almost constant in 0.15 to 0.18

because constant wind force acts on the windward surfaces. On the other hand, the wind

force coefficient in the across-wind direction fluctuates because of the vortex shedding.

The wind force coefficient acting on the both sides of a model has a mean value of 0.0.

Vortices are shed alternatively first from one side and then from the other one, thereby

inducing pressure difference. Like wind force coefficients in the along-wind and

transverse-wind directions, wind moment coefficients show similar patterns.

⇒ Section 6.4.3

In the power spectral density of wind force coefficients, the sharp peak in the square model appears at 1.0 Hz; the value of the largest peak in each model is 1.7 in the square model 1.2 in the setback model, 1.0 in helical model, and 0.8 in the corner recession model. In the power spectral density of wind moment coefficients, shape modified models show much smaller values, about 40% of the value of the square model.

⇒ Section 6.4.3

From the numerical analysis, it is observed that armed with aerodynamic modifications, these fluidic designed tall buildings can be aesthetically and innovatively designed by suppressing adverse effects by the wind. Therefore, engineers can achieve significant reduction in wind responses by providing these fluidic designed modifications.

Appendices

Appendix A: Model Mesh
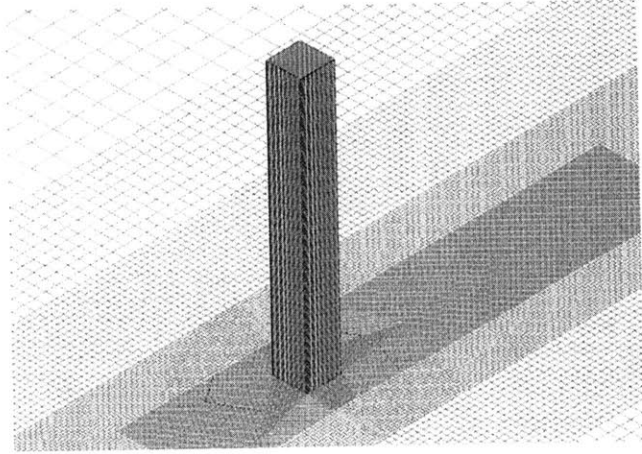
Figure 1: Square Model
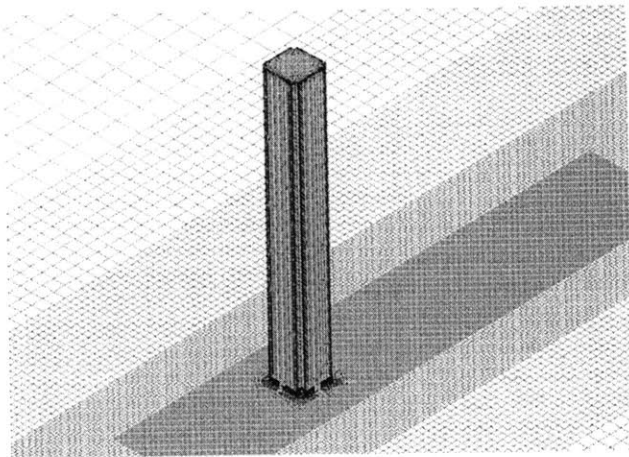
Figure 2: Corner Recession Model
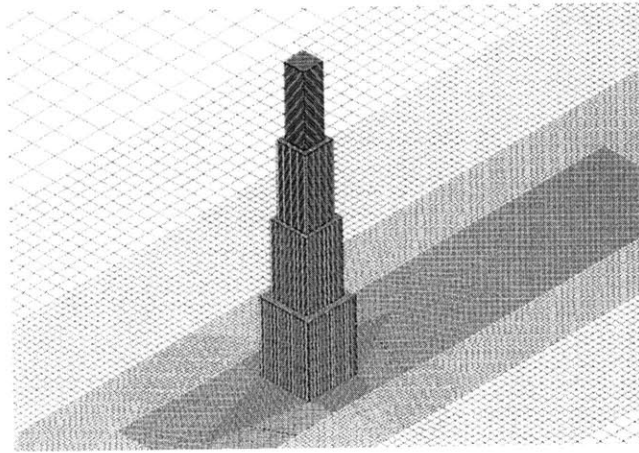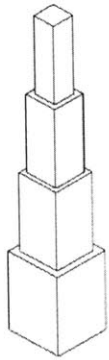
Figure 3: Setback Model
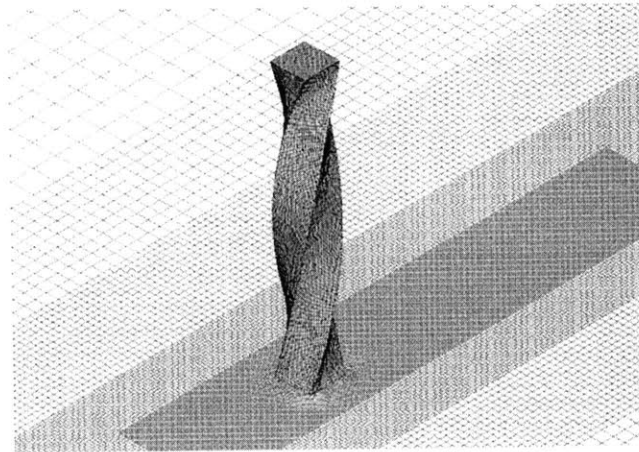
Figure 4: Helical Model

Table 1 Mesh Detailed

Model Mesh	Number of Elements	Number of Nodes
Square Model	8,969,474	9,107,692
Corner Recession Model	8,930,921	9,164,888
Setback Model	8,865,089	9,098,433
180 degree Helical Model	8,868,938	9,088,336

Appendix B: Brief Procedure in Numerical Analysis
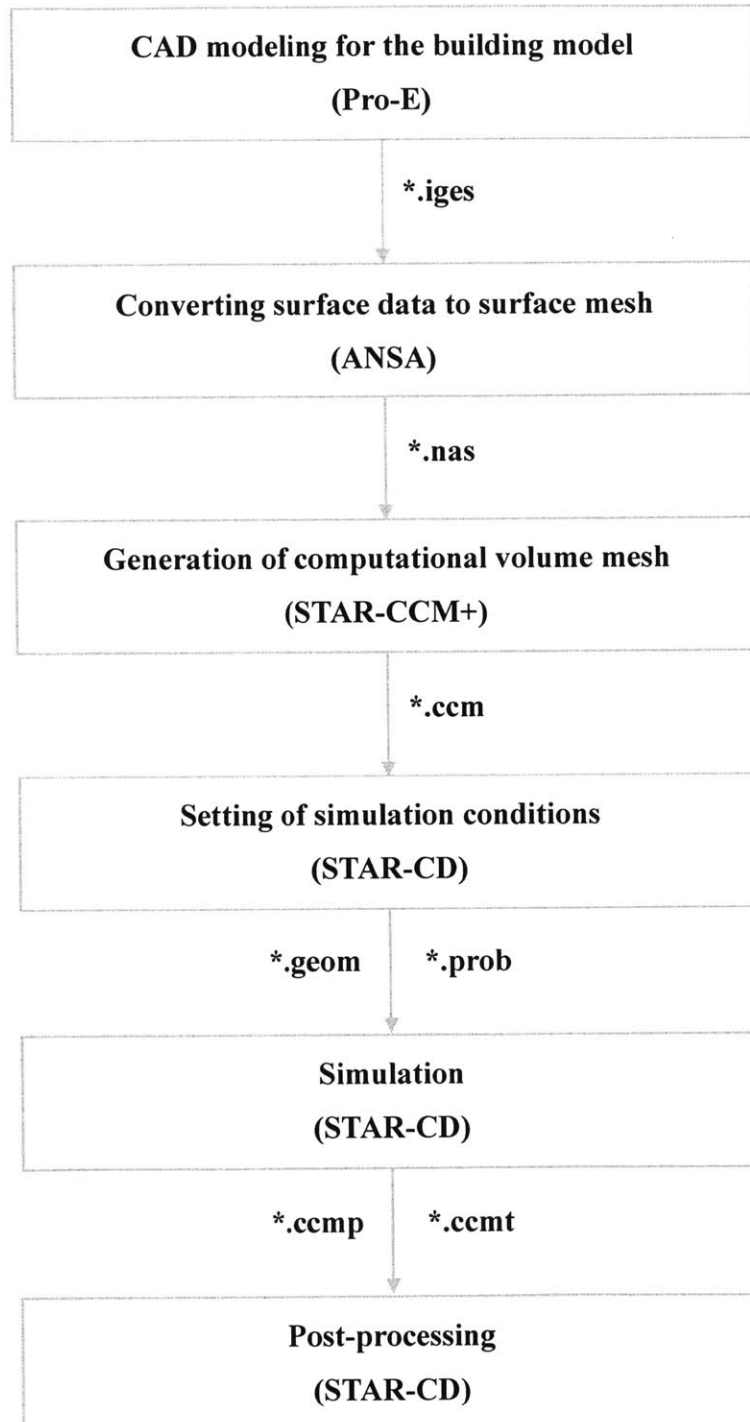
```
┌─────────────────────────────────────────────┐
│      CAD modeling for the building model      │
│                   (Pro-E)                     │
└─────────────────────────────────────────────┘
                       │ *.iges
                       ▼
┌─────────────────────────────────────────────┐
│    Converting surface data to surface mesh    │
│                   (ANSA)                      │
└─────────────────────────────────────────────┘
                       │ *.nas
                       ▼
┌─────────────────────────────────────────────┐
│    Generation of computational volume mesh    │
│                (STAR-CCM+)                    │
└─────────────────────────────────────────────┘
                       │ *.ccm
                       ▼
┌─────────────────────────────────────────────┐
│         Setting of simulation conditions      │
│                 (STAR-CD)                     │
└─────────────────────────────────────────────┘
            *.geom     │ *.prob
                       ▼
┌─────────────────────────────────────────────┐
│                  Simulation                   │
│                 (STAR-CD)                     │
└─────────────────────────────────────────────┘
            *.ccmp     │ *.ccmt
                       ▼
┌─────────────────────────────────────────────┐
│                Post-processing                │
│                 (STAR-CD)                     │
└─────────────────────────────────────────────┘
```

Flow characteristics around a square model (velocity)

TIME = 0.200000E-01

H=400

L   y   D

α = 0°

α

x

50

B=50   D=50

Square model (Tamura et al., 2010)

x-y section at z=0.25H

(z=0.25H)   (z=0.50H)   (z=0.75H)   (z=0.75H)

x-z section at z=0.25H
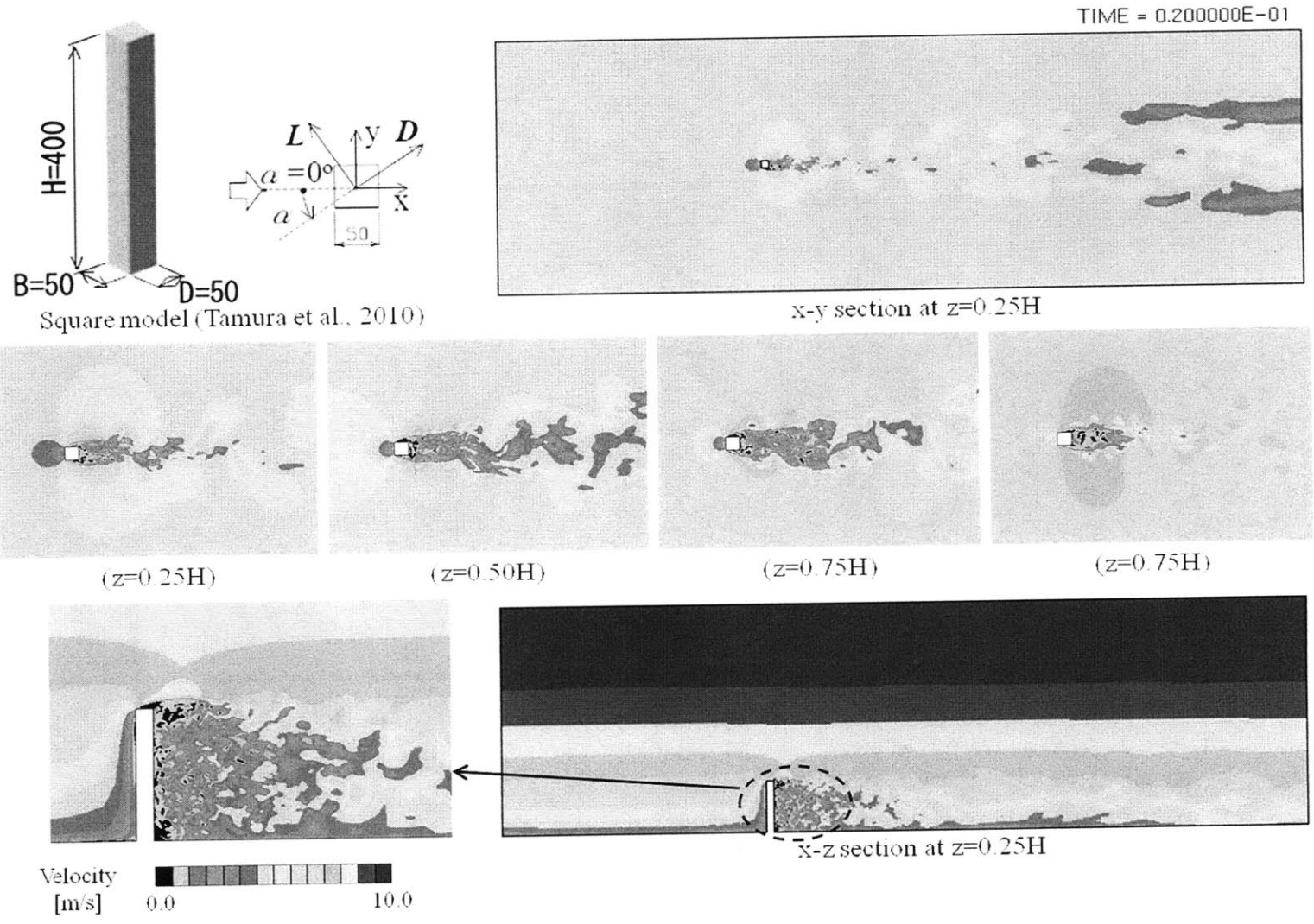
Velocity
[m/s]   0.0   10.0

Flow characteristics around a square model (pressure)

TIME = 0.200000E-01

Square model (Tamura et al., 2010)

x-y section at z=0.25H

H=400

B=50 D=50

L y D
α =0°
X
α
50

(z=0.25H)   (z=0.50H)   (z=0.75H)   (z=0.75H)

x-z section at z=0.25H

Pressure
[Pa]   -10.0   15.0
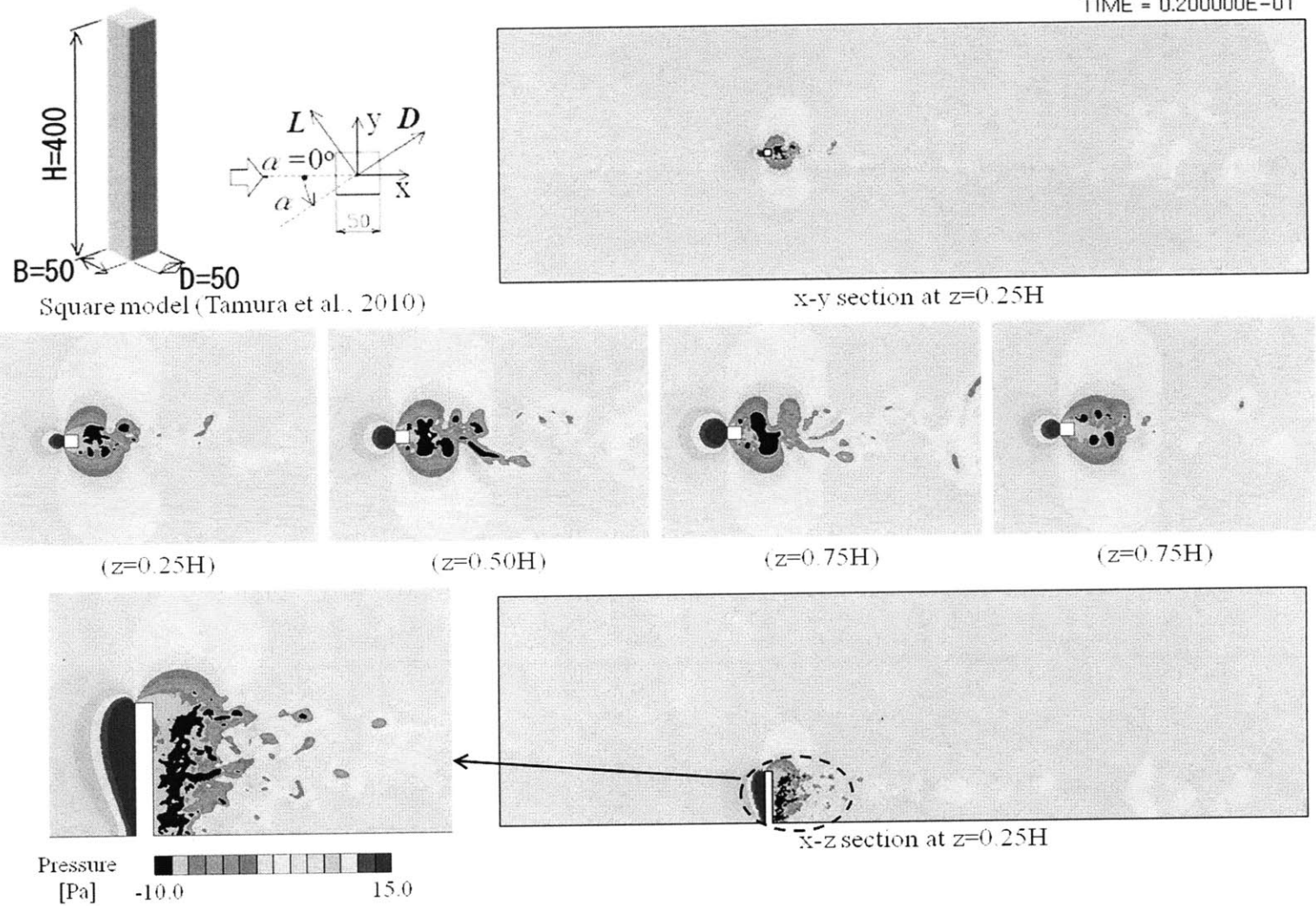
Flow characteristics around a corner recession model (velocity)
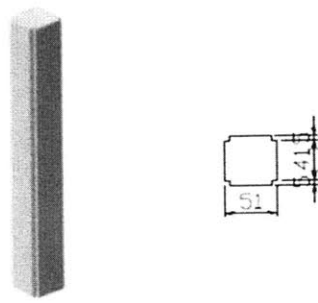
TIME = 0.200000E-01

Corner cut model (Tamura et al., 2010)
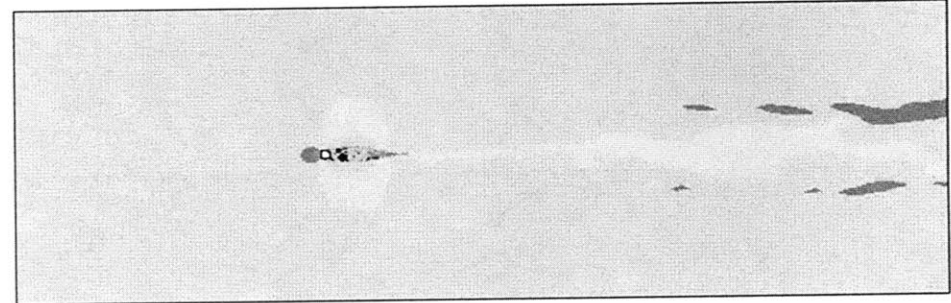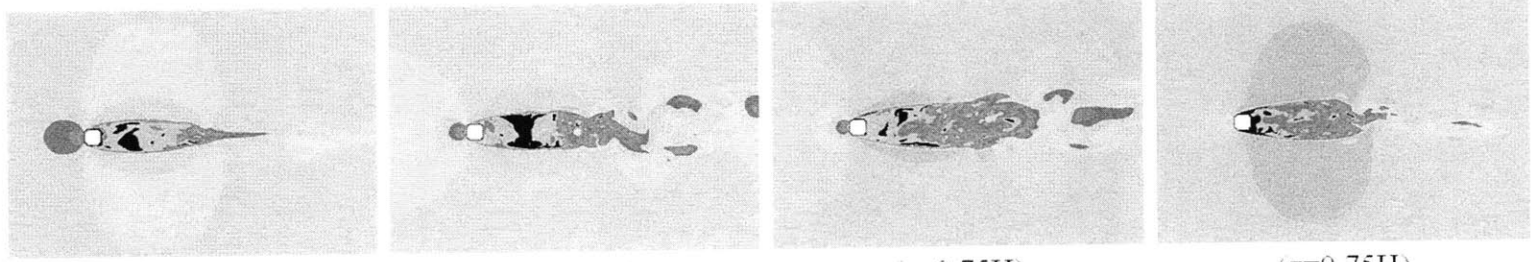
x-y section at z=0.25H

(z=0.25H)
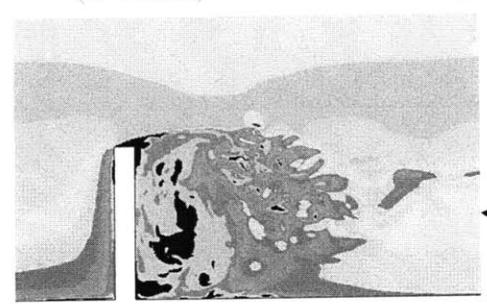
(z=0.50H)

(z=0.75H)

(z=0.75H)

x-z section at z=0.25H

Velocity
[m/s]   0.0   10.0
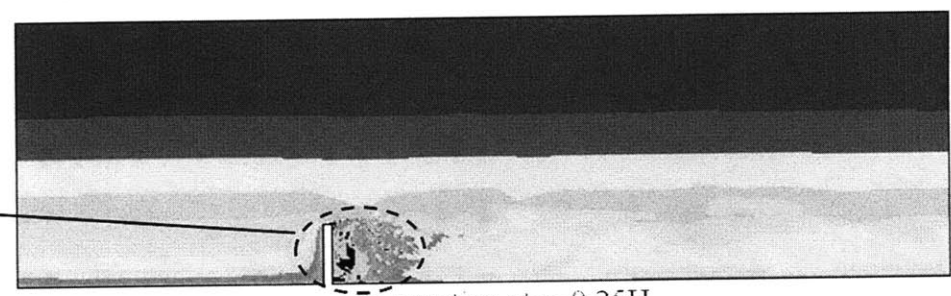
Flow characteristics around a corner recession model (pressure)

TIME = 0.200000E-01
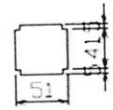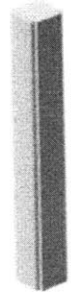
Corner cut model (Tamura et al., 2010)
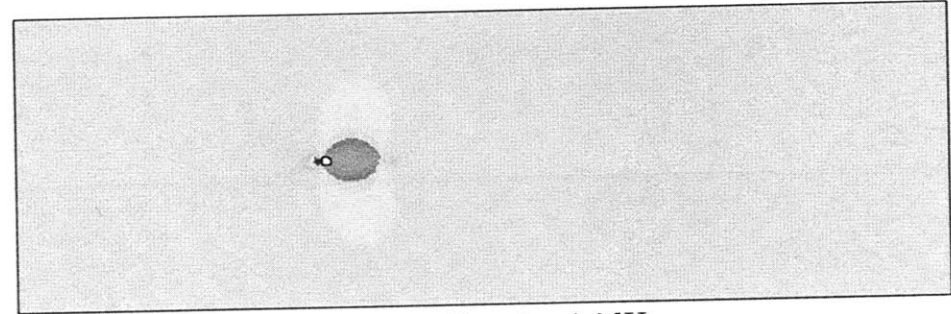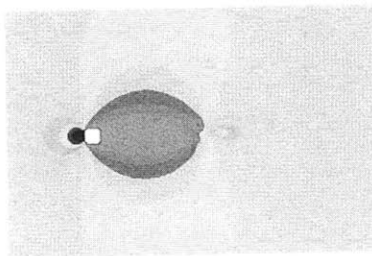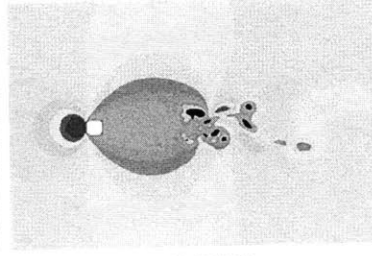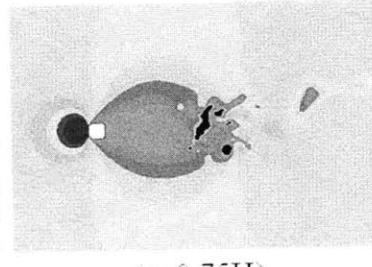
x-y section at z=0.25H
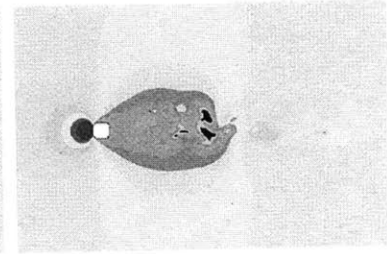
(z=0.25H)
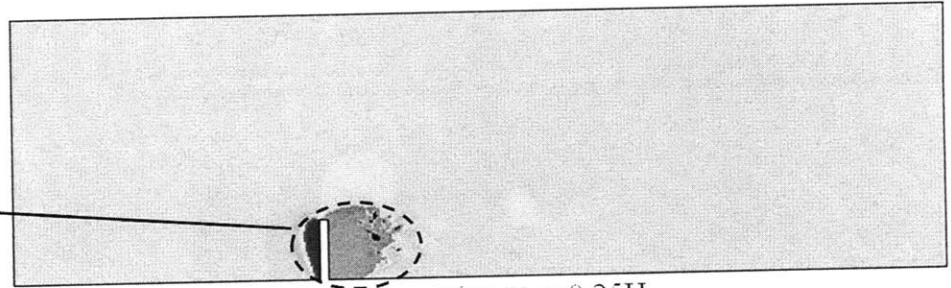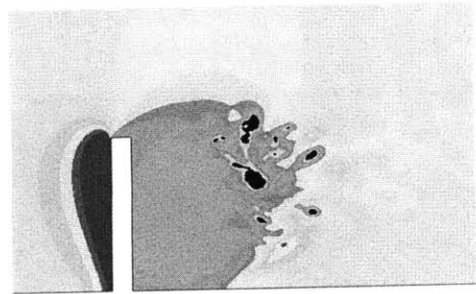
(z=0.50H)

(z=0.75H)

(z=0.75H)

x-z section at z=0.25H

Pressure
[Pa]   -10.0   15.0

Flow characteristics around a setback model (velocity)
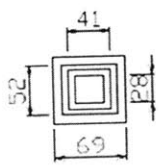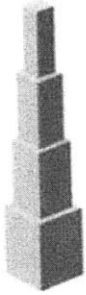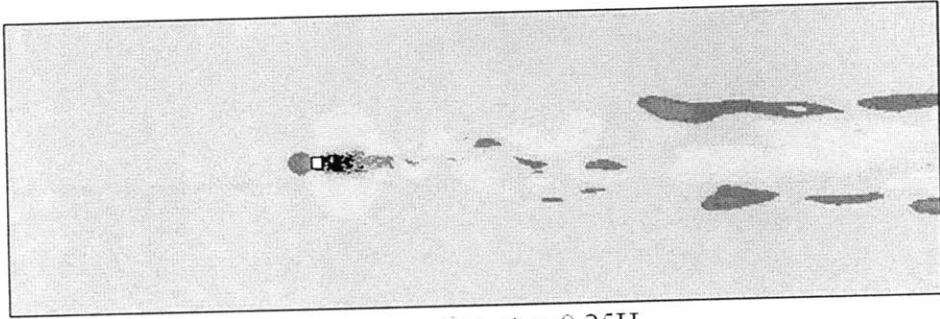
Setback model (Tamura et al., 2010)
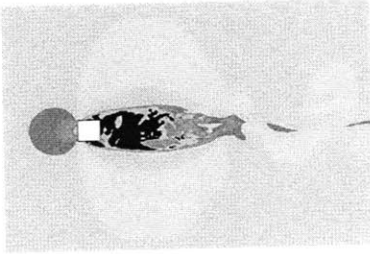
x-y section at z=0.25H
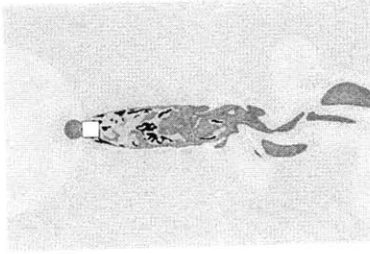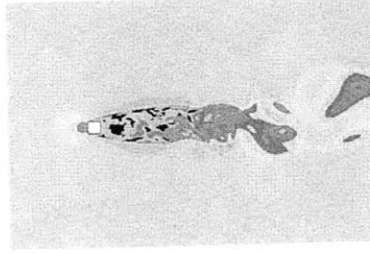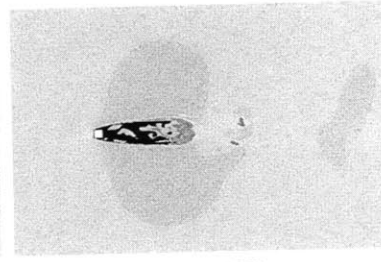
(z=0.25H)　　　　(z=0.50H)　　　　(z=0.75H)　　　　(z=0.75H)
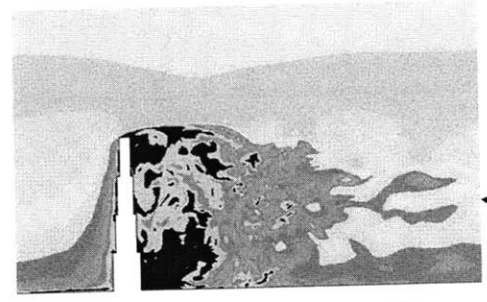
x-z section at z=0.25H

Velocity
[m/s]　　0.0　　　　　10.0

Flow characteristics around a setback model (pressure)

TIME = 0.200000E-01
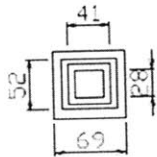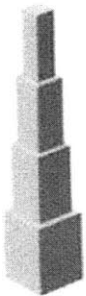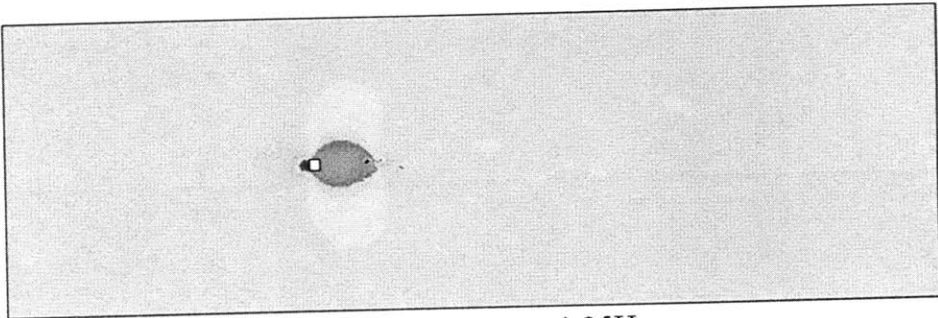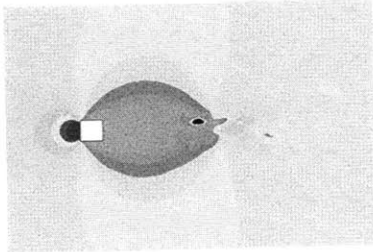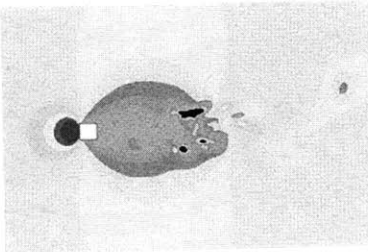
x-y section at z=0.25H

Setback model (Tamura et al., 2010)

41
52
69
P8
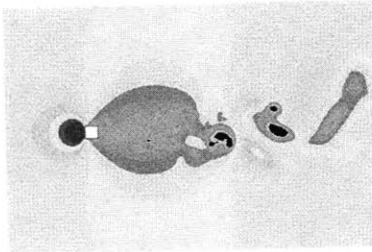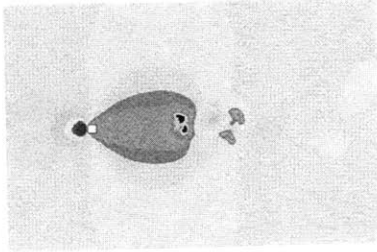
(z=0.25H)
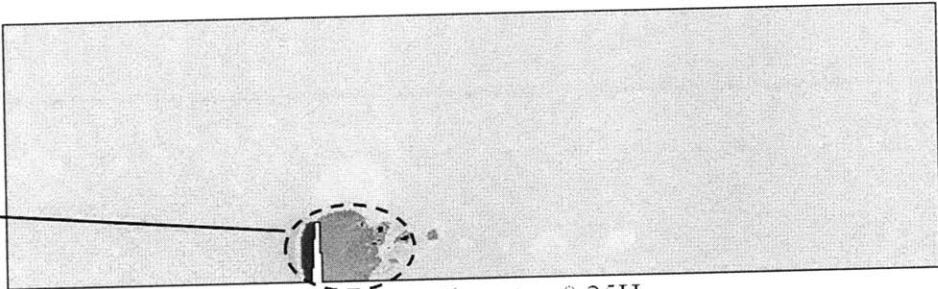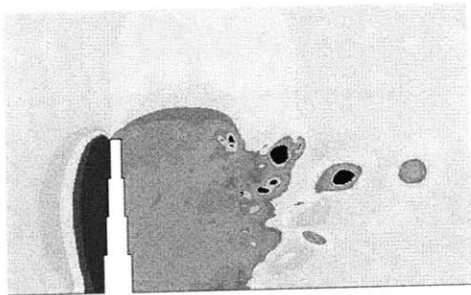
(z=0.50H)

(z=0.75H)

(z=0.75H)

x-z section at z=0.25H

Pressure [Pa]   -10.0   15.0

Flow characteristics around a 180° helical model (velocity)

TIME = 0.200000E-01
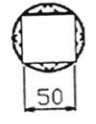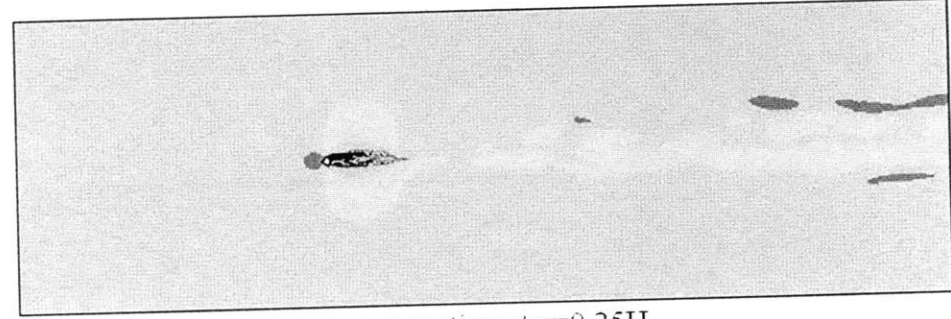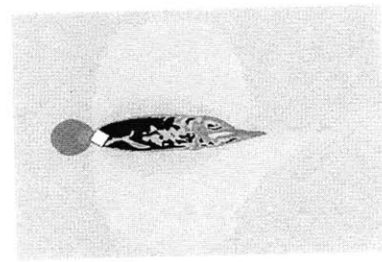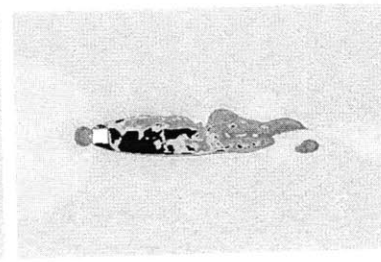
Helical model (Tamura et al., 2010)

x-y section at z=0.25H
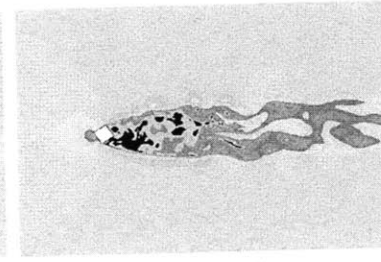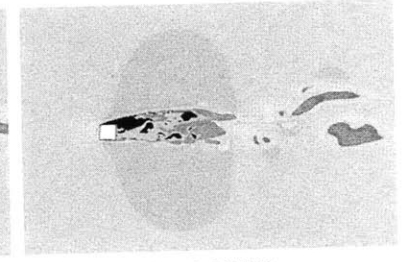
(z=0.25H)
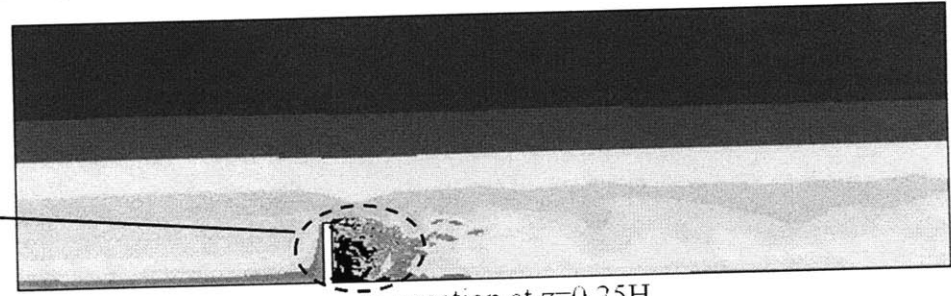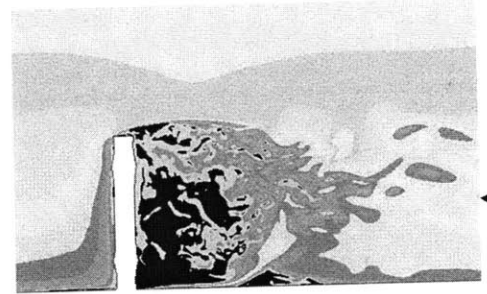
(z=0.50H)

(z=0.75H)

(z=0.75H)

x-z section at z=0.25H

Velocity [m/s]   0.0   10.0

Flow characteristics around a 180° helical model (pressure)

TIME = 0.200000E-01
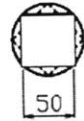
Helical model (Tamura et al., 2010)
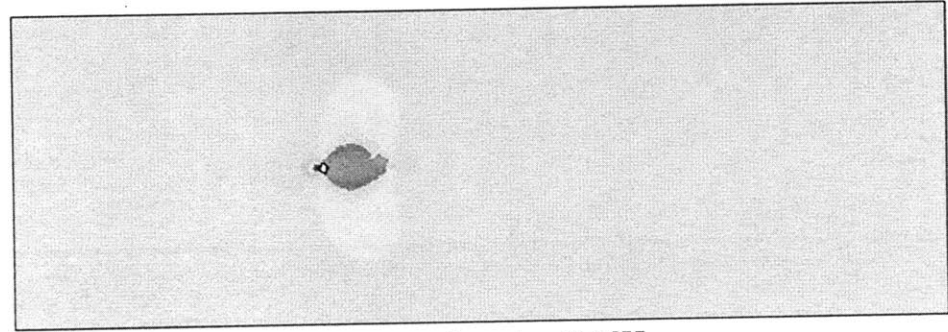
50
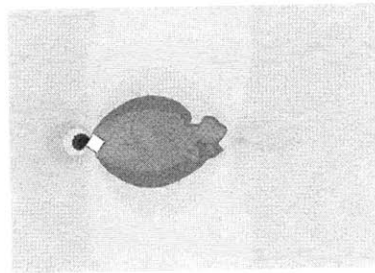
x-y section at z=0.25H
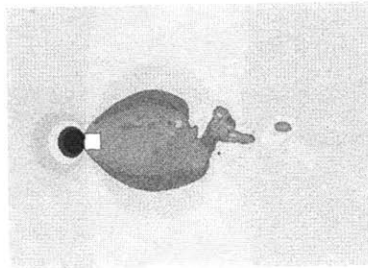
(z=0.25H)

(z=0.50H)
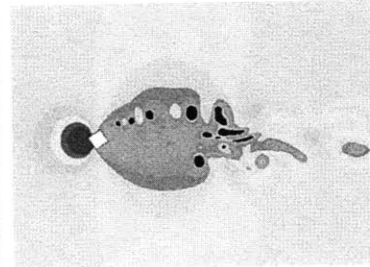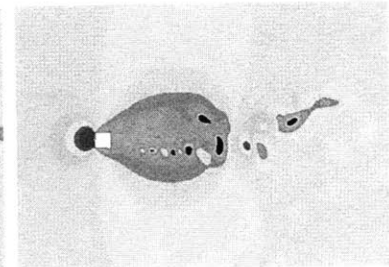
(z=0.75H)

(z=0.75H)
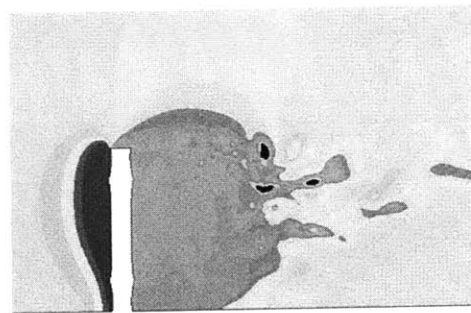
x-z section at z=0.25H

Pressure
[Pa]   -10.0   15.0
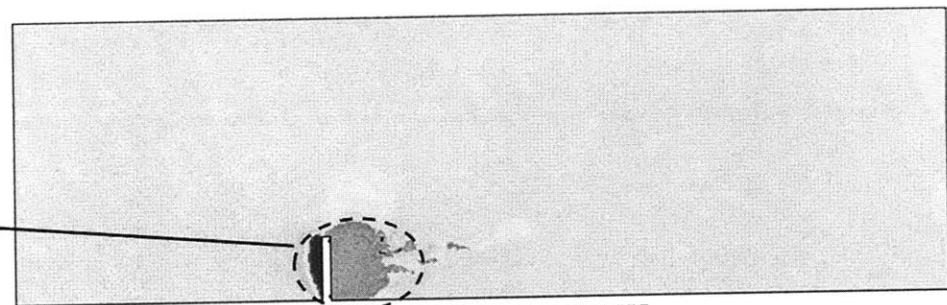
Appendix D: Post-processing for CFD simulation (STAR-CD V.4.14)

1. Mesh Generation, Analysis Features and Run Time Control
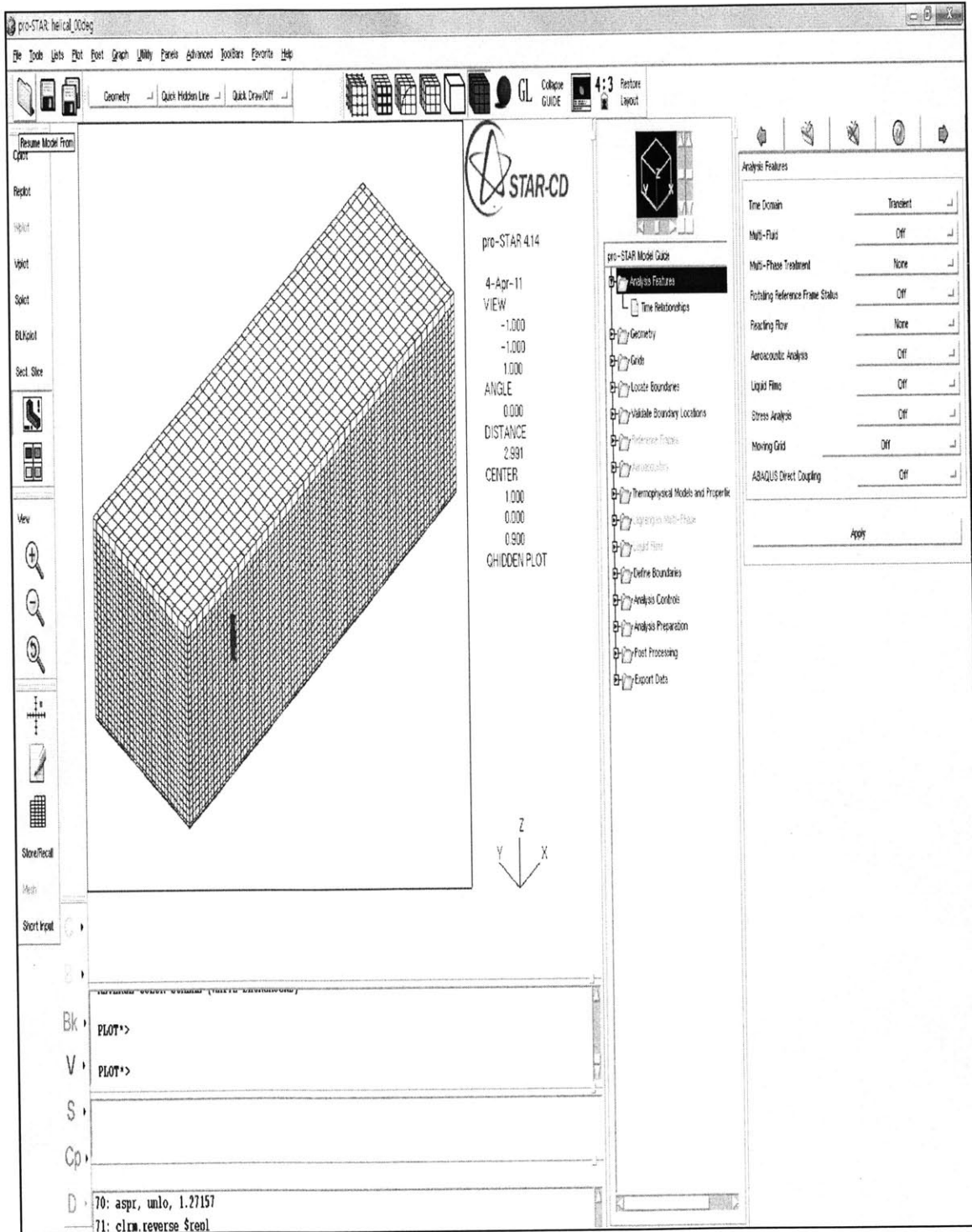
pro-STAR Model Guide

- Analysis Features
  - Time Relationships
- Geometry
- Grids
- Locate Boundaries
- Validate Boundary Locations
- Reference Frames
- Aeroacoustics
- Thermophysical Models and Propertie
- Lagrangian Multi-Phase
- Liquid Films
- Define Boundaries
- Analysis Controls
- Analysis Preparation
- Post Processing
- Export Data

Analysis Features

Time Domain	Transient
Multi-Fluid	Off
Multi-Phase Treatment	None
Rotating Reference Frame Status	Off
Reacting Flow	None
Aeroacoustic Analysis	Off
Liquid Films	Off
Stress Analysis	Off
Moving Grid	Off
ABAQUS Direct Coupling	Off

Apply
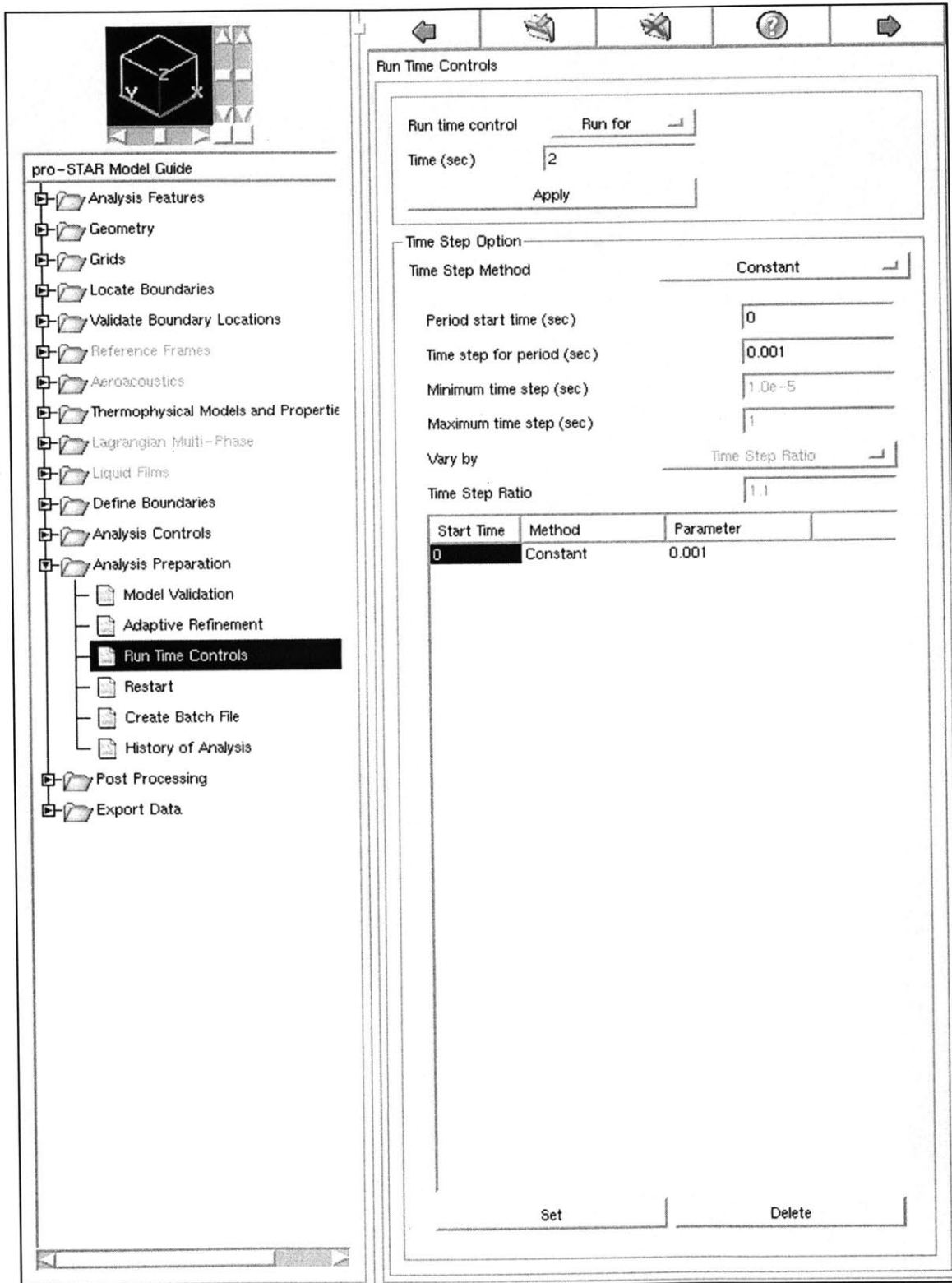
pro-STAR Model Guide

- Analysis Features
- Geometry
- Grids
- Locate Boundaries
- Validate Boundary Locations
- Reference Frames
- Aeroacoustics
- Thermophysical Models and Propertie
- Lagrangian Multi-Phase
- Liquid Films
- Define Boundaries
- Analysis Controls
- Analysis Preparation
  - Model Validation
  - Adaptive Refinement
  - Run Time Controls
  - Restart
  - Create Batch File
  - History of Analysis
- Post Processing
- Export Data

Run Time Controls

Run time control   Run for

Time (sec)   2

Apply

Time Step Option

Time Step Method   Constant

Period start time (sec)   0

Time step for period (sec)   0.001

Minimum time step (sec)   1.0e-5

Maximum time step (sec)   1

Vary by   Time Step Ratio

Time Step Ratio   1.1

Start Time	Method	Parameter	
0	Constant	0.001	

Set   Delete

2. Create Boundaries & Define Boundary Regions

	Type	Name
0	Wall	Default_Boundary_Region
1	Wall	face_top
2	Inlet	boun_inlet
3	Symplane	boun_slipwall_1
4	Symplane	boun_slipwall_2
5	Symplane	boun_slipwall_3
6	Outlet	boun_outlet
7	Wall	boun_ground
8	Wall	face_front
9	Wall	face_side_1
10	Wall	face_side_2
11	Wall	face_rear
12		

pro−STAR Model Guide

- Analysis Features
- Geometry
- Grids
- Locate Boundaries
  - Import Boundaries
  - Create Boundaries
- Validate Boundary Locations
- Reference Frames
- Aeroacoustics
- Thermophysical Models and Propertie
- Lagrangian Multi−Phase
- Liquid Films
- Define Boundaries
- Analysis Controls
- Analysis Preparation
- Post Processing
- Export Data

Create Boundaries

Regions | Cyclics | Couples | Patches

Boundary Regions

Type — Wall
Name — ult_Boundary_Region

Define | Delete

Create/Modify Boundaries

Action List

- Create by Picking Cell Faces
- Create by Picking a Zone
- Create by Picking Surface based on Edges
- Create by Picking Surface based on Vset
- Change Current Boundary Set
- Change Cursor Selected Region
- Change Zone
- Delete All in Region
- Delete Current Boundary Set
- Delete Cursor Selected Region
- Delete Zone

Apply

Compress | Merge
Plot All | Plot Region | Count

pro-STAR Model Guide

- ▷ 📁 Analysis Features
- ▷ 📁 Geometry
- ▷ 📁 Grids
- ▽ 📁 Locate Boundaries
  - 📄 Import Boundaries
  - 📄 Create Boundaries
- ▷ 📁 Validate Boundary Locations
- ▷ 📁 Reference Frames
- ▷ 📁 Aeroacoustics
- ▷ 📁 Thermophysical Models and Propertie
- ▷ 📁 Lagrangian Multi-Phase
- ▷ 📁 Liquid Films
- ▽ 📁 Define Boundaries
  - 📄 Define Boundary Regions
  - 📄 Scalar Boundaries
- ▷ 📁 Analysis Controls
- ▷ 📁 Analysis Preparation
- ▷ 📁 Post Processing
- ▷ 📁 Export Data

Define Boundary Regions

| Region Setup | Plot Boundary | Porous Couples |

	Region Type	Region Name
0	Wall	Default_Boundary_Region
1	Wall	face_top
2	Inlet	boun_inlet
3	Symplane	boun_slipwall_1
4	Symplane	boun_slipwall_2
5	Symplane	boun_slipwall_3
6	Outlet	boun_outlet
7	Wall	boun_ground

Region Type	Wall
Region Name	ult_Boundary_Region
User Option	Standard
Table Name	📁

Wall Parameters

Slip	No
Coordinate System	1
Omega (rpm)	0
Wall U (m/s)	0
Wall V (m/s)	0
Wall W (m/s)	0
Roughness	Standard
Elog	9
Displacement (m)	
A	
B	
C	
Wall Heat	Adiabatic
Emissivity	1
Reflectivity	0
Transmissivity	0
Solar Heating	Exposed

125

```
C******************************************************************
**
      SUBROUTINE BCDEFI(SCALAR,U,V,W,TE,ED,T,DEN,TURINT,RSU,V2P,F2P)
C     Boundary conditions at inlets
C******************************************************************
**
      REAL*8 VEL_REF,Z_REF,VEL_ALPHA,TUR_REF,TUR_ALPHA

      VEL_REF   = 7.0
      Z_REF     = 0.4
      VEL_ALPHA = 0.27

      TUR_REF   = 0.2
      TUR_ALPHA = -0.32

      IF (IREG.EQ.2) THEN
         U   = VEL_REF * (Z / Z_REF)**VEL_ALPHA
         V   = 0.0
         W   = 0.0
         TURINT = .TRUE.
         TE = TUR_REF * (Z / Z_REF)**TUR_ALPHA
         ED = 0.133
         DEN = 1.205
      ENDIF

      RETURN
      END
C******************************************************************
**
```

3. Material Properties (Fluids) and Turbulence Models (DES)

pro-STAR Model Guide	Material Properties (Fluids)

pro-STAR Model Guide

- ▶ Analysis Features
- ▶ Geometry
- ▶ Grids
- ▶ Locate Boundaries
- ▶ Validate Boundary Locations
- ▶ Reference Frames
- ▶ Aeroacoustics
- ▼ Thermophysical Models and Propertie
  - Thermal Options
  - Solid Stress Options
  - Gravity
  - ▼ Liquids and Gases
    - **Material Properties (Fluids)**
    - Turbulence Models
    - Thermal Models
    - Fluid Initialization
    - Monitoring and Reference D
    - Buoyancy
  - ▶ Eulerian Multi-Phase
  - ▶ Reacting Flow
  - ▶ Additional Scalars
  - ▶ Multifluid
  - ▶ Solids
  - ▶ Porosity
  - ▶ Sources
- ▶ Lagrangian Multi-Phase
- ▶ Liquid Films
- ▶ Define Boundaries
- ▶ Analysis Controls
- ▶ Analysis Preparation
- ▶ Post Processing
- ▶ Export Data

Material Properties (Fluids)

Define user material

Material # | 1 | AIR

Molecular Properties | Mechancial Properties

Density	Constant
Density (kg/m3)	1.205
Thermal Expan. Coef. (1/K)	0
a0 (kg/m3)	0
a1 (Pa)	0

Molecular Viscosity	Constant
mu (kg/ms)	1.81e-05
EN	1.81e-05
	Define Polynomial

Specific Heat	Constant
Cv (J/kgK)	1006
	Define Polynomial

Conductivity	Constant
k (W/mK)	0.02637
	Define Polynomial

Molecular Weight (kg/kmol)	28.96

Apply	Delete	Defaults

User Define

pro-STAR Model Guide

- Analysis Features
- Geometry
- Grids
- Locate Boundaries
- Validate Boundary Locations
- Reference Frames
- Aeroacoustics
- Thermophysical Models and Propertie
  - Thermal Options
  - Solid Stress Options
  - Gravity
  - Liquids and Gases
    - Material Properties (Fluids)
    - **Turbulence Models**
    - Thermal Models
    - Fluid Initialization
    - Monitoring and Reference D
    - Buoyancy
  - Eulerian Multi-Phase
  - Reacting Flow
  - Additional Scalars
  - Multifluid
  - Solids
  - Porosity
  - Sources
- Lagrangian Multi-Phase
- Liquid Films
- Define Boundaries
- Analysis Controls
- Analysis Preparation
- Post Processing
- Export Data

Turbulence Models

| Material # | 1 | AIR |
| Turbulence | | On |

| Turbulence | Near-wall Treatment | Multiphase Options |

| Model | k-Epsilon/High Reynolds Number |

C-Mu	0.09
C-Eps1	1.44
C-Eps2	1.92
C-Eps3	1.44
C-Eps4	-0.33
CAPPA	0.419
Prandtl (K.E.)	1
Prandtl (Eps)	1.219
Prandtl (Enth)	Value
User Define	0.9

DES | Blend
L | 0 | Vel | 0
Time Averaging
Step to start averaging | 1

Apply | User Define | Defaults

128

Appendix E:

Data of Pressure Characteristics of the Square Model and the Helical Model

	Square Model C_Mx	Helical Model C_Mx	Square Model C_My	Helical Model C_My
0	0.001095	0.001675	0.096911	0.085279
0.001	0.001067	0.001668	0.097023	0.085334
0.002	0.001032	0.001654	0.097102	0.085378
0.003	0.000975	0.001637	0.097142	0.085413
0.004	0.000888	0.001617	0.09714	0.085439
0.005	0.000772	0.001598	0.0971	0.085461
0.006	0.000634	0.001577	0.097033	0.085479
0.007	0.000489	0.001564	0.096953	0.085494
0.008	0.00035	0.001558	0.096875	0.085509
0.009	0.00023	0.00156	0.096813	0.085525
0.01	0.00014	0.001569	0.096779	0.085546
0.011	8.11E-05	0.001582	0.096773	0.08557
0.012	3.66E-05	0.001594	0.09679	0.085603
0.013	-8.9E-06	0.001604	0.096813	0.085643
0.014	-6.4E-05	0.001606	0.096826	0.085688
0.015	-0.00013	0.001605	0.096819	0.085735
0.016	-0.00022	0.001598	0.096794	0.085781
0.017	-0.00031	0.001586	0.096764	0.085828
0.018	-0.0004	0.00157	0.096742	0.085875
0.019	-0.00048	0.001554	0.096742	0.085923
0.02	-0.00053	0.001543	0.096772	0.085973
0.021	-0.00056	0.001534	0.096828	0.086023
0.022	-0.00057	0.001531	0.096901	0.086074
0.023	-0.00056	0.001533	0.096973	0.086125
0.024	-0.00055	0.001541	0.09703	0.08618
0.025	-0.00055	0.001549	0.097063	0.086234
0.026	-0.00056	0.001558	0.09707	0.086285
0.027	-0.00058	0.001566	0.097059	0.086331
0.028	-0.00061	0.001573	0.097042	0.086374
0.029	-0.00064	0.001581	0.097029	0.086415
0.03	-0.00068	0.001593	0.097027	0.086456
0.031	-0.00071	0.001606	0.097036	0.086498
0.032	-0.00074	0.001628	0.097052	0.086539
0.033	-0.00076	0.001651	0.097069	0.086581
0.034	-0.00077	0.001679	0.097084	0.08662
0.035	-0.00078	0.00171	0.097092	0.086657
0.036	-0.00078	0.00174	0.097093	0.086691
0.037	-0.00079	0.00177	0.097086	0.086724
0.038	-0.0008	0.001801	0.097074	0.086756
0.039	-0.00082	0.001834	0.097061	0.086787
0.04	-0.00085	0.001868	0.097051	0.086817
0.041	-0.00089	0.001902	0.097047	0.086847
0.042	-0.00091	0.001935	0.097053	0.086875
0.043	-0.00093	0.001971	0.097068	0.086904
0.044	-0.00093	0.002007	0.097093	0.086935
0.045	-0.00092	0.002044	0.097123	0.086965
0.046	-0.00089	0.002079	0.097157	0.086992
0.047	-0.00085	0.002114	0.097189	0.087013
0.048	-0.00079	0.002146	0.097216	0.087024
0.049	-0.00071	0.002172	0.09724	0.087031
0.05	-0.00063	0.002195	0.097255	0.08703
0.051	-0.00054	0.00221	0.097262	0.08703
0.052	-0.00044	0.00222	0.097262	0.08703
0.053	-0.00034	0.002227	0.097258	0.087031
0.054	-0.00024	0.002233	0.097255	0.087034
0.055	-0.00013	0.002239	0.097255	0.087038
0.056	-2.5E-05	0.002246	0.097265	0.087043
0.057	7.43E-05	0.002256	0.097282	0.087049
0.058	0.000159	0.002269	0.097298	0.087053
0.059	0.000227	0.002283	0.09731	0.087052
0.06	0.000274	0.002295	0.097311	0.087047
0.061	0.000302	0.002308	0.097299	0.087037
0.062	0.000315	0.002316	0.097276	0.087025
0.063	0.00032	0.002326	0.097251	0.087014
0.064	0.000322	0.002329	0.097227	0.087009
0.065	0.000323	0.002333	0.097204	0.087013
0.066	0.000325	0.002335	0.097185	0.087029
0.067	0.000326	0.002334	0.097167	0.087054
0.068	0.000324	0.002334	0.097145	0.087084
0.069	0.000313	0.002336	0.097114	0.087117
0.07	0.000287	0.00234	0.097079	0.08715
0.071	0.000251	0.002346	0.097038	0.087178
0.072	0.000201	0.002353	0.096995	0.087198
0.073	0.000141	0.002359	0.096953	0.087207
0.074	7.61E-05	0.002362	0.096917	0.087209
0.075	1.23E-05	0.002362	0.096889	0.087206
0.076	-3.9E-05	0.00236	0.096873	0.087204
0.077	-7.5E-05	0.002354	0.096871	0.087212
0.078	-9.2E-05	0.002347	0.096884	0.087232
0.079	-9.4E-05	0.002337	0.09691	0.087267
0.08	-8.3E-05	0.002324	0.096945	0.087312
0.081	-6.5E-05	0.002307	0.096977	0.08736
0.082	-4.5E-05	0.002289	0.097002	0.087405
0.083	-3E-05	0.002266	0.097011	0.08744
0.084	-2.4E-05	0.002245	0.097001	0.087466
0.085	-3.1E-05	0.002223	0.096975	0.087486
0.086	-5.8E-05	0.002207	0.09694	0.087504
0.087	-0.0001	0.002194	0.0969	0.087525
0.088	-0.00017	0.002183	0.096855	0.087553
0.089	-0.00025	0.002177	0.096812	0.08759
0.09	-0.00034	0.00217	0.096775	0.08764
0.091	-0.00044	0.002165	0.096742	0.087698
0.092	-0.00053	0.00216	0.096715	0.087765
0.093	-0.00062	0.002154	0.096692	0.087835
0.094	-0.0007	0.002149	0.096674	0.087903
0.095	-0.00078	0.002144	0.096662	0.087964
0.096	-0.00086	0.002142	0.096655	0.088017
0.097	-0.00094	0.002141	0.096653	0.088062
0.098	-0.00101	0.002142	0.096656	0.088102
0.099	-0.00108	0.002146	0.096663	0.088138
0.1	-0.00115	0.002148	0.096672	0.088174
0.101	-0.00121	0.002149	0.096685	0.088211
0.102	-0.00126	0.002153	0.0967	0.088251
0.103	-0.00131	0.002157	0.096724	0.088297
0.104	-0.00137	0.002165	0.096755	0.088342
0.105	-0.00143	0.002176	0.096791	0.088387
0.106	-0.00149	0.002188	0.096829	0.088427
0.107	-0.00154	0.002203	0.096865	0.088463
0.108	-0.00159	0.002216	0.0969	0.088494
0.109	-0.00163	0.002224	0.096923	0.088522
0.11	-0.00165	0.002232	0.096939	0.08855
0.111	-0.00166	0.002233	0.096948	0.088579
0.112	-0.00166	0.002229	0.096958	0.088613
0.113	-0.00167	0.002216	0.096974	0.088656
0.114	-0.00169	0.002195	0.096997	0.088704
0.115	-0.00172	0.002169	0.097018	0.088753
0.116	-0.00177	0.002136	0.097027	0.088799

0.117	-0.00183	0.002101	0.09702	0.088841
0.118	-0.00189	0.002063	0.096992	0.088872
0.119	-0.00194	0.002025	0.096952	0.088898
0.12	-0.002	0.001989	0.096904	0.088919
0.121	-0.00204	0.001955	0.096858	0.08894
0.122	-0.00208	0.001927	0.096816	0.088961
0.123	-0.0021	0.001904	0.096775	0.088982
0.124	-0.00211	0.001883	0.096735	0.089002
0.125	-0.0021	0.001866	0.096687	0.089016
0.126	-0.00208	0.001845	0.096633	0.089024
0.127	-0.00204	0.001824	0.096574	0.089029
0.128	-0.00198	0.0018	0.096521	0.089036
0.129	-0.00192	0.001774	0.09648	0.089047
0.13	-0.00185	0.001747	0.096453	0.089063
0.131	-0.00178	0.001718	0.096442	0.089085
0.132	-0.00171	0.001688	0.096441	0.08911
0.133	-0.00163	0.00166	0.096446	0.089134
0.134	-0.00153	0.001631	0.096445	0.089154
0.135	-0.00142	0.001602	0.096433	0.089165
0.136	-0.0013	0.001575	0.096404	0.089169
0.137	-0.00117	0.001553	0.09636	0.089165
0.138	-0.00102	0.001535	0.096305	0.089155
0.139	-0.00087	0.001522	0.096243	0.089143
0.14	-0.00072	0.001512	0.096183	0.089132
0.141	-0.00058	0.001506	0.096134	0.089127
0.142	-0.00045	0.001505	0.096098	0.089129
0.143	-0.00033	0.001503	0.096072	0.089139
0.144	-0.00023	0.001503	0.096052	0.089157
0.145	-0.00016	0.001505	0.096026	0.089178
0.146	-9.9E-05	0.001506	0.095993	0.089199
0.147	-4.6E-05	0.001508	0.095953	0.089221
0.148	1.24E-05	0.001506	0.095905	0.089237
0.149	8.52E-05	0.001505	0.09586	0.089252
0.15	0.000173	0.001501	0.095825	0.089268
0.151	0.000271	0.001497	0.0958	0.089287
0.152	0.000363	0.001494	0.095779	0.089308
0.153	0.000428	0.001489	0.095756	0.089333
0.154	0.000452	0.001485	0.095725	0.089359
0.155	0.000422	0.001481	0.09569	0.089387
0.156	0.00034	0.001475	0.095645	0.089415
0.157	0.000213	0.001469	0.095593	0.089444
0.158	5.63E-05	0.001462	0.09554	0.089472
0.159	-0.00011	0.001453	0.095478	0.089499
0.16	-0.00028	0.001447	0.095413	0.089525
0.161	-0.00043	0.001441	0.09535	0.08955
0.162	-0.00056	0.001436	0.095288	0.089575
0.163	-0.00067	0.001435	0.095235	0.0896
0.164	-0.00075	0.001433	0.095185	0.089624
0.165	-0.00084	0.001434	0.095141	0.08965
0.166	-0.00092	0.001437	0.095114	0.08968
0.167	-0.00102	0.001443	0.095105	0.089716
0.168	-0.00113	0.001454	0.09511	0.089758
0.169	-0.00124	0.001468	0.095123	0.089805
0.17	-0.00137	0.001485	0.095122	0.08985
0.171	-0.00149	0.001507	0.095097	0.08989
0.172	-0.00161	0.001529	0.095041	0.089921
0.173	-0.0017	0.00155	0.094964	0.089945
0.174	-0.00176	0.001566	0.094882	0.089967
0.175	-0.00178	0.001574	0.094806	0.089986
0.176	-0.00175	0.001573	0.094752	0.090008
0.177	-0.00171	0.00156	0.094722	0.090035
0.178	-0.00165	0.001538	0.094717	0.090069
0.179	-0.00161	0.00151	0.094725	0.090108
0.18	-0.0016	0.001477	0.094741	0.090153

0.181	-0.00162	0.001439	0.094756	0.090199
0.182	-0.00166	0.001404	0.094777	0.090249
0.183	-0.0017	0.001368	0.094805	0.090299
0.184	-0.00171	0.001336	0.094849	0.090351
0.185	-0.00169	0.001309	0.094902	0.0904
0.186	-0.00162	0.001288	0.094958	0.090443
0.187	-0.00151	0.001273	0.095016	0.090478
0.188	-0.00135	0.001265	0.095061	0.090505
0.189	-0.00117	0.001259	0.09509	0.090524
0.19	-0.00099	0.001253	0.095101	0.090537
0.191	-0.00081	0.001247	0.095104	0.09055
0.192	-0.00065	0.001232	0.095104	0.090565
0.193	-0.00051	0.001217	0.095113	0.090585
0.194	-0.00037	0.001196	0.095134	0.090611
0.195	-0.00024	0.001175	0.095167	0.090641
0.196	-1E-04	0.001155	0.095207	0.090674
0.197	5.36E-05	0.001137	0.095248	0.090706
0.198	0.000224	0.001124	0.095283	0.090736
0.199	0.000404	0.001116	0.095309	0.090764
0.2	0.000581	0.001114	0.095333	0.090793
0.201	0.000739	0.001119	0.095348	0.090824
0.202	0.000866	0.001129	0.095356	0.090856
0.203	0.000953	0.001144	0.095359	0.090891
0.204	0.000996	0.001164	0.09536	0.090931
0.205	0.001003	0.001188	0.095364	0.090973
0.206	0.000977	0.001217	0.095364	0.091019
0.207	0.000923	0.001252	0.095363	0.091068
0.208	0.000843	0.001292	0.095354	0.091121
0.209	0.000746	0.001341	0.095336	0.091175
0.21	0.000647	0.001398	0.095318	0.091233
0.211	0.000558	0.001464	0.095297	0.091291
0.212	0.000493	0.001538	0.095273	0.091347
0.213	0.000461	0.001618	0.09524	0.091396
0.214	0.000457	0.001704	0.095205	0.091443
0.215	0.000463	0.001788	0.095168	0.091486
0.216	0.000462	0.001873	0.095131	0.091529
0.217	0.000441	0.001954	0.095099	0.091573
0.218	0.000395	0.002031	0.095073	0.091619
0.219	0.000321	0.002103	0.095056	0.09167
0.22	0.000235	0.002166	0.095043	0.091722
0.221	0.000151	0.00222	0.09503	0.091771
0.222	8.62E-05	0.002266	0.095017	0.091818
0.223	4.51E-05	0.002304	0.094999	0.091859
0.224	3.6E-05	0.002333	0.094978	0.091894
0.225	4.96E-05	0.002355	0.094955	0.091926
0.226	6.74E-05	0.00237	0.094934	0.091957
0.227	6.98E-05	0.002381	0.094927	0.091993
0.228	4.42E-05	0.00239	0.094927	0.092034
0.229	-9.3E-06	0.002401	0.094928	0.092079
0.23	-8.1E-05	0.002416	0.094921	0.092123
0.231	-0.00017	0.002442	0.094902	0.092167
0.232	-0.00026	0.002477	0.094864	0.092207
0.233	-0.00034	0.002521	0.094809	0.092244
0.234	-0.00042	0.00257	0.094737	0.092275
0.235	-0.00047	0.002622	0.09465	0.092304
0.236	-0.00047	0.002668	0.094556	0.092328
0.237	-0.00044	0.002709	0.094456	0.092347
0.238	-0.00037	0.002745	0.094357	0.092362
0.239	-0.00026	0.002781	0.094253	0.092371
0.24	-0.00012	0.002818	0.09415	0.092377
0.241	1.93E-05	0.00286	0.094047	0.092379
0.242	0.000145	0.002906	0.093952	0.092381
0.243	0.000244	0.002954	0.093886	0.09239
0.244	0.000306	0.003004	0.093861	0.092411

0.245	0.000339	0.003055	0.093876	0.092445
0.246	0.000353	0.003105	0.093931	0.09249
0.247	0.000366	0.003154	0.094014	0.092545
0.248	0.000381	0.003199	0.094113	0.092605
0.249	0.000397	0.003246	0.094213	0.092667
0.25	0.000407	0.003293	0.094302	0.09273
0.251	0.000405	0.003337	0.094375	0.092791
0.252	0.000386	0.003382	0.094437	0.09285
0.253	0.000354	0.003422	0.094493	0.092906
0.254	0.000314	0.003457	0.094549	0.092961
0.255	0.000267	0.003484	0.0946	0.093009
0.256	0.000212	0.003506	0.094644	0.093055
0.257	0.000152	0.003524	0.094679	0.093097
0.258	9.32E-05	0.00354	0.094701	0.093134
0.259	4.28E-05	0.003556	0.094711	0.093168
0.26	7.31E-07	0.003576	0.09471	0.093198
0.261	-3.4E-05	0.003602	0.0947	0.093225
0.262	-6.2E-05	0.003638	0.094679	0.093251
0.263	-7.9E-05	0.003685	0.094651	0.093273
0.264	-7.8E-05	0.003742	0.094617	0.093291
0.265	-4.7E-05	0.003808	0.094575	0.093301
0.266	2.22E-05	0.003882	0.094536	0.093304
0.267	0.000124	0.003961	0.094506	0.093302
0.268	0.000247	0.004043	0.094483	0.093298
0.269	0.000363	0.004123	0.094474	0.093294
0.27	0.000442	0.0042	0.09448	0.093295
0.271	0.000482	0.004268	0.094507	0.093303
0.272	0.000496	0.004329	0.094547	0.093316
0.273	0.000512	0.004386	0.094591	0.093328
0.274	0.000548	0.004443	0.094624	0.093334
0.275	0.000614	0.004504	0.094649	0.093336
0.276	0.000707	0.00457	0.094665	0.093332
0.277	0.000818	0.004644	0.094672	0.093326
0.278	0.000937	0.004722	0.094675	0.093319
0.279	0.001057	0.004797	0.094676	0.093314
0.28	0.001168	0.004868	0.094676	0.09331
0.281	0.001258	0.004931	0.094676	0.093309
0.282	0.001326	0.004986	0.094687	0.093317
0.283	0.001359	0.005032	0.094705	0.093331
0.284	0.001358	0.005071	0.094733	0.093355
0.285	0.001327	0.00511	0.094761	0.093383
0.286	0.001284	0.005145	0.094784	0.093413
0.287	0.001245	0.005187	0.094794	0.09344
0.288	0.001226	0.005236	0.094786	0.093461
0.289	0.001226	0.005292	0.094751	0.093473
0.29	0.001253	0.005355	0.094697	0.093475
0.291	0.001294	0.005423	0.094635	0.093473
0.292	0.001343	0.005494	0.094576	0.093468
0.293	0.001394	0.00556	0.094528	0.093464
0.294	0.001423	0.005617	0.094494	0.093465
0.295	0.001421	0.005663	0.094472	0.093473
0.296	0.001388	0.005702	0.094472	0.093491
0.297	0.001336	0.005738	0.09449	0.093516
0.298	0.00129	0.005774	0.094519	0.093544
0.299	0.001286	0.005814	0.094541	0.093567
0.3	0.001335	0.00586	0.094549	0.093581
0.301	0.00144	0.005917	0.094544	0.093587
0.302	0.00159	0.005981	0.094531	0.093587
0.303	0.001762	0.006051	0.094507	0.093582
0.304	0.001932	0.006123	0.094487	0.09358
0.305	0.002073	0.006193	0.094485	0.093586
0.306	0.002169	0.006257	0.094505	0.093606
0.307	0.002217	0.006315	0.094542	0.093639
0.308	0.002221	0.006362	0.094591	0.093683

0.309	0.002197	0.006399	0.094644	0.093732
0.31	0.002158	0.006424	0.094693	0.093784
0.311	0.00212	0.006438	0.094735	0.093833
0.312	0.002093	0.006436	0.094769	0.093877
0.313	0.002083	0.006422	0.094784	0.093915
0.314	0.002097	0.006392	0.094769	0.093943
0.315	0.00213	0.006348	0.094725	0.093962
0.316	0.002178	0.006294	0.094659	0.093975
0.317	0.002224	0.006234	0.094582	0.093986
0.318	0.002257	0.006175	0.094514	0.094002
0.319	0.002268	0.006125	0.094471	0.094027
0.32	0.002246	0.006088	0.094465	0.094066
0.321	0.002203	0.006064	0.094506	0.094116
0.322	0.002143	0.006047	0.094578	0.094174
0.323	0.00209	0.006032	0.094662	0.09423
0.324	0.002062	0.006018	0.094728	0.094278
0.325	0.002073	0.006001	0.094756	0.094308
0.326	0.002125	0.005987	0.094742	0.09432
0.327	0.002198	0.005974	0.094701	0.09432
0.328	0.002277	0.005966	0.094662	0.094318
0.329	0.002341	0.005962	0.09465	0.094323
0.33	0.002368	0.005961	0.094679	0.094343
0.331	0.002348	0.005963	0.09475	0.094382
0.332	0.002271	0.005964	0.094843	0.094437
0.333	0.002141	0.005964	0.094948	0.094503
0.334	0.001967	0.005963	0.095052	0.094577
0.335	0.001759	0.005958	0.095134	0.094651
0.336	0.001544	0.005952	0.09519	0.094721
0.337	0.001349	0.005943	0.095208	0.094779
0.338	0.001192	0.00593	0.095171	0.094818
0.339	0.001078	0.005913	0.095089	0.094839
0.34	0.001006	0.005893	0.09498	0.094847
0.341	0.000973	0.00587	0.094866	0.094847
0.342	0.000966	0.005847	0.09477	0.094848
0.343	0.000976	0.005823	0.094718	0.094857
0.344	0.000997	0.005795	0.094719	0.09488
0.345	0.001029	0.005768	0.094772	0.094915
0.346	0.001075	0.005738	0.09486	0.094956
0.347	0.001141	0.005708	0.094953	0.094994
0.348	0.001225	0.005677	0.095031	0.095026
0.349	0.001313	0.005644	0.095079	0.095049
0.35	0.001392	0.00561	0.095088	0.095064
0.351	0.001453	0.005568	0.095062	0.095072
0.352	0.001506	0.005521	0.095015	0.095078
0.353	0.001547	0.005464	0.09496	0.095084
0.354	0.001575	0.0054	0.094913	0.095094
0.355	0.001576	0.005328	0.094887	0.095112
0.356	0.00154	0.005254	0.094894	0.095144
0.357	0.001463	0.005177	0.094941	0.095192
0.358	0.001353	0.0051	0.095014	0.095253
0.359	0.001222	0.005025	0.09509	0.095317
0.36	0.00108	0.004953	0.095158	0.095382
0.361	0.000934	0.004884	0.095212	0.095443
0.362	0.000783	0.004817	0.095236	0.095498
0.363	0.000621	0.004756	0.095229	0.095544
0.364	0.000452	0.004699	0.095184	0.095581
0.365	0.000284	0.004647	0.095106	0.095606
0.366	0.000131	0.004601	0.095013	0.095623
0.367	8.16E-06	0.004558	0.094918	0.095633
0.368	-8E-05	0.004518	0.094848	0.095644
0.369	-0.00014	0.004477	0.094811	0.095658
0.37	-0.00018	0.004427	0.094811	0.095679
0.371	-0.00022	0.004371	0.094837	0.095706
0.372	-0.00026	0.004305	0.09487	0.095737

0.373	-0.00031	0.004237	0.094898	0.095768
0.374	-0.00036	0.004168	0.094915	0.095797
0.375	-0.00041	0.004103	0.094914	0.095824
0.376	-0.00046	0.004042	0.094898	0.095849
0.377	-0.0005	0.003987	0.094873	0.095871
0.378	-0.00053	0.003938	0.09485	0.095892
0.379	-0.00053	0.003896	0.094842	0.095917
0.38	-0.00052	0.003857	0.094851	0.095944
0.381	-0.00049	0.003819	0.094879	0.095974
0.382	-0.00045	0.003778	0.094923	0.096007
0.383	-0.00041	0.00373	0.094977	0.096042
0.384	-0.00036	0.003676	0.095035	0.096078
0.385	-0.00034	0.003611	0.095087	0.096115
0.386	-0.00034	0.003541	0.095133	0.096152
0.387	-0.00034	0.003468	0.095171	0.096188
0.388	-0.00036	0.003391	0.0952	0.096224
0.389	-0.00039	0.003312	0.095222	0.096257
0.39	-0.00042	0.003229	0.095243	0.096289
0.391	-0.00044	0.003145	0.095256	0.096318
0.392	-0.00046	0.003058	0.095268	0.096344
0.393	-0.00047	0.00297	0.095274	0.096366
0.394	-0.00046	0.00288	0.09527	0.096383
0.395	-0.00043	0.002788	0.095255	0.096396
0.396	-0.0004	0.002695	0.095231	0.096406
0.397	-0.00037	0.002598	0.095199	0.096414
0.398	-0.00036	0.002499	0.095157	0.096421
0.399	-0.00036	0.002403	0.095111	0.09643
0.4	-0.00038	0.002308	0.095066	0.096445
0.401	-0.00042	0.002218	0.095031	0.096465
0.402	-0.00046	0.002129	0.095008	0.096491
0.403	-0.00051	0.002045	0.094996	0.096517
0.404	-0.00055	0.001961	0.094991	0.096543
0.405	-0.00058	0.001881	0.094979	0.096563
0.406	-0.00059	0.001804	0.094949	0.096575
0.407	-0.0006	0.00173	0.094894	0.096578
0.408	-0.00062	0.001657	0.094813	0.096573
0.409	-0.00064	0.001584	0.094715	0.096563
0.41	-0.00068	0.00151	0.094607	0.096552
0.411	-0.00074	0.001435	0.094499	0.096541
0.412	-0.00082	0.001357	0.094407	0.096535
0.413	-0.00091	0.001275	0.094336	0.096532
0.414	-0.001	0.001188	0.094293	0.096535
0.415	-0.00109	0.001095	0.094272	0.096541
0.416	-0.00116	0.000997	0.094265	0.096547
0.417	-0.00123	0.000894	0.094261	0.096555
0.418	-0.00129	0.00079	0.094244	0.096558
0.419	-0.00135	0.000687	0.094208	0.096559
0.42	-0.00142	0.000593	0.094153	0.096557
0.421	-0.00149	0.000505	0.094083	0.096552
0.422	-0.00157	0.000431	0.094014	0.096551
0.423	-0.00165	0.000368	0.093956	0.096555
0.424	-0.00173	0.000313	0.093928	0.09657
0.425	-0.0018	0.000263	0.093933	0.096595
0.426	-0.00186	0.000211	0.09397	0.096626
0.427	-0.00189	0.000155	0.094023	0.096661
0.428	-0.00189	9.29E-05	0.09408	0.096693
0.429	-0.00188	2.08E-05	0.094127	0.096721
0.43	-0.00184	-5.7E-05	0.094154	0.096741
0.431	-0.00181	-0.00014	0.094162	0.096756
0.432	-0.00178	-0.00022	0.094148	0.096768
0.433	-0.00176	-0.00028	0.094122	0.09678
0.434	-0.00175	-0.00034	0.094091	0.096796
0.435	-0.00175	-0.00038	0.094064	0.096816
0.436	-0.00174	-0.0004	0.094049	0.096842

0.437	-0.00171	-0.00042	0.09405	0.09687
0.438	-0.00166	-0.00043	0.094066	0.096901
0.439	-0.0016	-0.00042	0.094092	0.09693
0.44	-0.00152	-0.00042	0.094119	0.096958
0.441	-0.00146	-0.00041	0.094144	0.096985
0.442	-0.00142	-0.00039	0.094161	0.097013
0.443	-0.00141	-0.00037	0.09416	0.09704
0.444	-0.00143	-0.00035	0.09414	0.097067
0.445	-0.00147	-0.00033	0.094103	0.097094
0.446	-0.00151	-0.00031	0.094063	0.097124
0.447	-0.00154	-0.00028	0.094022	0.097154
0.448	-0.00153	-0.00023	0.093988	0.097185
0.449	-0.0015	-0.00019	0.093963	0.097216
0.45	-0.00143	-0.00013	0.093944	0.097245
0.451	-0.00135	-7.8E-05	0.093931	0.097273
0.452	-0.00127	-2.4E-05	0.093917	0.097299
0.453	-0.00119	2.22E-05	0.093901	0.097325
0.454	-0.00114	5.68E-05	0.093881	0.09735
0.455	-0.00111	8.47E-05	0.093862	0.097377
0.456	-0.0011	0.000105	0.093846	0.097407
0.457	-0.00111	0.00012	0.093835	0.097441
0.458	-0.00111	0.000129	0.09383	0.097476
0.459	-0.0011	0.000136	0.09383	0.097509
0.46	-0.00108	0.000138	0.09383	0.097537
0.461	-0.00104	0.000142	0.09383	0.097561
0.462	-0.00099	0.000151	0.093833	0.097582
0.463	-0.00094	0.000162	0.093834	0.097599
0.464	-0.00089	0.000179	0.093833	0.097616
0.465	-0.00086	0.000206	0.093836	0.097638
0.466	-0.00084	0.000249	0.093841	0.097663
0.467	-0.00083	0.000303	0.093844	0.097691
0.468	-0.00083	0.000371	0.093846	0.097721
0.469	-0.00084	0.000446	0.093842	0.097754
0.47	-0.00085	0.000529	0.093837	0.097789
0.471	-0.00085	0.000614	0.093824	0.097824
0.472	-0.00086	0.000705	0.093808	0.097859
0.473	-0.00087	0.000806	0.093797	0.097898
0.474	-0.00089	0.000912	0.093787	0.097941
0.475	-0.00091	0.001027	0.093776	0.097986
0.476	-0.00095	0.001145	0.093758	0.098032
0.477	-0.001	0.001267	0.093737	0.098077
0.478	-0.00106	0.001387	0.093708	0.098119
0.479	-0.00112	0.001506	0.093678	0.098161
0.48	-0.00117	0.001626	0.093651	0.0982
0.481	-0.00122	0.001748	0.093631	0.098242
0.482	-0.00127	0.001867	0.093616	0.098284
0.483	-0.00131	0.001986	0.093606	0.098329
0.484	-0.00134	0.0021	0.093599	0.098373
0.485	-0.00138	0.002207	0.093595	0.09842
0.486	-0.00141	0.002306	0.093593	0.098465
0.487	-0.00145	0.002391	0.093588	0.098508
0.488	-0.00148	0.002462	0.093582	0.098548
0.489	-0.00152	0.002516	0.093573	0.098585
0.49	-0.00156	0.002552	0.093568	0.098621
0.491	-0.0016	0.00257	0.093565	0.098656
0.492	-0.00163	0.002573	0.093567	0.09869
0.493	-0.00166	0.00256	0.093574	0.098724
0.494	-0.00169	0.002536	0.093579	0.098755
0.495	-0.00171	0.002503	0.093584	0.098782
0.496	-0.00173	0.002466	0.093587	0.098806
0.497	-0.00174	0.002432	0.093591	0.098828
0.498	-0.00175	0.0024	0.093599	0.09885
0.499	-0.00175	0.002372	0.093614	0.098873
0.5	-0.00175	0.002347	0.093634	0.098898

0.501	-0.00175	0.002334	0.093658	0.098926
0.502	-0.00174	0.002317	0.093679	0.098952
0.503	-0.00172	0.002303	0.093696	0.098976
0.504	-0.00169	0.00229	0.093709	0.098997
0.505	-0.00166	0.002273	0.093722	0.099018
0.506	-0.00161	0.002259	0.093735	0.099038
0.507	-0.00156	0.002242	0.093751	0.09906
0.508	-0.0015	0.002227	0.093766	0.099082
0.509	-0.00144	0.002215	0.093777	0.099103
0.51	-0.00136	0.002203	0.093779	0.099121
0.511	-0.00128	0.002198	0.093777	0.09914
0.512	-0.0012	0.002197	0.09377	0.099156
0.513	-0.00112	0.002196	0.093755	0.09917
0.514	-0.00103	0.002193	0.093735	0.099184
0.515	-0.00094	0.002188	0.093711	0.099196
0.516	-0.00085	0.002182	0.093687	0.099209
0.517	-0.00077	0.002178	0.093668	0.099224
0.518	-0.00068	0.002179	0.093662	0.099245
0.519	-0.0006	0.002184	0.093669	0.09927
0.52	-0.00053	0.002193	0.093676	0.099296
0.521	-0.00047	0.002201	0.093677	0.099318
0.522	-0.00042	0.002208	0.093665	0.099337
0.523	-0.00039	0.002209	0.093636	0.099353
0.524	-0.00038	0.002206	0.093595	0.099368
0.525	-0.00039	0.002197	0.093548	0.099384
0.526	-0.00041	0.002182	0.093501	0.099404
0.527	-0.00043	0.002168	0.093455	0.099426
0.528	-0.00046	0.002159	0.093407	0.099448
0.529	-0.00049	0.002158	0.093358	0.099469
0.53	-0.00052	0.002166	0.093313	0.099489
0.531	-0.00055	0.002179	0.093273	0.099511
0.532	-0.00057	0.002198	0.093235	0.099532
0.533	-0.00059	0.002219	0.093198	0.099553
0.534	-0.00061	0.002238	0.09316	0.099573
0.535	-0.00062	0.002251	0.093122	0.09959
0.536	-0.00063	0.002257	0.093082	0.099606
0.537	-0.00063	0.002252	0.093036	0.099617
0.538	-0.00063	0.002239	0.09298	0.09963
0.539	-0.00065	0.002219	0.092914	0.099643
0.54	-0.00068	0.00219	0.092845	0.099662
0.541	-0.00073	0.002158	0.09278	0.099686
0.542	-0.0008	0.002126	0.092719	0.099717
0.543	-0.00088	0.0021	0.092664	0.099752
0.544	-0.00095	0.002083	0.092613	0.099787
0.545	-0.00101	0.002078	0.092564	0.099821
0.546	-0.00104	0.002085	0.092525	0.099856
0.547	-0.00107	0.002105	0.092489	0.099889
0.548	-0.00109	0.002137	0.092466	0.099925
0.549	-0.00109	0.002175	0.092454	0.099962
0.55	-0.0011	0.002211	0.092457	0.100002
0.551	-0.00109	0.002243	0.092471	0.10004
0.552	-0.00107	0.002263	0.09249	0.100075
0.553	-0.00105	0.002267	0.092508	0.100105
0.554	-0.00101	0.002257	0.092525	0.100129
0.555	-0.00097	0.002237	0.09254	0.100148
0.556	-0.00092	0.002213	0.092556	0.100164
0.557	-0.00088	0.002188	0.092577	0.100176
0.558	-0.00083	0.002159	0.092605	0.100186
0.559	-0.00079	0.002131	0.092637	0.100195
0.56	-0.00073	0.002101	0.092671	0.1002
0.561	-0.00067	0.002065	0.092708	0.100204
0.562	-0.00058	0.002026	0.092751	0.100208
0.563	-0.00048	0.001982	0.0928	0.100213
0.564	-0.00037	0.001933	0.092858	0.100218

0.565	-0.00023	0.001882	0.092925	0.100227
0.566	-9.6E-05	0.00183	0.092994	0.100237
0.567	4.44E-05	0.001782	0.093064	0.100248
0.568	0.000176	0.001739	0.093125	0.100257
0.569	0.000293	0.001706	0.093177	0.100267
0.57	0.000391	0.00168	0.093212	0.100275
0.571	0.000468	0.001662	0.093231	0.100283
0.572	0.000525	0.001651	0.09323	0.100288
0.573	0.000574	0.001643	0.093214	0.100293
0.574	0.000625	0.001639	0.093191	0.100299
0.575	0.000687	0.001632	0.093165	0.100306
0.576	0.000762	0.001625	0.09314	0.100315
0.577	0.000847	0.001613	0.093115	0.100322
0.578	0.000941	0.001595	0.093094	0.100332
0.579	0.001039	0.001574	0.093074	0.100338
0.58	0.001135	0.001548	0.093059	0.100345
0.581	0.001228	0.001516	0.093053	0.100351
0.582	0.001309	0.00148	0.093052	0.100361
0.583	0.001376	0.001444	0.093054	0.100369
0.584	0.001427	0.001414	0.093057	0.100382
0.585	0.001467	0.001389	0.093058	0.100395
0.586	0.001501	0.00137	0.093055	0.100411
0.587	0.001536	0.001352	0.093043	0.100427
0.588	0.001575	0.00133	0.093023	0.100442
0.589	0.001621	0.001306	0.092998	0.100458
0.59	0.001672	0.001276	0.092971	0.100474
0.591	0.001713	0.001244	0.092948	0.100493
0.592	0.001725	0.001215	0.092935	0.100518
0.593	0.001703	0.001193	0.092942	0.10055
0.594	0.001641	0.001188	0.09297	0.100594
0.595	0.001544	0.001195	0.093015	0.100647
0.596	0.001424	0.001217	0.093068	0.100704
0.597	0.001289	0.001249	0.093118	0.100763
0.598	0.00115	0.001285	0.093158	0.100822
0.599	0.001012	0.001312	0.093185	0.100878
0.6	0.00088	0.001326	0.0932	0.10093
0.601	0.000752	0.001323	0.093202	0.100976
0.602	0.000627	0.0013	0.093205	0.10102
0.603	0.000507	0.001256	0.093212	0.101058
0.604	0.000393	0.001202	0.093226	0.101094
0.605	0.000286	0.001138	0.093246	0.101125
0.606	0.000187	0.001073	0.093271	0.101157
0.607	8.84E-05	0.001013	0.093289	0.101185
0.608	-1E-05	0.000961	0.093302	0.101212
0.609	-0.00012	0.00092	0.093302	0.101238
0.61	-0.00024	0.000893	0.093292	0.101265
0.611	-0.00036	0.000875	0.093271	0.101291
0.612	-0.00047	0.000863	0.093244	0.101313
0.613	-0.00055	0.000855	0.09321	0.101333
0.614	-0.00062	0.000852	0.093182	0.101354
0.615	-0.00067	0.000853	0.093159	0.101376
0.616	-0.00072	0.000859	0.093142	0.101402
0.617	-0.00077	0.000869	0.093124	0.101428
0.618	-0.00082	0.000877	0.093103	0.101455
0.619	-0.00087	0.000886	0.093078	0.101482
0.62	-0.00093	0.000898	0.093042	0.101507
0.621	-0.00099	0.000913	0.093004	0.101528
0.622	-0.00103	0.000936	0.09297	0.101548
0.623	-0.00105	0.000966	0.092945	0.101564
0.624	-0.00104	0.000994	0.092928	0.101578
0.625	-0.00101	0.001018	0.092928	0.101591
0.626	-0.00096	0.001034	0.092935	0.101605
0.627	-0.0009	0.001044	0.092953	0.101622
0.628	-0.00083	0.001049	0.092967	0.101639

0.629	-0.00076	0.00105	0.09297	0.101655
0.63	-0.00068	0.001052	0.092963	0.101667
0.631	-0.00059	0.001055	0.092949	0.101677
0.632	-0.00049	0.001061	0.092941	0.101687
0.633	-0.00038	0.001067	0.092944	0.101696
0.634	-0.00025	0.001073	0.092962	0.101706
0.635	-0.00013	0.001083	0.092998	0.101722
0.636	-2.5E-05	0.001099	0.093048	0.101744
0.637	5.43E-05	0.001123	0.093106	0.101774
0.638	9.78E-05	0.001153	0.093163	0.101811
0.639	0.000103	0.001187	0.09321	0.10185
0.64	7.52E-05	0.001225	0.09324	0.101891
0.641	3.02E-05	0.001267	0.093257	0.101932
0.642	-2.4E-05	0.001315	0.093263	0.101973
0.643	-7.3E-05	0.001363	0.093262	0.10201
0.644	-0.00011	0.001416	0.093258	0.102045
0.645	-0.00015	0.001475	0.093257	0.102081
0.646	-0.00018	0.001543	0.093264	0.10212
0.647	-0.00022	0.001619	0.093281	0.10216
0.648	-0.00028	0.001701	0.093305	0.102203
0.649	-0.00037	0.001782	0.093334	0.10225
0.65	-0.00051	0.001855	0.093363	0.102302
0.651	-0.00069	0.001919	0.093399	0.102359
0.652	-0.0009	0.001972	0.093434	0.102419
0.653	-0.00114	0.002018	0.09347	0.102481
0.654	-0.00139	0.00206	0.093511	0.102543
0.655	-0.00162	0.002101	0.093552	0.1026
0.656	-0.00181	0.002146	0.093589	0.102649
0.657	-0.00196	0.002187	0.093612	0.102687
0.658	-0.00207	0.002224	0.093622	0.102716
0.659	-0.00214	0.002254	0.093615	0.102735
0.66	-0.00217	0.002276	0.093599	0.102749
0.661	-0.00218	0.002296	0.09358	0.102763
0.662	-0.00219	0.002315	0.09356	0.102778
0.663	-0.0022	0.002336	0.093542	0.102793
0.664	-0.00221	0.002355	0.093529	0.102811
0.665	-0.00221	0.00237	0.093519	0.102829
0.666	-0.0022	0.00238	0.093508	0.102843
0.667	-0.00215	0.002386	0.093499	0.102853
0.668	-0.00206	0.002394	0.093486	0.102857
0.669	-0.00194	0.002406	0.093471	0.102857
0.67	-0.0018	0.002428	0.09345	0.102853
0.671	-0.00165	0.002457	0.093431	0.102851
0.672	-0.0015	0.002494	0.09342	0.102854
0.673	-0.00136	0.002534	0.093422	0.102865
0.674	-0.00122	0.00257	0.093434	0.102885
0.675	-0.0011	0.002596	0.093459	0.102912
0.676	-0.00099	0.002604	0.093496	0.102949
0.677	-0.0009	0.002583	0.09354	0.102989
0.678	-0.00083	0.002531	0.093587	0.103033
0.679	-0.00078	0.002446	0.093631	0.103078
0.68	-0.00076	0.002339	0.093672	0.103124
0.681	-0.00075	0.002221	0.093709	0.10317
0.682	-0.00075	0.002107	0.093738	0.103213
0.683	-0.00074	0.002009	0.09375	0.103251
0.684	-0.00071	0.001933	0.093741	0.103281
0.685	-0.00064	0.001876	0.093697	0.103299
0.686	-0.00054	0.001834	0.093631	0.103306
0.687	-0.00041	0.001796	0.093536	0.103302
0.688	-0.00026	0.001756	0.093435	0.103292
0.689	-8.8E-05	0.001713	0.093331	0.103277
0.69	9.15E-05	0.001669	0.093233	0.103261
0.691	0.000271	0.001625	0.093153	0.10325
0.692	0.00045	0.001586	0.093085	0.103241
0.693	0.000634	0.001555	0.093037	0.103237
0.694	0.000827	0.001536	0.093012	0.10324
0.695	0.001033	0.001532	0.093006	0.103249
0.696	0.001249	0.001544	0.093021	0.103268
0.697	0.001458	0.001569	0.093072	0.1033
0.698	0.001656	0.001607	0.09315	0.103346
0.699	0.00184	0.001658	0.093256	0.103405
0.7	0.001993	0.001714	0.09338	0.103473
0.701	0.002099	0.001773	0.093519	0.103554
0.702	0.002156	0.001823	0.093667	0.103643
0.703	0.00217	0.001859	0.093816	0.103738
0.704	0.002163	0.001878	0.093955	0.103831
0.705	0.002154	0.001878	0.094074	0.103918
0.706	0.002157	0.001868	0.094156	0.10399
0.707	0.002189	0.001849	0.094184	0.10404
0.708	0.002259	0.00183	0.094163	0.104069
0.709	0.002373	0.001815	0.0941	0.104076
0.71	0.00253	0.001807	0.094015	0.104067
0.711	0.002725	0.001807	0.093929	0.10405
0.712	0.002935	0.001814	0.093857	0.104029
0.713	0.003133	0.001829	0.093806	0.104011
0.714	0.003299	0.001849	0.093791	0.104003
0.715	0.00341	0.001873	0.093809	0.104007
0.716	0.003452	0.001894	0.093849	0.104022
0.717	0.003435	0.001916	0.093911	0.104047
0.718	0.003376	0.001936	0.094	0.104084
0.719	0.003301	0.001953	0.094094	0.104123
0.72	0.00323	0.001974	0.094191	0.104164
0.721	0.003177	0.001997	0.094279	0.1042
0.722	0.003137	0.002029	0.094346	0.104231
0.723	0.003098	0.002069	0.094399	0.10426
0.724	0.00304	0.002113	0.094441	0.104292
0.725	0.002948	0.002163	0.094478	0.10433
0.726	0.002806	0.002217	0.094508	0.104375
0.727	0.002601	0.002273	0.094534	0.104429
0.728	0.002333	0.002332	0.094549	0.104488
0.729	0.002014	0.002385	0.094544	0.104546
0.73	0.001658	0.002433	0.094515	0.104601
0.731	0.001286	0.002472	0.094463	0.10465
0.732	0.000922	0.002507	0.094388	0.104691
0.733	0.000585	0.002537	0.094295	0.104723
0.734	0.0003	0.002565	0.094196	0.104748
0.735	7.65E-05	0.002592	0.094109	0.104771
0.736	-9.2E-05	0.002624	0.094044	0.104795
0.737	-0.00022	0.002656	0.094005	0.10482
0.738	-0.00033	0.002686	0.093982	0.104848
0.739	-0.00045	0.002712	0.093963	0.104875
0.74	-0.0006	0.00273	0.093934	0.104904
0.741	-0.00079	0.002736	0.093878	0.104929
0.742	-0.00103	0.002735	0.093796	0.104953
0.743	-0.00128	0.002729	0.093686	0.104972
0.744	-0.00151	0.002723	0.093563	0.104989
0.745	-0.00169	0.002719	0.093453	0.105002
0.746	-0.00178	0.002717	0.093388	0.105021
0.747	-0.0018	0.002712	0.093376	0.105046
0.748	-0.00176	0.002713	0.093425	0.105083
0.749	-0.00171	0.002713	0.09352	0.10513
0.75	-0.00167	0.002709	0.093637	0.105184
0.751	-0.00169	0.002701	0.093753	0.105242
0.752	-0.00175	0.002686	0.093843	0.105296
0.753	-0.00187	0.002665	0.093891	0.105341
0.754	-0.00199	0.002641	0.093894	0.105373
0.755	-0.0021	0.002614	0.093877	0.105394
0.756	-0.00217	0.002585	0.093863	0.105412

0.757	-0.00218	0.002557	0.093868	0.105431
0.758	-0.00215	0.002528	0.093909	0.105456
0.759	-0.00205	0.0025	0.09399	0.105486
0.76	-0.0019	0.002476	0.094097	0.105518
0.761	-0.00171	0.002453	0.094205	0.105545
0.762	-0.00149	0.002437	0.094295	0.105566
0.763	-0.00125	0.00242	0.094347	0.105572
0.764	-0.00099	0.002401	0.094354	0.105565
0.765	-0.00076	0.002381	0.09433	0.105555
0.766	-0.00058	0.002356	0.094281	0.105544
0.767	-0.00046	0.002328	0.094213	0.105537
0.768	-0.00042	0.002297	0.094142	0.105539
0.769	-0.00044	0.002266	0.094065	0.105543
0.77	-0.00047	0.00224	0.093995	0.10555
0.771	-0.00051	0.002215	0.093938	0.105559
0.772	-0.00052	0.002193	0.0939	0.105568
0.773	-0.00045	0.002177	0.093889	0.105574
0.774	-0.00031	0.002164	0.093904	0.105577
0.775	-0.00011	0.002157	0.093959	0.105583
0.776	8.62E-05	0.002151	0.09404	0.105595
0.777	0.000229	0.002146	0.094127	0.105615
0.778	0.000281	0.002142	0.094198	0.105639
0.779	0.000234	0.002137	0.09425	0.105672
0.78	0.000114	0.002135	0.094291	0.10571
0.781	-5.8E-05	0.002135	0.094329	0.105754
0.782	-0.00023	0.002139	0.094367	0.105799
0.783	-0.00037	0.002151	0.094413	0.105841
0.784	-0.00042	0.002172	0.094474	0.105877
0.785	-0.00038	0.002204	0.094556	0.105911
0.786	-0.00025	0.002245	0.094652	0.105941
0.787	-5.4E-05	0.002294	0.094756	0.105968
0.788	0.000172	0.002348	0.094854	0.105992
0.789	0.000384	0.002402	0.094925	0.106014
0.79	0.00054	0.002454	0.094954	0.106031
0.791	0.000604	0.002501	0.094927	0.106042
0.792	0.000571	0.002539	0.09485	0.106051
0.793	0.000455	0.002575	0.09474	0.106058
0.794	0.000279	0.002603	0.094622	0.106067
0.795	8.02E-05	0.002626	0.094523	0.106085
0.796	-0.0001	0.002649	0.094456	0.106108
0.797	-0.00025	0.002671	0.09443	0.10614
0.798	-0.00035	0.002702	0.094442	0.106177
0.799	-0.00039	0.002736	0.094474	0.106213
0.8	-0.00038	0.002773	0.094516	0.106246
0.801	-0.00033	0.002807	0.09456	0.106275
0.802	-0.00026	0.002834	0.094613	0.106301
0.803	-0.0002	0.002849	0.094685	0.106335
0.804	-0.00018	0.002852	0.094773	0.106376
0.805	-0.00021	0.002845	0.094877	0.106427
0.806	-0.00027	0.002838	0.094999	0.106489
0.807	-0.00033	0.002832	0.095139	0.106558
0.808	-0.00033	0.002837	0.095296	0.106628
0.809	-0.00027	0.002856	0.095463	0.106696
0.81	-0.00013	0.002887	0.095622	0.106755
0.811	5.86E-05	0.002927	0.095766	0.106808
0.812	0.00024	0.002969	0.095879	0.106855
0.813	0.000374	0.003008	0.095953	0.106897
0.814	0.000427	0.003044	0.095992	0.106939
0.815	0.000394	0.003071	0.096003	0.106984
0.816	0.000298	0.003092	0.095994	0.107031
0.817	0.000168	0.003107	0.095985	0.107082
0.818	3.52E-05	0.003121	0.095981	0.107137
0.819	-7.2E-05	0.003128	0.095986	0.107193
0.82	-0.00014	0.003136	0.096001	0.10725

0.821	-0.00016	0.00314	0.096028	0.107304
0.822	-0.00013	0.003141	0.09607	0.107358
0.823	-8.6E-05	0.003138	0.096121	0.107412
0.824	-5.6E-05	0.003129	0.096166	0.107464
0.825	-7E-05	0.003113	0.096189	0.107512
0.826	-0.00015	0.003091	0.096181	0.107558
0.827	-0.00032	0.003064	0.096139	0.107602
0.828	-0.00055	0.003033	0.096067	0.107646
0.829	-0.00082	0.003001	0.095987	0.107692
0.83	-0.0011	0.002968	0.095923	0.107743
0.831	-0.00134	0.002938	0.095899	0.1078
0.832	-0.00153	0.002908	0.095931	0.107866
0.833	-0.00167	0.002881	0.09601	0.107936
0.834	-0.00175	0.002858	0.096114	0.108007
0.835	-0.00181	0.002839	0.096216	0.108073
0.836	-0.00188	0.002827	0.096284	0.10813
0.837	-0.00198	0.002821	0.096303	0.108176
0.838	-0.00213	0.002819	0.096272	0.108212
0.839	-0.00231	0.002819	0.096204	0.108243
0.84	-0.00252	0.002821	0.096123	0.108274
0.841	-0.00272	0.002823	0.096058	0.108311
0.842	-0.0029	0.002821	0.096031	0.108356
0.843	-0.00303	0.002819	0.096051	0.10841
0.844	-0.00309	0.002817	0.096112	0.108468
0.845	-0.00309	0.002817	0.096198	0.108525
0.846	-0.00305	0.002823	0.096285	0.108577
0.847	-0.00298	0.002836	0.09635	0.108617
0.848	-0.0029	0.002861	0.096386	0.108648
0.849	-0.00283	0.002901	0.096383	0.108667
0.85	-0.00278	0.002954	0.096346	0.108677
0.851	-0.00273	0.003019	0.096294	0.108684
0.852	-0.0027	0.003089	0.096249	0.108693
0.853	-0.00267	0.003164	0.096221	0.108706
0.854	-0.00263	0.003241	0.096223	0.108724
0.855	-0.00257	0.003314	0.096257	0.108745
0.856	-0.00246	0.003379	0.09632	0.108766
0.857	-0.00232	0.003439	0.096399	0.108786
0.858	-0.00215	0.003488	0.096474	0.108801
0.859	-0.00197	0.003522	0.096522	0.108808
0.86	-0.00182	0.003547	0.096528	0.108806
0.861	-0.0017	0.003561	0.096482	0.108797
0.862	-0.00162	0.003563	0.096397	0.108782
0.863	-0.00159	0.003561	0.096294	0.108768
0.864	-0.00159	0.003551	0.096192	0.108759
0.865	-0.00159	0.003541	0.096112	0.108756
0.866	-0.00159	0.00353	0.09607	0.108762
0.867	-0.00156	0.003522	0.096072	0.108777
0.868	-0.00148	0.003523	0.096119	0.108802
0.869	-0.00135	0.003534	0.096197	0.108831
0.87	-0.00119	0.003556	0.096287	0.108859
0.871	-0.001	0.003587	0.09637	0.108885
0.872	-0.0008	0.003626	0.096436	0.108906
0.873	-0.00061	0.003676	0.096476	0.108922
0.874	-0.00042	0.003727	0.096495	0.108936
0.875	-0.00027	0.003776	0.096494	0.108949
0.876	-0.00014	0.003821	0.096484	0.108964
0.877	-5E-05	0.003856	0.096472	0.108985
0.878	2.77E-05	0.003876	0.096466	0.10901
0.879	0.000105	0.003883	0.096468	0.109036
0.88	0.000195	0.00388	0.096478	0.109063
0.881	0.000303	0.003868	0.096489	0.109087
0.882	0.000438	0.003855	0.096494	0.109105
0.883	0.000598	0.003839	0.096484	0.109114
0.884	0.000762	0.00382	0.096463	0.109119

0.885	0.000916	0.003795	0.096435	0.109122
0.886	0.001053	0.003765	0.096411	0.109127
0.887	0.001163	0.003726	0.096403	0.109138
0.888	0.001244	0.003682	0.096418	0.10916
0.889	0.001295	0.003635	0.096461	0.109193
0.89	0.001328	0.003594	0.096518	0.109232
0.891	0.001358	0.003559	0.096577	0.109272
0.892	0.001396	0.00353	0.096637	0.109311
0.893	0.001449	0.003509	0.096699	0.10935
0.894	0.001522	0.003492	0.096759	0.109386
0.895	0.001604	0.003477	0.096824	0.109423
0.896	0.001676	0.003462	0.096893	0.109464
0.897	0.001727	0.003447	0.096949	0.109507
0.898	0.00174	0.003428	0.096983	0.109552
0.899	0.001712	0.003412	0.096993	0.109598
0.9	0.00165	0.003401	0.096968	0.109639
0.901	0.001563	0.003394	0.09692	0.109679
0.902	0.001464	0.003389	0.096861	0.109717
0.903	0.001361	0.003387	0.0968	0.109753
0.904	0.001265	0.003382	0.096746	0.109788
0.905	0.001179	0.003372	0.096709	0.109825
0.906	0.001096	0.003358	0.096688	0.109866
0.907	0.001005	0.003336	0.096675	0.109909
0.908	0.000901	0.003309	0.096661	0.109954
0.909	0.000781	0.003274	0.096631	0.109996
0.91	0.000638	0.003235	0.096591	0.110038
0.911	0.000474	0.003193	0.096541	0.11008
0.912	0.000289	0.00315	0.096481	0.11012
0.913	8.86E-05	0.003105	0.096417	0.110162
0.914	-0.00012	0.003059	0.096362	0.110204
0.915	-0.00031	0.00301	0.096319	0.110248
0.916	-0.00049	0.002966	0.096298	0.110292
0.917	-0.00063	0.002927	0.096296	0.110333
0.918	-0.00073	0.002901	0.096317	0.110373
0.919	-0.00079	0.002885	0.09635	0.110411
0.92	-0.00083	0.002876	0.096388	0.110445
0.921	-0.00086	0.002869	0.096418	0.110473
0.922	-0.00091	0.002864	0.096429	0.110496
0.923	-0.00099	0.002858	0.096414	0.110514
0.924	-0.00109	0.002857	0.096374	0.110527
0.925	-0.00121	0.002863	0.096312	0.110537
0.926	-0.00134	0.00288	0.096235	0.110544
0.927	-0.00145	0.002908	0.096162	0.110551
0.928	-0.00153	0.002942	0.096105	0.110559
0.929	-0.00158	0.002973	0.096082	0.110575
0.93	-0.0016	0.002995	0.096104	0.1106
0.931	-0.00157	0.003	0.096162	0.110634
0.932	-0.00154	0.002991	0.096246	0.110677
0.933	-0.00151	0.002968	0.09633	0.110724
0.934	-0.00151	0.002938	0.0964	0.110776
0.935	-0.00156	0.002906	0.096447	0.110829
0.936	-0.00165	0.002875	0.096475	0.110882
0.937	-0.00176	0.002851	0.096484	0.110932
0.938	-0.00188	0.002833	0.096487	0.110981
0.939	-0.002	0.00282	0.096496	0.11103
0.94	-0.0021	0.002808	0.096523	0.111081
0.941	-0.00216	0.002792	0.096572	0.111134
0.942	-0.00218	0.002774	0.096641	0.111189
0.943	-0.00217	0.002747	0.096722	0.111242
0.944	-0.00213	0.00272	0.096797	0.11129
0.945	-0.00207	0.002688	0.096852	0.111326
0.946	-0.00199	0.002661	0.096876	0.111352
0.947	-0.00192	0.002639	0.096868	0.111367
0.948	-0.00185	0.002629	0.096839	0.111377

0.949	-0.00178	0.002632	0.096808	0.111386
0.95	-0.00174	0.002648	0.096788	0.111401
0.951	-0.00173	0.002676	0.096786	0.111421
0.952	-0.00173	0.002713	0.096802	0.11145
0.953	-0.00174	0.00276	0.096832	0.111479
0.954	-0.00177	0.002815	0.096867	0.111512
0.955	-0.0018	0.002875	0.096888	0.111541
0.956	-0.00182	0.002938	0.096877	0.111559
0.957	-0.00183	0.002997	0.096818	0.111564
0.958	-0.00184	0.003046	0.096722	0.111556
0.959	-0.00183	0.003082	0.09661	0.111542
0.96	-0.00181	0.0031	0.096505	0.111527
0.961	-0.00178	0.0031	0.096429	0.111517
0.962	-0.00174	0.003086	0.096398	0.111516
0.963	-0.00166	0.003063	0.096417	0.111524
0.964	-0.00154	0.003043	0.096483	0.11154
0.965	-0.00138	0.003032	0.096592	0.111565
0.966	-0.00117	0.003042	0.096714	0.11159
0.967	-0.00092	0.003064	0.096822	0.11161
0.968	-0.00066	0.003097	0.096894	0.111619
0.969	-0.0004	0.003126	0.096929	0.111618
0.97	-0.00015	0.00315	0.096934	0.111611
0.971	5.87E-05	0.003159	0.096909	0.111598
0.972	0.000228	0.003157	0.096862	0.111585
0.973	0.000354	0.003145	0.096797	0.111573
0.974	0.000447	0.00313	0.096723	0.111565
0.975	0.000516	0.003119	0.09664	0.111559
0.976	0.000567	0.003115	0.096548	0.111553
0.977	0.000602	0.003118	0.096444	0.111548
0.978	0.000614	0.003125	0.096331	0.111541
0.979	0.000595	0.003126	0.096219	0.111538
0.98	0.000548	0.003115	0.096126	0.111539
0.981	0.000476	0.003091	0.096058	0.111548
0.982	0.00039	0.003059	0.096017	0.111564
0.983	0.000302	0.003019	0.096002	0.111587
0.984	0.000221	0.002977	0.096009	0.111615
0.985	0.000158	0.002933	0.096031	0.111642
0.986	0.000112	0.002888	0.09607	0.111672
0.987	8.29E-05	0.00285	0.09612	0.111702
0.988	5.39E-05	0.002819	0.09617	0.111729
0.989	2.08E-05	0.002803	0.096201	0.111752
0.99	-3.3E-05	0.002802	0.096202	0.111767
0.991	-0.0001	0.002814	0.096167	0.111775
0.992	-0.00018	0.002835	0.096107	0.111778
0.993	-0.00026	0.002856	0.096037	0.111779
0.994	-0.00033	0.002867	0.095978	0.111784
0.995	-0.0004	0.002862	0.095943	0.111798
0.996	-0.00047	0.00284	0.095933	0.111821
0.997	-0.00052	0.002801	0.095931	0.111847
0.998	-0.00057	0.002749	0.095934	0.111875
0.999	-0.00061	0.002694	0.095934	0.111903
1	-0.00065	0.002638	0.095916	0.111928
1.001	-0.00068	0.002585	0.095878	0.111948
1.002	-0.00072	0.002538	0.095825	0.111968
1.003	-0.00077	0.002499	0.095766	0.111989
1.004	-0.00082	0.002473	0.095714	0.112016
1.005	-0.00087	0.002465	0.095671	0.112049
1.006	-0.00091	0.002483	0.095651	0.112089
1.007	-0.00094	0.002519	0.095648	0.112133
1.008	-0.00095	0.002559	0.095653	0.112178
1.009	-0.00095	0.002585	0.095657	0.112222
1.01	-0.00093	0.002589	0.095664	0.112262
1.011	-0.00091	0.002576	0.095667	0.112301
1.012	-0.00089	0.002559	0.095673	0.112339

1.013	-0.00088	0.002554	0.095689	0.112382
1.014	-0.0009	0.002569	0.095714	0.112429
1.015	-0.00094	0.002608	0.095746	0.112479
1.016	-0.00098	0.002674	0.095775	0.112532
1.017	-0.00103	0.00276	0.095788	0.11258
1.018	-0.00107	0.002862	0.095776	0.112624
1.019	-0.0011	0.002968	0.09574	0.112662
1.02	-0.00111	0.003076	0.095685	0.112697
1.021	-0.00112	0.003172	0.095618	0.112728
1.022	-0.00113	0.003245	0.095556	0.112759
1.023	-0.00114	0.003286	0.095504	0.11279
1.024	-0.00114	0.003287	0.095467	0.112823
1.025	-0.00113	0.003248	0.095437	0.112853
1.026	-0.00111	0.003179	0.09541	0.112881
1.027	-0.00107	0.003084	0.095377	0.112905
1.028	-0.00103	0.002982	0.095334	0.112923
1.029	-0.00097	0.002885	0.095277	0.112937
1.03	-0.00091	0.002807	0.095215	0.112951
1.031	-0.00085	0.002744	0.095151	0.112963
1.032	-0.00078	0.002696	0.095093	0.112978
1.033	-0.00072	0.002657	0.09504	0.112992
1.034	-0.00065	0.002621	0.095002	0.113009
1.035	-0.00058	0.002586	0.094987	0.11303
1.036	-0.00051	0.002552	0.09499	0.113054
1.037	-0.00044	0.002514	0.095009	0.11308
1.038	-0.00037	0.002476	0.095031	0.113107
1.039	-0.00029	0.00244	0.095052	0.113134
1.04	-0.00021	0.002407	0.095067	0.113156
1.041	-0.00013	0.002378	0.095078	0.113177
1.042	-4.6E-05	0.002355	0.095088	0.113194
1.043	3.5E-05	0.002336	0.095101	0.113211
1.044	0.000114	0.002327	0.095121	0.11323
1.045	0.000192	0.002329	0.09514	0.113249
1.046	0.000268	0.002339	0.095155	0.113267
1.047	0.000338	0.002345	0.095171	0.113285
1.048	0.000402	0.002346	0.095177	0.113301
1.049	0.000457	0.002343	0.095175	0.113316
1.05	0.000507	0.002329	0.095174	0.113328
1.051	0.000553	0.002303	0.095174	0.113338
1.052	0.000601	0.002268	0.095183	0.113347
1.053	0.00065	0.002226	0.095199	0.113358
1.054	0.000706	0.002184	0.095222	0.113368
1.055	0.000765	0.002156	0.095246	0.11338
1.056	0.000833	0.00214	0.09526	0.113391
1.057	0.000907	0.002143	0.09526	0.113402
1.058	0.000984	0.002163	0.095246	0.113411
1.059	0.001066	0.002191	0.095222	0.113417
1.06	0.001142	0.002219	0.095197	0.113419
1.061	0.001215	0.002241	0.095173	0.11342
1.062	0.001282	0.002254	0.095149	0.113419
1.063	0.001343	0.002258	0.095129	0.113421
1.064	0.001398	0.00225	0.095117	0.113432
1.065	0.001451	0.002238	0.095111	0.113453
1.066	0.001499	0.002225	0.09511	0.113484
1.067	0.001541	0.002217	0.095107	0.113521
1.068	0.001574	0.002219	0.095099	0.113562
1.069	0.001594	0.002236	0.095084	0.113605
1.07	0.001598	0.002266	0.095057	0.113645
1.071	0.001586	0.002308	0.09502	0.113682
1.072	0.00156	0.002357	0.094979	0.113719
1.073	0.001525	0.002402	0.094946	0.113757
1.074	0.001487	0.002437	0.094924	0.113798
1.075	0.001455	0.00246	0.094923	0.113843
1.076	0.00143	0.00247	0.094946	0.113891

1.077	0.001413	0.002471	0.094982	0.113938
1.078	0.001403	0.002474	0.095026	0.113982
1.079	0.001402	0.002485	0.095072	0.114022
1.08	0.001407	0.002502	0.095116	0.114057
1.081	0.001417	0.00253	0.095153	0.114086
1.082	0.00143	0.002571	0.095181	0.114111
1.083	0.001439	0.002626	0.095196	0.11413
1.084	0.001438	0.002693	0.095192	0.114144
1.085	0.001422	0.002774	0.095179	0.114159
1.086	0.001383	0.002859	0.095155	0.114175
1.087	0.001319	0.002948	0.09513	0.114197
1.088	0.001229	0.00303	0.095106	0.114226
1.089	0.001117	0.003098	0.095081	0.114262
1.09	0.000991	0.003151	0.095058	0.114305
1.091	0.000863	0.003187	0.095037	0.114351
1.092	0.000743	0.00321	0.095016	0.114399
1.093	0.00063	0.003225	0.094992	0.114444
1.094	0.000522	0.003236	0.094969	0.114489
1.095	0.000418	0.003253	0.094944	0.114535
1.096	0.000316	0.003277	0.09492	0.114581
1.097	0.000218	0.003312	0.094902	0.114627
1.098	0.000124	0.003348	0.094905	0.114675
1.099	3.18E-05	0.003382	0.09493	0.114727
1.1	-5.5E-05	0.003413	0.094971	0.114781
1.101	-0.00014	0.003433	0.095018	0.114834
1.102	-0.00022	0.003441	0.095059	0.114883
1.103	-0.00029	0.003438	0.095089	0.114929
1.104	-0.00036	0.003427	0.095106	0.11497
1.105	-0.00042	0.003413	0.095113	0.11501
1.106	-0.00049	0.003402	0.095111	0.115049
1.107	-0.00054	0.003401	0.095102	0.115087
1.108	-0.00059	0.003412	0.095089	0.115124
1.109	-0.00061	0.003437	0.095078	0.115162
1.11	-0.00062	0.003476	0.095072	0.115201
1.111	-0.0006	0.003521	0.095075	0.11524
1.112	-0.00058	0.003574	0.095084	0.115282
1.113	-0.00054	0.003624	0.095094	0.115324
1.114	-0.0005	0.00367	0.0951	0.115364
1.115	-0.00046	0.003707	0.095102	0.115403
1.116	-0.00042	0.003729	0.095097	0.115438
1.117	-0.00039	0.003737	0.095092	0.115467
1.118	-0.00036	0.003732	0.09509	0.11549
1.119	-0.00033	0.003713	0.095095	0.115506
1.12	-0.0003	0.003688	0.095107	0.115516
1.121	-0.00027	0.003663	0.095122	0.115519
1.122	-0.00024	0.003643	0.095135	0.115517
1.123	-0.00022	0.003632	0.095142	0.115511
1.124	-0.0002	0.003626	0.095141	0.115504
1.125	-0.00017	0.003623	0.095135	0.1155
1.126	-0.00014	0.003622	0.095129	0.115499
1.127	-9E-05	0.003621	0.095128	0.115503
1.128	-3.3E-05	0.00361	0.095131	0.115511
1.129	3.17E-05	0.003593	0.095134	0.115521
1.13	0.0001	0.003574	0.095132	0.115533
1.131	0.00017	0.003552	0.095117	0.115542
1.132	0.000241	0.003532	0.095083	0.115548
1.133	0.000309	0.003514	0.095038	0.115553
1.134	0.000373	0.003499	0.094984	0.115558
1.135	0.000425	0.003484	0.094919	0.115565
1.136	0.000465	0.003471	0.094851	0.115574
1.137	0.000495	0.003455	0.09478	0.115585
1.138	0.000521	0.003435	0.094714	0.115597
1.139	0.000547	0.003411	0.094662	0.115611
1.14	0.000582	0.003378	0.094631	0.115628

1.141	0.000632	0.003338	0.094624	0.115647
1.142	0.000693	0.003286	0.094637	0.115666
1.143	0.00076	0.003228	0.094659	0.115687
1.144	0.00083	0.003162	0.094688	0.115708
1.145	0.000899	0.003095	0.094721	0.115731
1.146	0.000959	0.003025	0.094751	0.115754
1.147	0.001008	0.002962	0.094774	0.115776
1.148	0.001038	0.002904	0.094791	0.115798
1.149	0.001051	0.002857	0.094814	0.115822
1.15	0.001046	0.002815	0.094849	0.115851
1.151	0.001027	0.002777	0.094894	0.115882
1.152	0.000996	0.002739	0.094944	0.115916
1.153	0.000962	0.002694	0.094998	0.115948
1.154	0.00093	0.002643	0.095052	0.115979
1.155	0.000905	0.002585	0.095096	0.116007
1.156	0.000894	0.002521	0.095133	0.116028
1.157	0.000887	0.002453	0.095161	0.116045
1.158	0.000881	0.002387	0.095178	0.116059
1.159	0.00086	0.002326	0.095184	0.116072
1.16	0.000818	0.002273	0.095179	0.116085
1.161	0.000741	0.002233	0.095165	0.1161
1.162	0.000634	0.002207	0.095141	0.116117
1.163	0.0005	0.002193	0.09511	0.116135
1.164	0.000353	0.002185	0.095076	0.116154
1.165	0.000208	0.002182	0.095048	0.116176
1.166	7.1E-05	0.00218	0.095029	0.116199
1.167	-5.5E-05	0.002174	0.095021	0.116225
1.168	-0.00017	0.002164	0.095024	0.116252
1.169	-0.00028	0.00215	0.095039	0.116284
1.17	-0.00038	0.002135	0.095055	0.116317
1.171	-0.00049	0.00212	0.095069	0.116351
1.172	-0.0006	0.002113	0.095078	0.116384
1.173	-0.0007	0.002114	0.095088	0.116416
1.174	-0.00079	0.002126	0.095099	0.116448
1.175	-0.00087	0.002148	0.095116	0.116481
1.176	-0.00093	0.002179	0.095138	0.116515
1.177	-0.00096	0.002218	0.095165	0.116549
1.178	-0.00097	0.002259	0.095201	0.116584
1.179	-0.00094	0.002301	0.095249	0.116618
1.18	-0.00087	0.002342	0.095302	0.11665
1.181	-0.00077	0.002386	0.095361	0.11668
1.182	-0.00065	0.002431	0.09542	0.116707
1.183	-0.00051	0.002481	0.095476	0.116735
1.184	-0.00038	0.002535	0.095524	0.116766
1.185	-0.00025	0.002598	0.09556	0.1168
1.186	-0.00012	0.002668	0.095589	0.116838
1.187	9.28E-06	0.002748	0.095615	0.11688
1.188	0.000147	0.002839	0.095636	0.116923
1.189	0.000296	0.002935	0.095659	0.116964
1.19	0.000457	0.003039	0.095677	0.117002
1.191	0.000627	0.003142	0.095689	0.117038
1.192	0.000796	0.00324	0.095701	0.117072
1.193	0.00096	0.003328	0.095709	0.11711
1.194	0.00111	0.003407	0.095711	0.117148
1.195	0.001246	0.003482	0.095701	0.117186
1.196	0.001368	0.003551	0.095685	0.117225
1.197	0.001479	0.00362	0.095665	0.117262
1.198	0.001583	0.003689	0.095658	0.117302
1.199	0.001685	0.003753	0.095663	0.117341
1.2	0.001792	0.003812	0.095678	0.117378
1.201	0.001904	0.003858	0.095701	0.117414
1.202	0.002024	0.003886	0.095729	0.117446
1.203	0.002157	0.003891	0.095764	0.117475
1.204	0.002306	0.003877	0.095803	0.117498
1.205	0.002467	0.003852	0.095843	0.117518
1.206	0.002638	0.003825	0.095881	0.117536
1.207	0.002809	0.003801	0.09591	0.11755
1.208	0.002977	0.003783	0.095927	0.117564
1.209	0.003131	0.003772	0.095935	0.117578
1.21	0.003271	0.003771	0.095936	0.117593
1.211	0.003388	0.003777	0.095935	0.117611
1.212	0.003485	0.003786	0.095937	0.117634
1.213	0.003561	0.003792	0.095941	0.117661
1.214	0.003614	0.00379	0.095948	0.117691
1.215	0.003643	0.003779	0.095952	0.117719
1.216	0.003649	0.00375	0.095953	0.117748
1.217	0.003634	0.003706	0.095943	0.117777
1.218	0.003599	0.003647	0.095923	0.117805
1.219	0.003543	0.003584	0.095898	0.117838
1.22	0.003464	0.003515	0.095861	0.117873
1.221	0.003362	0.003444	0.095818	0.117911
1.222	0.003236	0.003371	0.095772	0.117951
1.223	0.003091	0.003293	0.095732	0.117993
1.224	0.002934	0.003204	0.095706	0.118035
1.225	0.002776	0.003108	0.095698	0.118081
1.226	0.002629	0.003003	0.095707	0.118128
1.227	0.0025	0.002892	0.095725	0.118176
1.228	0.002392	0.002779	0.095747	0.118227
1.229	0.002304	0.002666	0.09577	0.11828
1.23	0.002227	0.002561	0.095781	0.118331
1.231	0.002152	0.002463	0.095776	0.118381
1.232	0.00207	0.002378	0.095755	0.118428
1.233	0.001979	0.002305	0.095718	0.11847
1.234	0.001876	0.002253	0.095667	0.118507
1.235	0.001763	0.002222	0.095606	0.118539
1.236	0.001644	0.002211	0.095536	0.118567
1.237	0.001519	0.00222	0.09546	0.118594
1.238	0.001392	0.002244	0.095384	0.118623
1.239	0.001268	0.002276	0.095308	0.118654
1.24	0.001155	0.002315	0.095238	0.118688
1.241	0.001053	0.002357	0.095178	0.118726
1.242	0.000968	0.002399	0.095132	0.118766
1.243	0.000898	0.002446	0.095092	0.118804
1.244	0.000837	0.002489	0.095066	0.118841
1.245	0.000773	0.002528	0.095041	0.118875
1.246	0.000698	0.00256	0.095023	0.118908
1.247	0.000606	0.002577	0.095002	0.118938
1.248	0.000501	0.002584	0.094977	0.118966
1.249	0.000396	0.002579	0.09495	0.118992
1.25	0.000297	0.002565	0.094933	0.119019
1.251	0.000221	0.002546	0.094932	0.119048
1.252	0.000177	0.002523	0.094949	0.119078
1.253	0.000171	0.002495	0.094984	0.119106
1.254	0.000207	0.002467	0.095031	0.119133
1.255	0.000279	0.002438	0.095083	0.119158
1.256	0.000371	0.00242	0.09513	0.119178
1.257	0.000469	0.002412	0.095163	0.119194
1.258	0.000558	0.002417	0.095177	0.119208
1.259	0.000631	0.002434	0.095181	0.119221
1.26	0.000678	0.002462	0.095172	0.119236
1.261	0.000699	0.002498	0.09516	0.119255
1.262	0.000699	0.002538	0.09515	0.119277
1.263	0.000694	0.002582	0.095145	0.119304
1.264	0.000693	0.002624	0.095146	0.119336
1.265	0.000703	0.002665	0.095151	0.119373
1.266	0.000733	0.0027	0.095153	0.119409
1.267	0.000776	0.00273	0.095151	0.119447
1.268	0.000818	0.002756	0.095141	0.119486

1.269	0.00084	0.002778	0.095124	0.119526
1.27	0.000828	0.002798	0.095096	0.119565
1.271	0.000774	0.002816	0.09506	0.119603
1.272	0.000684	0.002831	0.095025	0.119639
1.273	0.000567	0.002844	0.094996	0.119678
1.274	0.000438	0.002855	0.094988	0.119721
1.275	0.000309	0.002862	0.095007	0.119772
1.276	0.000197	0.002866	0.09505	0.119829
1.277	0.000101	0.002863	0.095115	0.119891
1.278	2.99E-05	0.002851	0.095187	0.119953
1.279	-2.1E-05	0.002827	0.095254	0.120012
1.28	-5.7E-05	0.002789	0.095303	0.120064
1.281	-8.6E-05	0.002738	0.095323	0.120105
1.282	-0.00012	0.002672	0.095308	0.120136
1.283	-0.00016	0.002596	0.095262	0.120156
1.284	-0.00021	0.002513	0.095194	0.12017
1.285	-0.00028	0.002429	0.095115	0.12018
1.286	-0.00037	0.002349	0.095041	0.120191
1.287	-0.00046	0.002278	0.09498	0.120204
1.288	-0.00056	0.002219	0.094936	0.120222
1.289	-0.00066	0.002169	0.094913	0.120245
1.29	-0.00075	0.002123	0.09491	0.120274
1.291	-0.00082	0.002084	0.094919	0.120302
1.292	-0.00087	0.002049	0.094927	0.120328
1.293	-0.0009	0.002014	0.094929	0.120346
1.294	-0.00091	0.00198	0.094926	0.120363
1.295	-0.00091	0.001947	0.094912	0.120375
1.296	-0.00092	0.001914	0.094892	0.120386
1.297	-0.00094	0.001887	0.094869	0.120398
1.298	-0.00098	0.001862	0.094849	0.120412
1.299	-0.00104	0.00184	0.094842	0.120433
1.3	-0.00111	0.001821	0.094852	0.120459
1.301	-0.00118	0.001802	0.094884	0.120492
1.302	-0.00123	0.001783	0.094934	0.120528
1.303	-0.00126	0.001761	0.095005	0.120569
1.304	-0.00127	0.001734	0.095092	0.120611
1.305	-0.00125	0.001697	0.095191	0.120656
1.306	-0.00121	0.001644	0.095291	0.120699
1.307	-0.00117	0.001576	0.095377	0.120739
1.308	-0.00114	0.001492	0.095435	0.120772
1.309	-0.00114	0.0014	0.095467	0.120804
1.31	-0.00117	0.001306	0.095478	0.120834
1.311	-0.00123	0.001218	0.095477	0.120865
1.312	-0.00131	0.00114	0.095476	0.1209
1.313	-0.00139	0.001076	0.095491	0.12094
1.314	-0.00147	0.001026	0.09553	0.120986
1.315	-0.00152	0.000981	0.095588	0.121034
1.316	-0.00154	0.000939	0.095661	0.121083
1.317	-0.00155	0.000892	0.09573	0.121128
1.318	-0.00155	0.000838	0.095783	0.121167
1.319	-0.00153	0.000774	0.095807	0.121195
1.32	-0.00152	0.000701	0.095802	0.121216
1.321	-0.0015	0.000625	0.095779	0.121231
1.322	-0.00149	0.000545	0.095751	0.121244
1.323	-0.00149	0.000473	0.095737	0.121263
1.324	-0.00148	0.000412	0.095745	0.121287
1.325	-0.00146	0.000366	0.09578	0.12132
1.326	-0.00144	0.00034	0.095835	0.121358
1.327	-0.0014	0.000332	0.095906	0.121399
1.328	-0.00133	0.00034	0.095981	0.121438
1.329	-0.00123	0.000356	0.096057	0.121474
1.33	-0.0011	0.000374	0.096131	0.121505
1.331	-0.00094	0.00039	0.096205	0.121534
1.332	-0.00077	0.0004	0.096271	0.121562

1.333	-0.00063	0.000409	0.096321	0.12159
1.334	-0.00054	0.000422	0.096352	0.12162
1.335	-0.00051	0.000439	0.096361	0.121653
1.336	-0.00052	0.000463	0.096344	0.121683
1.337	-0.00058	0.000496	0.096307	0.121712
1.338	-0.00064	0.000539	0.096261	0.121736
1.339	-0.00069	0.00059	0.09622	0.121758
1.34	-0.00071	0.00064	0.096195	0.121778
1.341	-0.0007	0.000687	0.096195	0.121799
1.342	-0.00066	0.000726	0.096217	0.121825
1.343	-0.00061	0.000753	0.096254	0.121855
1.344	-0.00057	0.000775	0.096286	0.121889
1.345	-0.00055	0.000797	0.096303	0.121924
1.346	-0.00056	0.000823	0.096297	0.121959
1.347	-0.00062	0.000858	0.096274	0.121995
1.348	-0.00071	0.000903	0.096248	0.122034
1.349	-0.00083	0.000952	0.096233	0.12208
1.35	-0.00096	0.001005	0.096243	0.122133
1.351	-0.00109	0.001057	0.096279	0.122191
1.352	-0.00121	0.001104	0.096332	0.122253
1.353	-0.00131	0.001147	0.096396	0.122312
1.354	-0.00136	0.001188	0.09647	0.12237
1.355	-0.00137	0.001229	0.096548	0.122423
1.356	-0.00135	0.00127	0.096617	0.122468
1.357	-0.00131	0.001307	0.096668	0.122505
1.358	-0.00129	0.001335	0.096692	0.122534
1.359	-0.00131	0.001353	0.096689	0.122557
1.36	-0.00137	0.001365	0.096651	0.122575
1.361	-0.00147	0.001371	0.096591	0.122591
1.362	-0.00161	0.001382	0.096516	0.122607
1.363	-0.00175	0.001401	0.09644	0.122626
1.364	-0.00188	0.001428	0.096373	0.122646
1.365	-0.00197	0.001463	0.096322	0.122667
1.366	-0.00203	0.001505	0.096289	0.12269
1.367	-0.00205	0.001547	0.096272	0.122715
1.368	-0.00205	0.001589	0.096271	0.122743
1.369	-0.00204	0.001628	0.096272	0.122772
1.37	-0.00201	0.001661	0.096267	0.1228
1.371	-0.00199	0.001685	0.096258	0.122828
1.372	-0.00198	0.001695	0.096241	0.122856
1.373	-0.00196	0.001692	0.096218	0.12288
1.374	-0.00193	0.001677	0.096195	0.122904
1.375	-0.00189	0.001656	0.09619	0.122929
1.376	-0.00182	0.001631	0.09621	0.122957
1.377	-0.00173	0.001609	0.096257	0.122989
1.378	-0.00162	0.001596	0.096321	0.123022
1.379	-0.0015	0.001587	0.09639	0.123055
1.38	-0.00136	0.001584	0.09645	0.123085
1.381	-0.00122	0.001589	0.096489	0.123109
1.382	-0.00107	0.0016	0.096506	0.123128
1.383	-0.00093	0.001615	0.096502	0.123143
1.384	-0.0008	0.00163	0.096475	0.123153
1.385	-0.00067	0.001642	0.096431	0.123159
1.386	-0.00056	0.001649	0.096374	0.123161
1.387	-0.00044	0.001651	0.096314	0.12316
1.388	-0.00032	0.001657	0.096253	0.123157
1.389	-0.00021	0.001671	0.096196	0.123151
1.39	-8.9E-05	0.001696	0.096142	0.123145
1.391	2.08E-05	0.001739	0.096093	0.123139
1.392	0.000129	0.001798	0.096047	0.123135
1.393	0.000231	0.001863	0.096005	0.123133
1.394	0.000326	0.00193	0.095968	0.123134
1.395	0.000412	0.001993	0.095935	0.123137
1.396	0.000486	0.00205	0.095902	0.123143

1.397	0.000554	0.002099	0.095875	0.123151
1.398	0.000616	0.002142	0.095845	0.123159
1.399	0.00067	0.002185	0.095814	0.123168
1.4	0.00072	0.002225	0.09578	0.123178
1.401	0.000763	0.002268	0.095741	0.123186
1.402	0.0008	0.002313	0.095696	0.123191
1.403	0.000825	0.00236	0.095648	0.123194
1.404	0.000841	0.002406	0.095596	0.123196
1.405	0.000843	0.002454	0.095545	0.123202
1.406	0.000835	0.002499	0.095495	0.12321
1.407	0.000821	0.002543	0.095451	0.123223
1.408	0.000808	0.002582	0.095409	0.123236
1.409	0.000802	0.002613	0.095367	0.12325
1.41	0.000805	0.002633	0.095324	0.123263
1.411	0.000813	0.002636	0.095283	0.123274
1.412	0.000818	0.002626	0.095242	0.123284
1.413	0.000807	0.0026	0.095201	0.12329
1.414	0.000776	0.002564	0.095155	0.123292
1.415	0.000727	0.002528	0.095105	0.123293
1.416	0.000662	0.002494	0.095048	0.123291
1.417	0.000586	0.002469	0.094993	0.12329
1.418	0.000512	0.002452	0.094946	0.123295
1.419	0.000448	0.002441	0.094915	0.123307
1.42	0.000393	0.00243	0.094897	0.123326
1.421	0.00035	0.00241	0.094888	0.123346
1.422	0.000318	0.002383	0.094886	0.123367
1.423	0.000295	0.002346	0.094883	0.123386
1.424	0.000279	0.002298	0.094877	0.123402
1.425	0.000268	0.002245	0.094861	0.123414
1.426	0.000259	0.002182	0.094835	0.123423
1.427	0.00025	0.002117	0.094801	0.12343
1.428	0.00024	0.002056	0.09476	0.123438
1.429	0.000227	0.002004	0.094714	0.123446
1.43	0.000211	0.001966	0.094668	0.123458
1.431	0.000196	0.001941	0.09462	0.123472
1.432	0.000188	0.001929	0.094576	0.123488
1.433	0.000192	0.001923	0.094536	0.123509
1.434	0.000213	0.001921	0.094501	0.123531
1.435	0.000251	0.001908	0.094467	0.123554
1.436	0.000305	0.001882	0.094434	0.123577
1.437	0.000366	0.001836	0.0944	0.123597
1.438	0.000429	0.00177	0.094361	0.123614
1.439	0.000488	0.001687	0.094318	0.123625
1.44	0.000539	0.001594	0.094266	0.12363
1.441	0.000577	0.001495	0.09421	0.123631
1.442	0.000605	0.0014	0.094148	0.123626
1.443	0.000626	0.001312	0.094083	0.123618
1.444	0.000642	0.001247	0.094017	0.123608
1.445	0.000655	0.0012	0.093954	0.123599
1.446	0.000671	0.001163	0.093897	0.123589
1.447	0.000688	0.00113	0.093848	0.123583
1.448	0.000709	0.001096	0.093808	0.12358
1.449	0.000728	0.001054	0.093776	0.12358
1.45	0.000739	0.001004	0.093748	0.123581
1.451	0.000744	0.000948	0.093724	0.123586
1.452	0.000736	0.000889	0.093699	0.123591
1.453	0.000719	0.000829	0.09367	0.123597
1.454	0.000694	0.000775	0.093633	0.123602
1.455	0.000668	0.000735	0.093593	0.123608
1.456	0.000643	0.000708	0.093549	0.123616
1.457	0.000624	0.000699	0.093506	0.123625
1.458	0.000606	0.000702	0.093464	0.123637
1.459	0.000589	0.00071	0.093426	0.12365
1.46	0.000568	0.00072	0.093396	0.123664

1.461	0.000538	0.000728	0.093373	0.123678
1.462	0.000499	0.000727	0.093358	0.123694
1.463	0.000451	0.000723	0.093347	0.123712
1.464	0.000397	0.000712	0.093339	0.12373
1.465	0.000343	0.000698	0.093326	0.123749
1.466	0.00029	0.000683	0.093305	0.123767
1.467	0.000243	0.000671	0.093277	0.123785
1.468	0.000205	0.000665	0.093242	0.123802
1.469	0.000177	0.000668	0.093211	0.123818
1.47	0.000158	0.00068	0.093186	0.123835
1.471	0.000142	0.000699	0.093169	0.123852
1.472	0.000126	0.000718	0.093163	0.123872
1.473	0.000108	0.000734	0.093167	0.123892
1.474	8.28E-05	0.000742	0.093178	0.123914
1.475	5.11E-05	0.000739	0.093184	0.123933
1.476	1.19E-05	0.000729	0.093186	0.12395
1.477	-3.1E-05	0.000707	0.093178	0.123962
1.478	-7.1E-05	0.000675	0.093159	0.123969
1.479	-9.9E-05	0.00064	0.093134	0.123974
1.48	-0.00011	0.000608	0.093106	0.123977
1.481	-0.00012	0.000586	0.093077	0.123981
1.482	-0.00011	0.000574	0.093049	0.123986
1.483	-8.9E-05	0.000582	0.093026	0.123992
1.484	-6.5E-05	0.000604	0.093003	0.124
1.485	-3.7E-05	0.000636	0.09298	0.124009
1.486	-1E-05	0.000676	0.092956	0.124017
1.487	1.71E-05	0.000717	0.092931	0.124025
1.488	4.59E-05	0.000758	0.092902	0.124029
1.489	7.73E-05	0.000795	0.092872	0.124032
1.49	0.000112	0.000824	0.092839	0.124033
1.491	0.000149	0.000845	0.092804	0.124033
1.492	0.000187	0.000851	0.092766	0.124034
1.493	0.000227	0.000844	0.09273	0.124038
1.494	0.000268	0.000825	0.092699	0.124046
1.495	0.00031	0.000805	0.092664	0.124057
1.496	0.000353	0.000787	0.092626	0.124071
1.497	0.000399	0.000772	0.09259	0.124088
1.498	0.000448	0.000766	0.092554	0.124103
1.499	0.000503	0.000765	0.09252	0.124117
1.5	0.000554	0.000768	0.092488	0.124129